



INFIERI 2013

University of Oxford

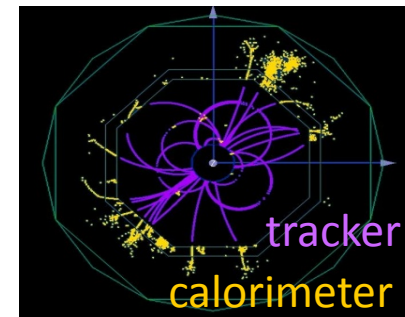
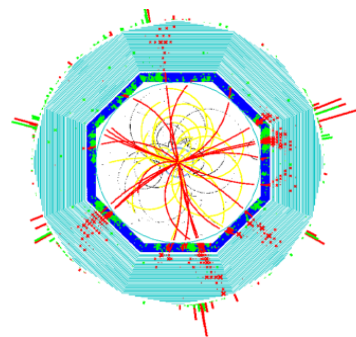


Intelligent PMTs versus SiPMs



Véronique PUILL

... High Energy Physics



Calorimetry: readout of organic and inorganic scintillators, lead glass, scint. or quartz fibres

→ visible light

→ 10s to 10000s of photons

PMT

HPD

Particle Identification Detection of Cherenkov light

→ UV/blue light

→ single photons

SiPM

MCP-PMT

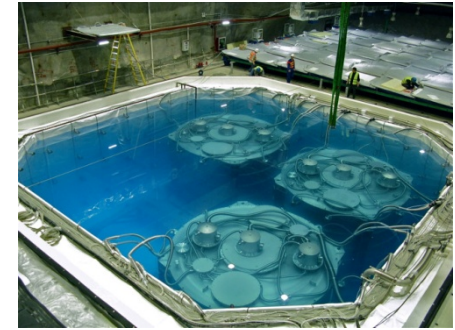
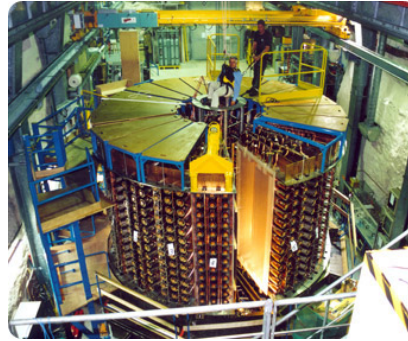
Tracking: readout of scintillating fibers

→ visible light

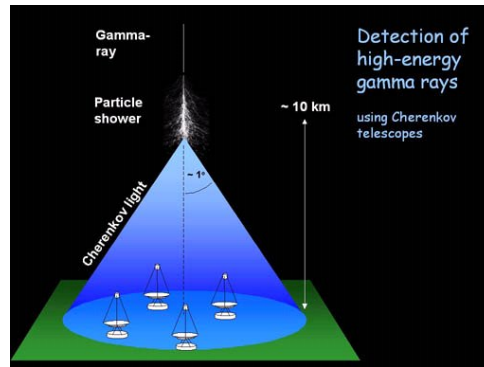
→ few photons

APD

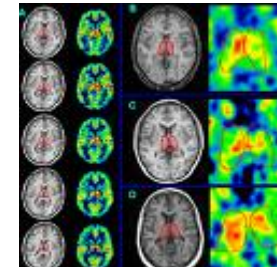
... Neutrino Experiments



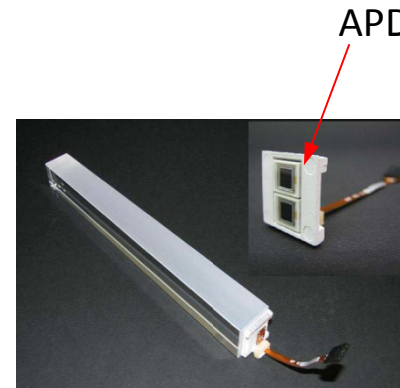
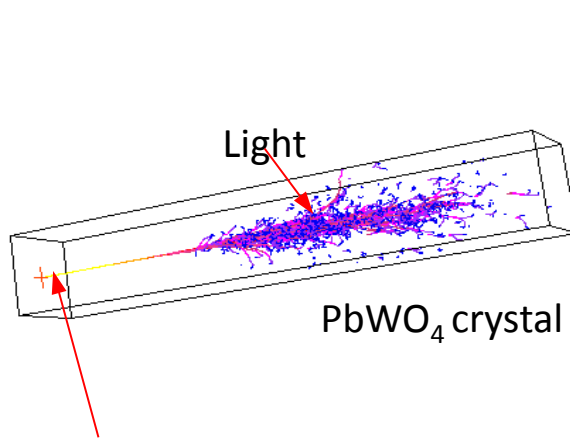
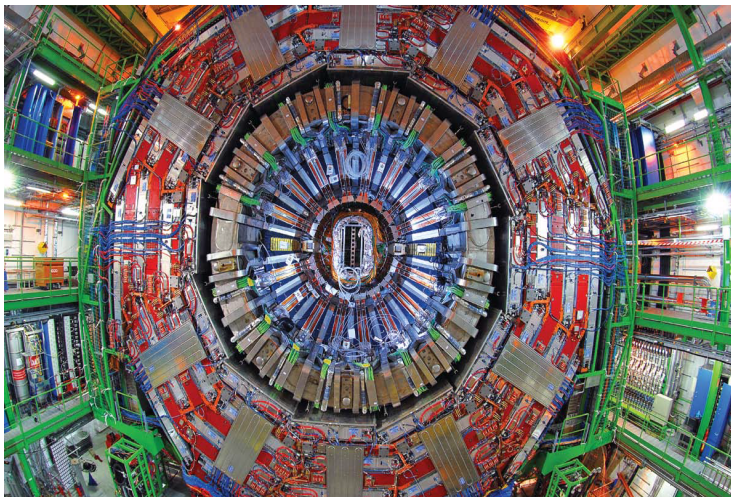
... Astrophysics : IACT (imaging Atmospheric Cherenkov Telescopes)



... Medical systems : imagery, cancer treatment, ..

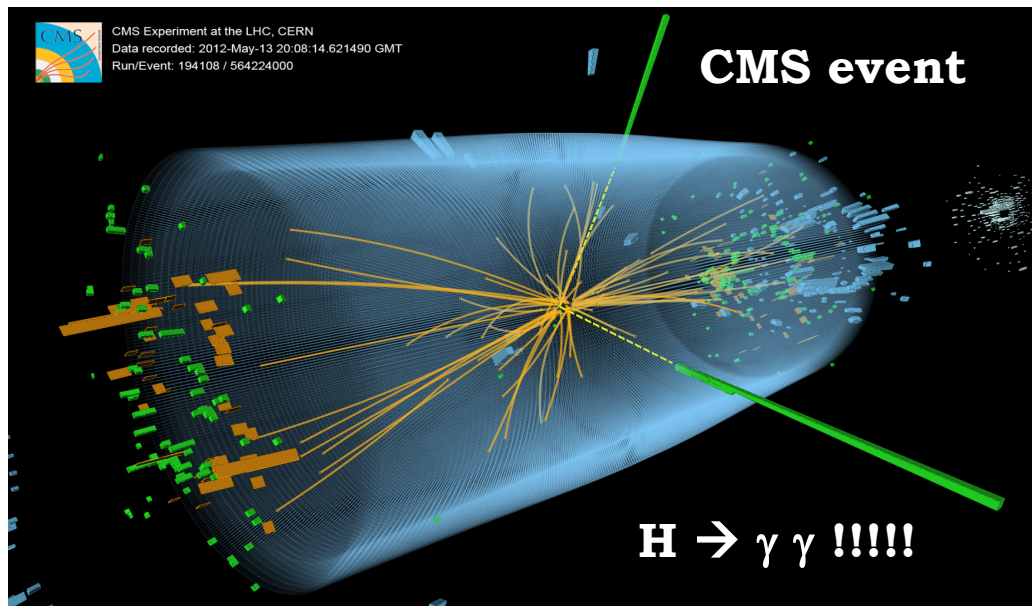


Example: CMS ECAL

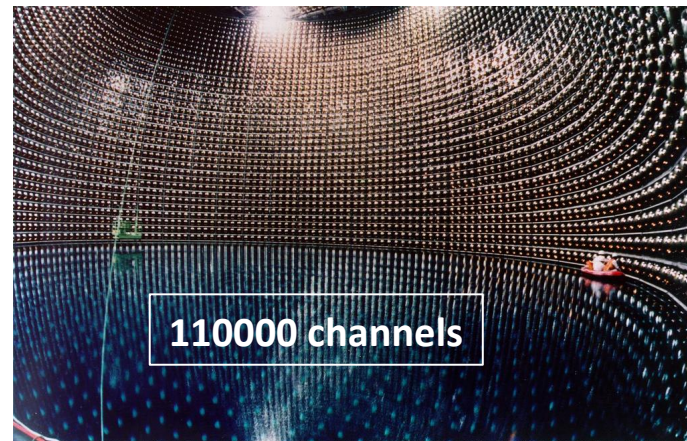
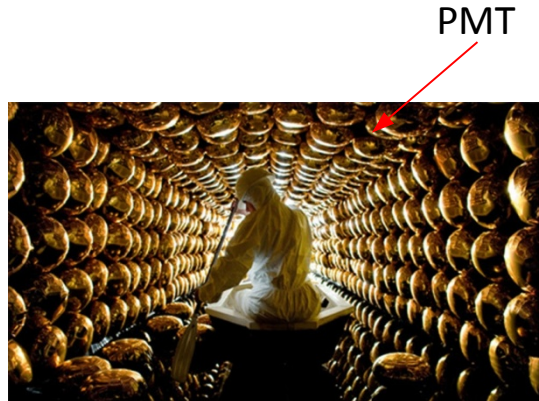
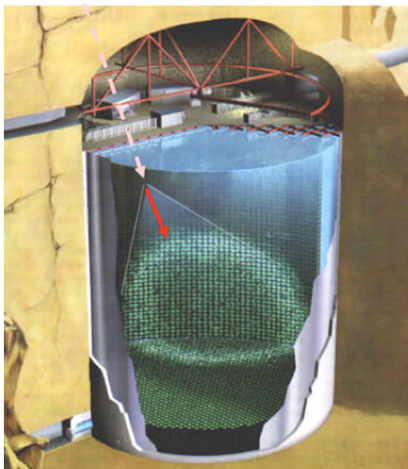


impact of e- or γ coming from electromagnetic showers

80000 channels

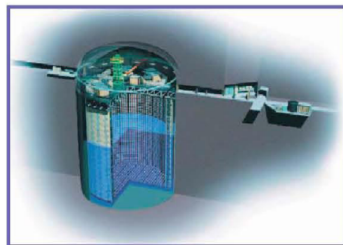


Super Kamiokande



T2K: Tokai-to-Kamioka

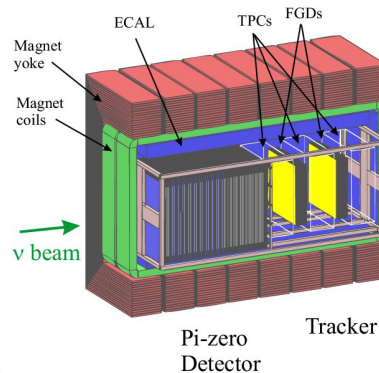
2nd generation long baseline neutrino oscillation experiment



Super-Kamiokande
(ICRR, Univ. Tokyo)



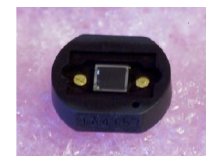
60000 channels



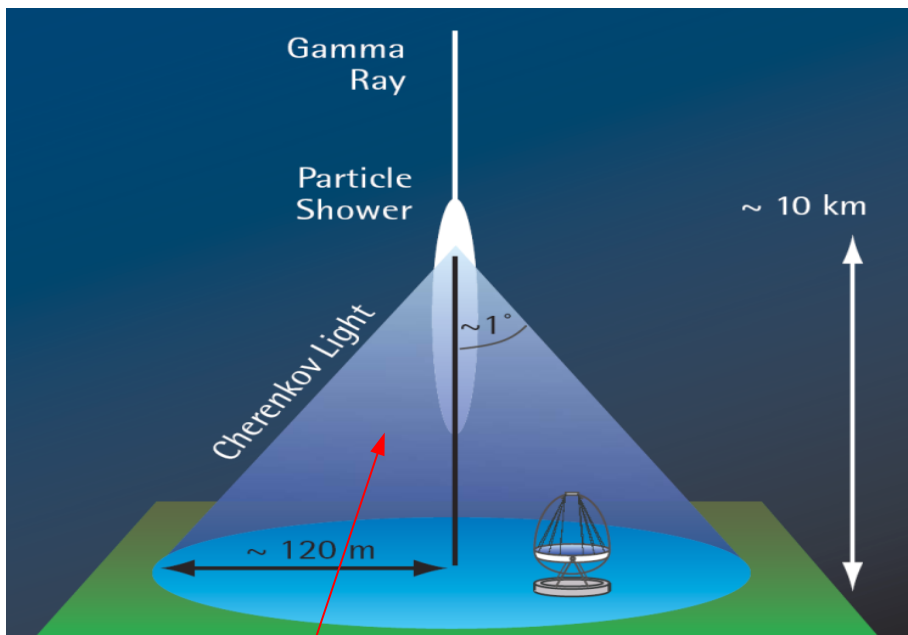
J-PARC Main Ring
(KEK-JAEA, Tokai)



SiPM



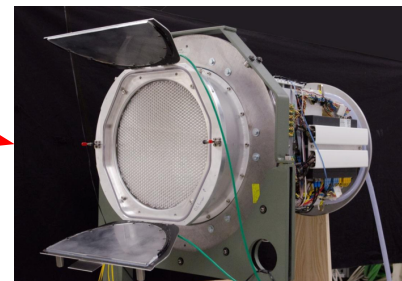
Detection of the very faint light flashes from air showers induced by cosmic rays



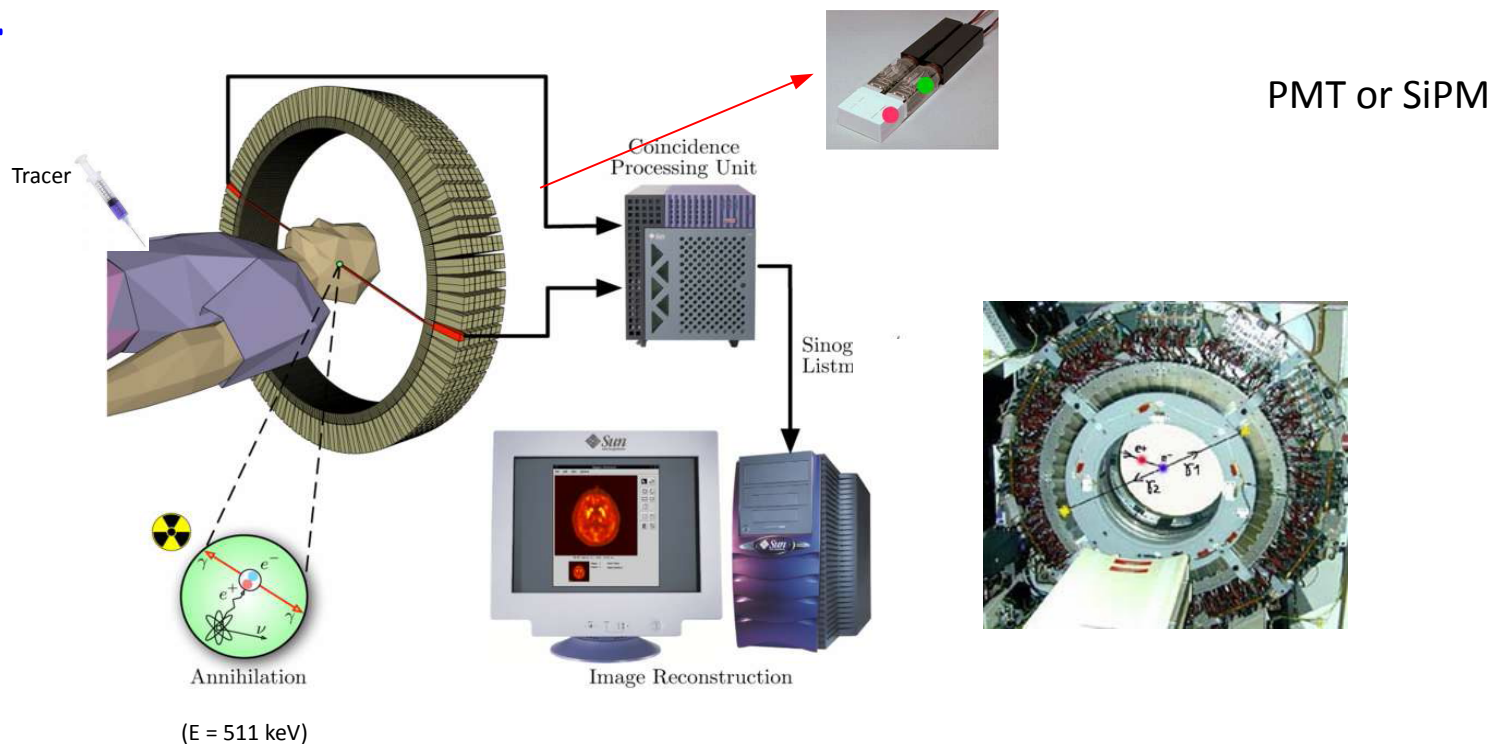
Cherenkov light detection

1500 – 2000 channels/camera

PMT or SiPM

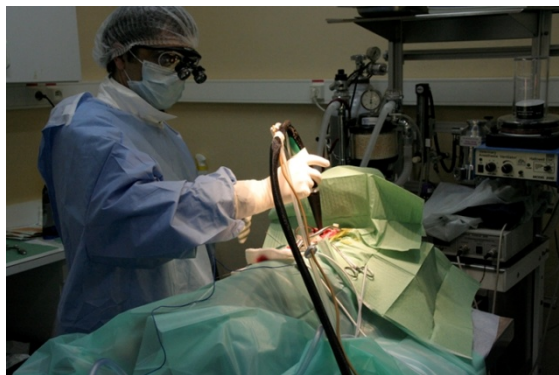


PET



Radio-isotopic probes

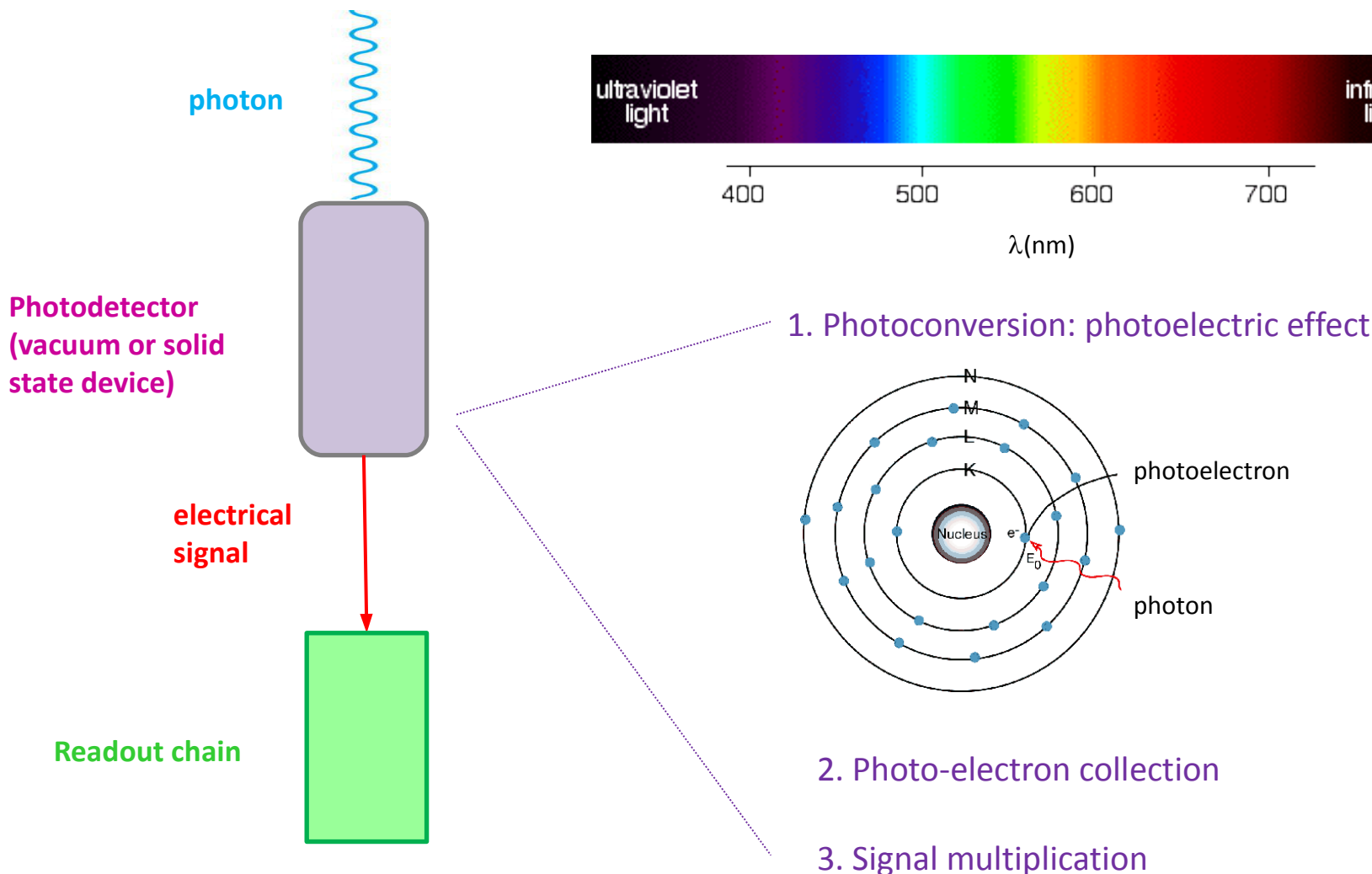
PMT or SiPM



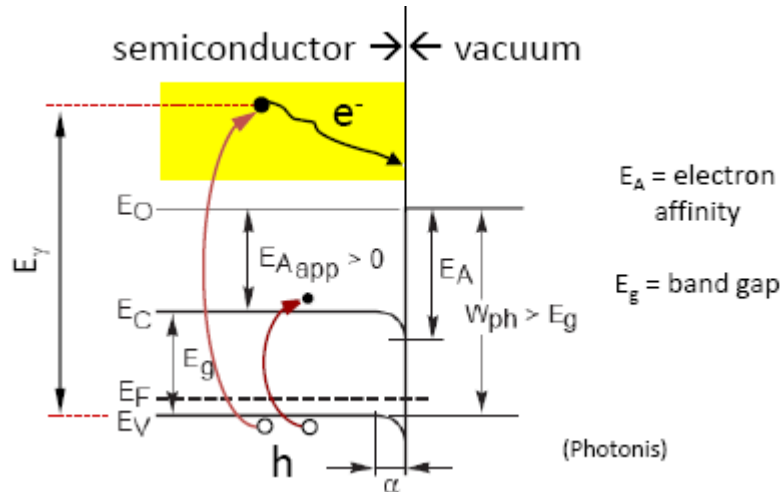
Outline

- Basic principle of the Photodetection
- Key parameters of the Photodetectors
- The Vacuum photodetectors
- The Silicon photodetectors

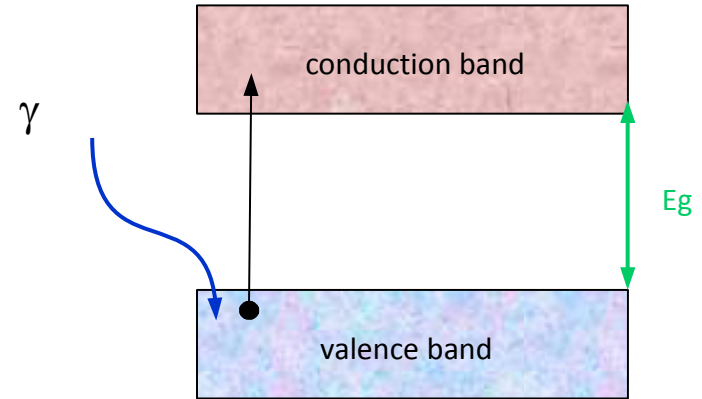
Goal of the Photodetection: convert Photons into a detectable electrical signal



in vacuum devices



in semiconductor devices



1 or 3 steps process:

Step 1: Absorption of the photon (γ) in the material and generation of electrons. If $E_\gamma > E_g$, electrons are lifted to conduction band

→ for Si-photodetector this leads to a photocurrent: **internal photoelectric effect**

→ for vacuum device (PMT, MCP-PMT, ...), 2 more steps are needed to detect a signal:

external photoelectric effect

Step 2: diffusion of the electrons through the material toward the boundary to vacuum. The escape depth L depends on the material.

Step 3: electrons with sufficient excess energy (larger energy than the work function) reaching the surface escape from it

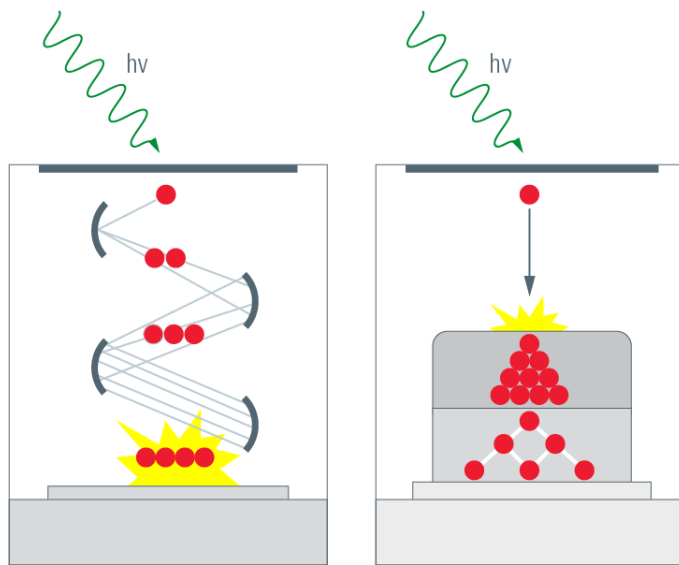
Once created, the photo-electrons (vacuum devices) or electron/hole pair (Si photodetector) can be lost (absorption, recombination)



Need of a good **collection efficiency (C_E)**: probability to transfer the primary p.e or e/h to the amplification region or readout channel

Step 3: the signal multiplication

The primary photo-electron or electron/hole pair is amplified (photodetector with **internal gain**)





Key parameters of the photodetectors

- Sensitivity
- Noise
- Gain
- Linearity
- Time response

Probability that the incident photon (N_γ) generates a photoelectron (N_{pe})

Quantum efficiency

Sensitivity x Gain x N_{pe}

$$Q\varepsilon[\%] = \frac{N_{pe}}{N_\gamma}$$

Radiant sensitivity

$$S[\text{mA/W}] \approx \frac{Q\varepsilon[\%] \times \lambda[\text{nm}] \times qe}{h \times c}$$

$$= \frac{Q\varepsilon[\%] \times \lambda[\text{nm}]}{124}$$

Photo detection efficiency : combined probability to produce a photoelectron and to detect it

$$PDE[\%] = Q\varepsilon[\%] \times C_E[\%] \quad \text{for a PMT}$$

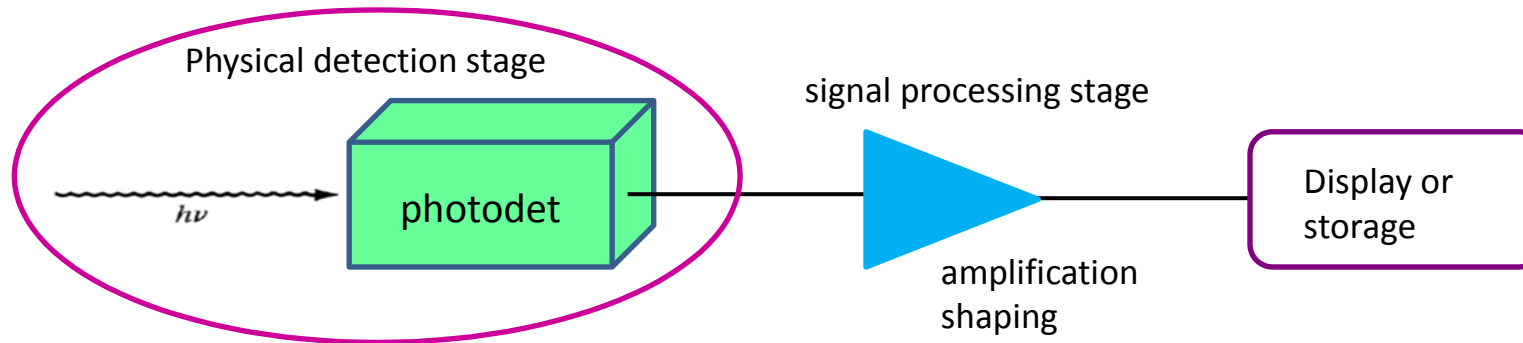
$$PDE[\%] = \mathcal{E}_{geom}[\%] \times Q\varepsilon[\%] \times P_{trig}[\%] \quad \text{for a SiPM}$$

C_E : collection efficiency

\mathcal{E}_{geom} : geometrical factor

P_{trig} : triggering probability

Principal noises associated with photodetectors :



Shot noise:

statistical nature of the production and collection of photo-generated electrons upon optical illumination (the statistics follow a Poisson process)

Dark current noise:

the current that continues to flow through the bias circuit in the absence of the light :

- ❖ **bulk dark current** due to thermally generated charges
- ❖ **surface dark current** due to surface defects

The dark noise depends a lot on the threshold → not a big issue when we want to detect hundreds or thousands of photons but in the case of very weak incident flux

The photodetector output current fluctuates.
The noise in this signal arises from 2 sources:

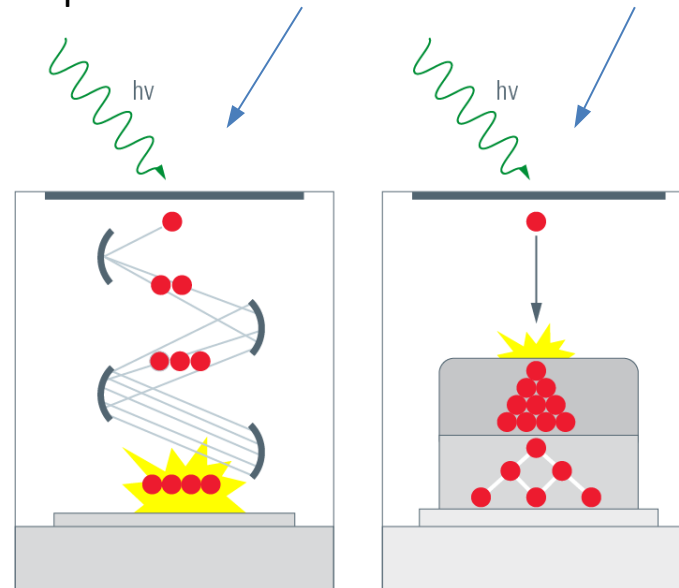
- randomness in the photon arrivals
- randomness in the carrier multiplication process

The statistical fluctuation of the avalanche multiplication which widens the response of a photodetector to a given photon signal beyond what would be expected from simple photoelectron statistics (Poisson) is characterized by the **excess noise factor ENF**

$$ENF = 1 + \frac{\sigma_M^2}{M^2}$$

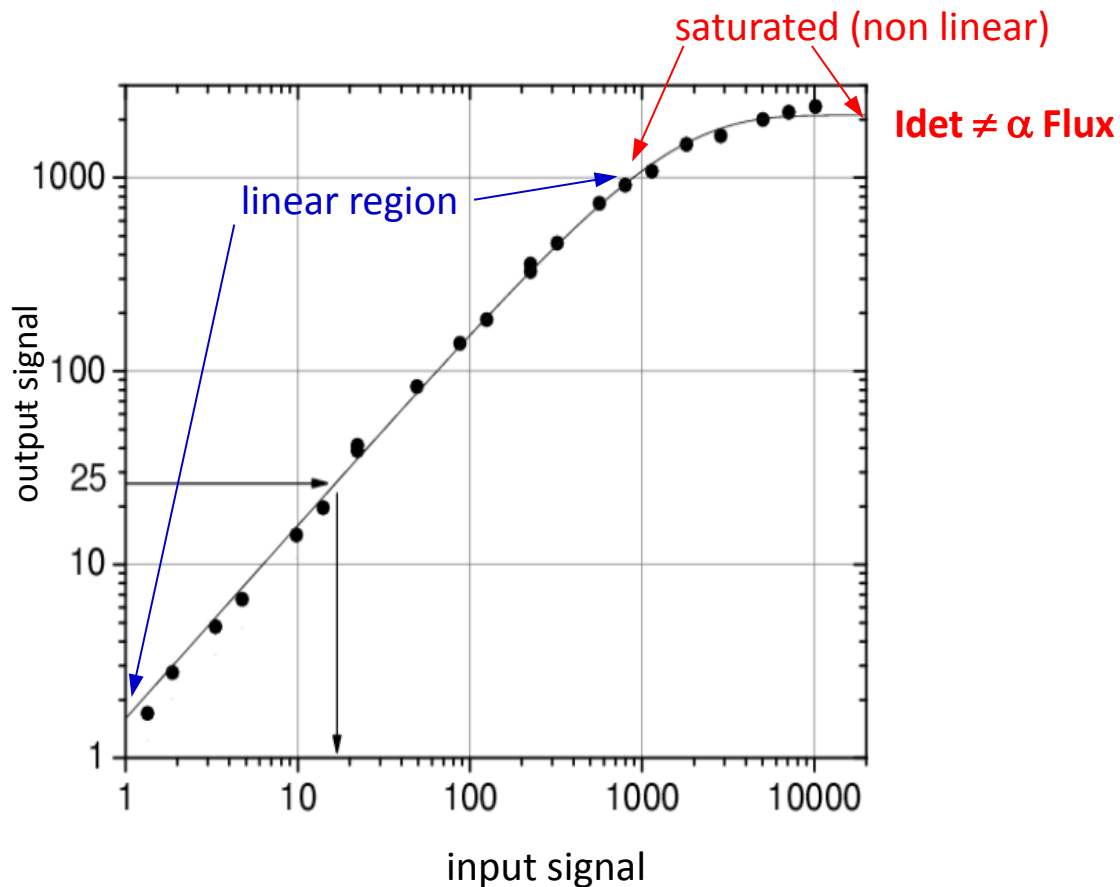
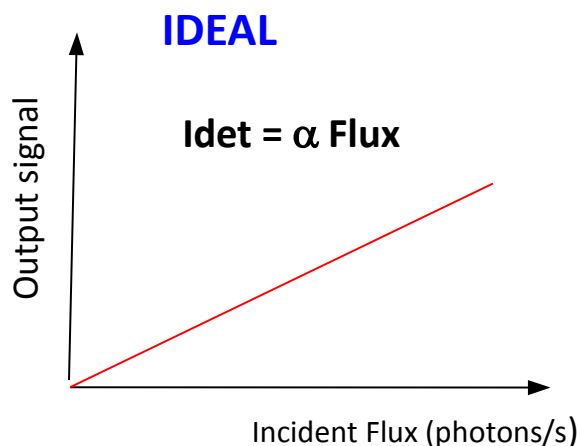
- ENF**
- ❖ impacts the photon counting capability for low light measurements
 - ❖ deteriorates the stochastic term in the energy resolution of a calorimeter

Gain process in a PMT and in an APD or SiPM

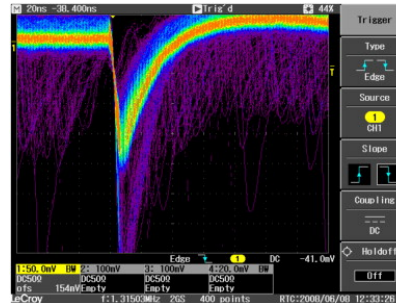
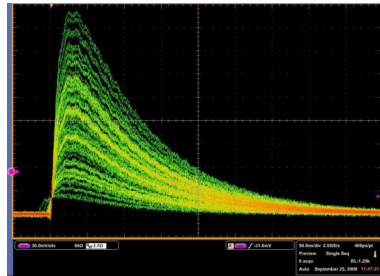
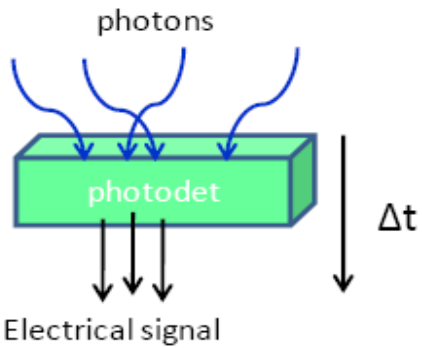


M: gain of the photodetector

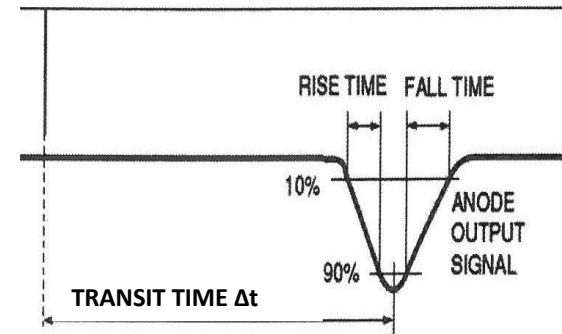
Ideally, the photocurrent response of the photodetector is linear with incident radiation over a wide range. Any variation in responsivity with incident radiation represents a variation in the linearity of the detector



Saturation: issue for the measurement of large number of photons (calorimeter)



★ light travels 300 μm in 1 ps



Timing parameters of the signal:

- Rise time, fall time (or decay time)
- Duration
- Transit time (Δt): time between the arrival of the photon and the electrical signal
- Transit time spread (TTS): transit time variation between different events → timing resolution

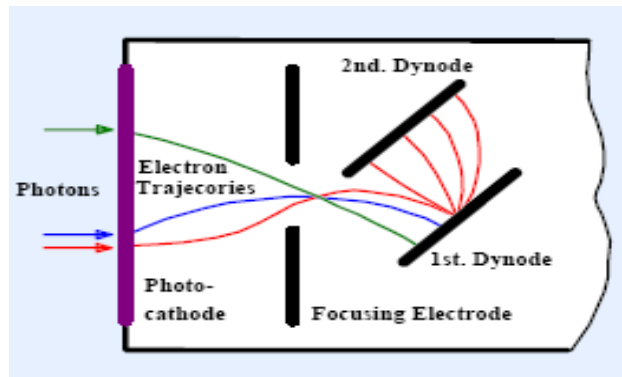


Fig. 13: Different electron trajectories cause different transit times in a PMT

Photodetectors parameters

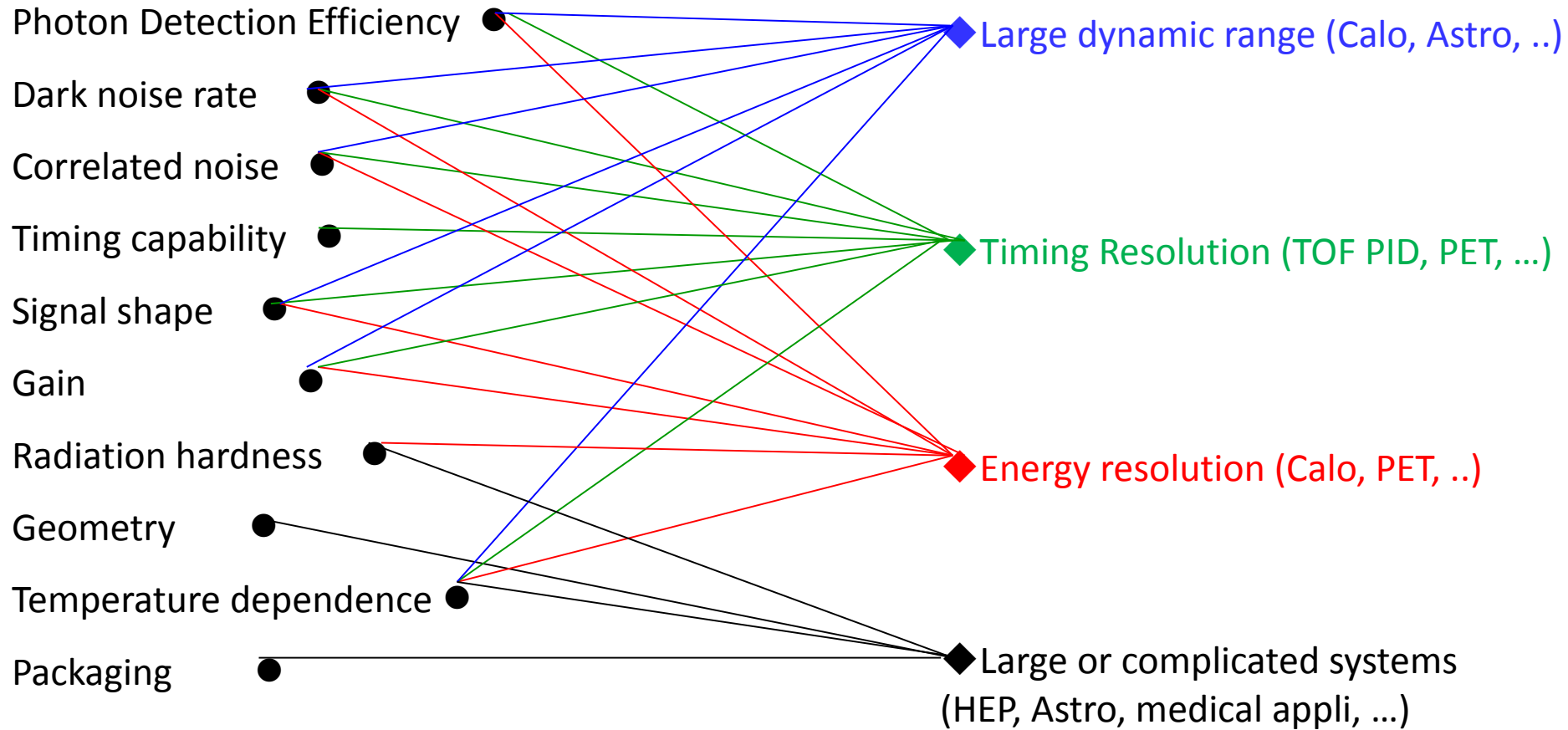
- Photon Detection Efficiency ●
- Dark noise rate ●
- Correlated noise ●
- Timing capability ●
- Signal shape ●
- Gain ●
- Radiation hardness ●
- Geometry ●
- Temperature dependence ●
- Packaging ●

System requirements

- ◆ Large dynamic range (Calo, Astro, ..)
- ◆ Timing Resolution (TOF PID, PET, ...)
- ◆ Energy resolution (Calo, PET, ..)
- ◆ Large or complicated systems (HEP, Astro, medical appli, ...)

Photodetectors parameters

System requirements





Vacuum Photodetectors

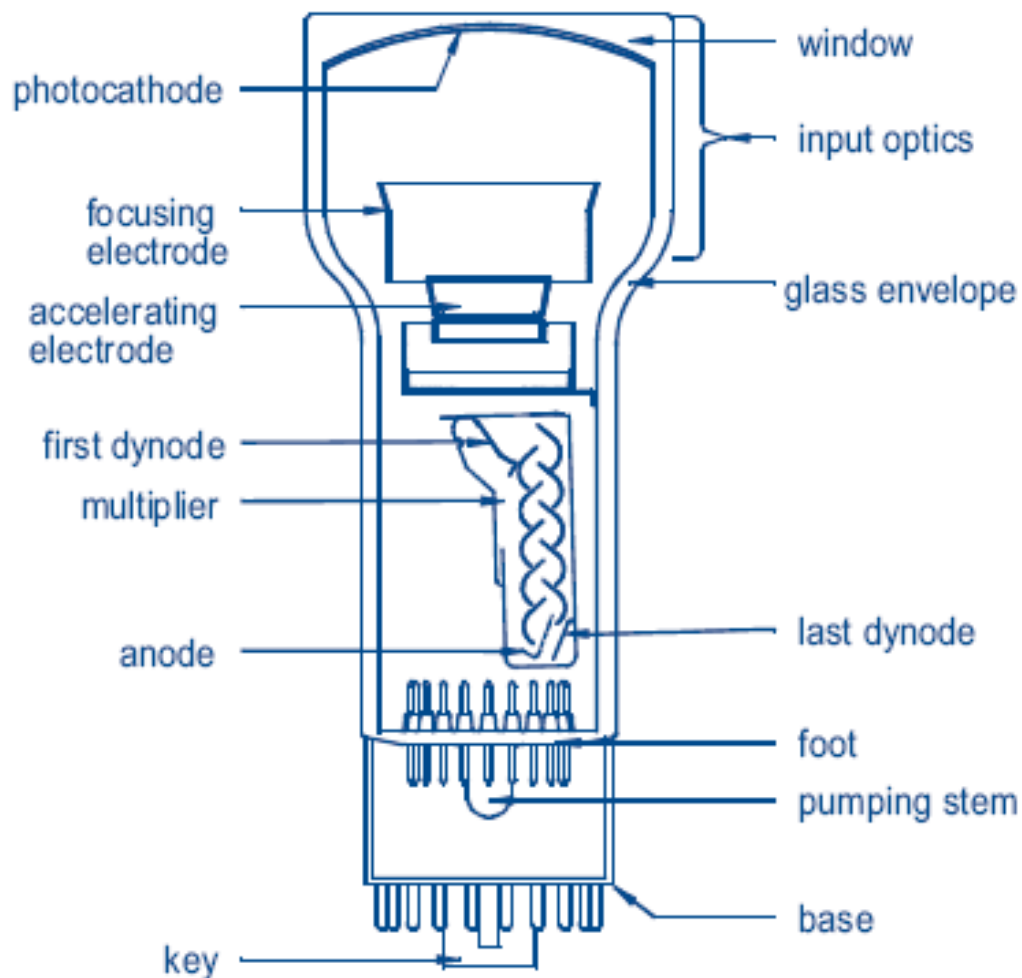
- Photomultipliers

- Micro Channel Plate Photomultipliers



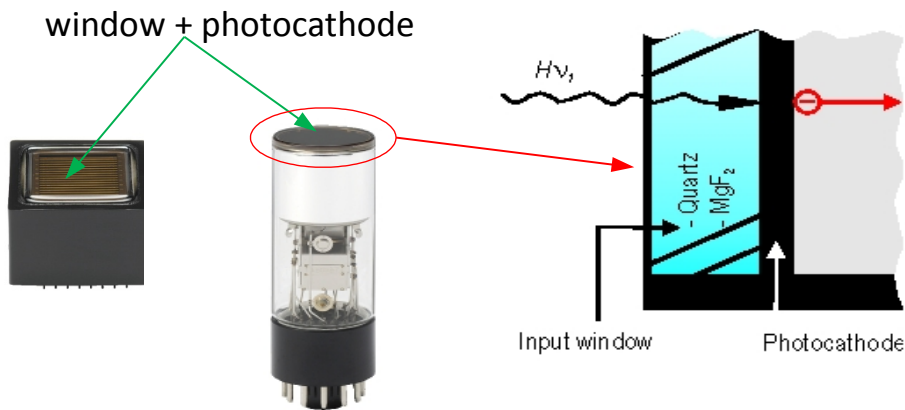
HAMAMATSU
PHOTON IS OUR BUSINESS

ET Enterprises
electron tubes



R976

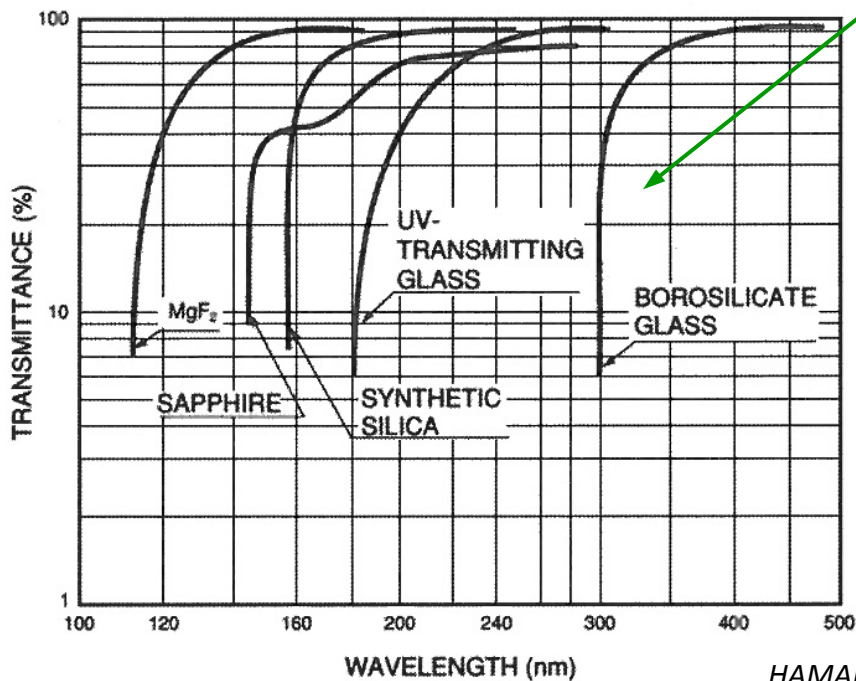
PHOTONIS PMT book



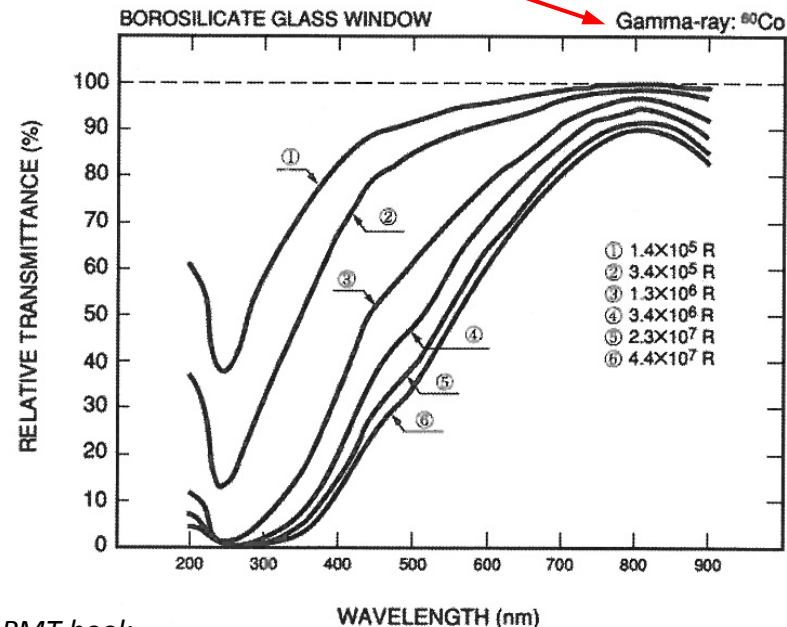
glass envelopes for PMTs



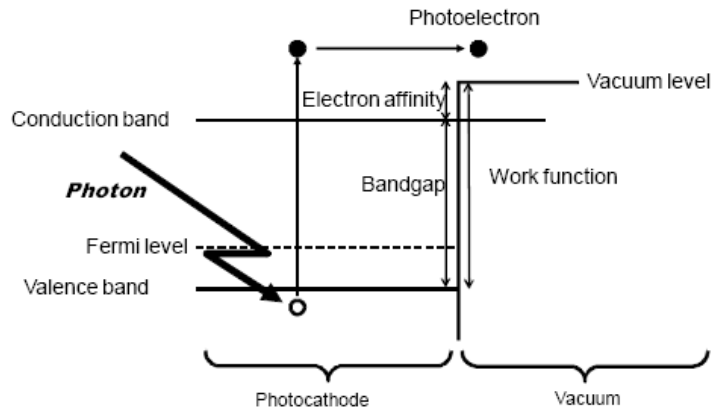
Transmittance of different material for the window



The choice of the window depends on the **wavelength of the light** we want to detect but also on the **radioactive environment**.

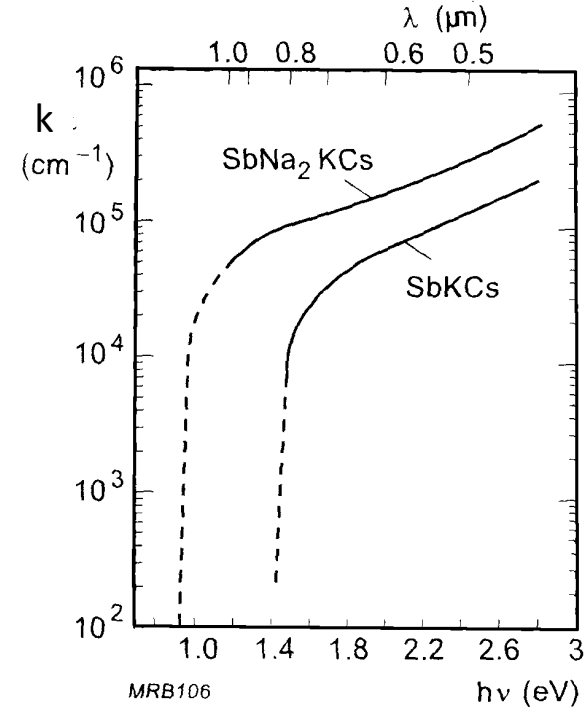


Band model for alkali photocathode



1. photon absorption and generation of an e-/hole
2. pair diffusion of the e- to the surface
3. emission of the e- in the vacuum

Light absorption in photocathode



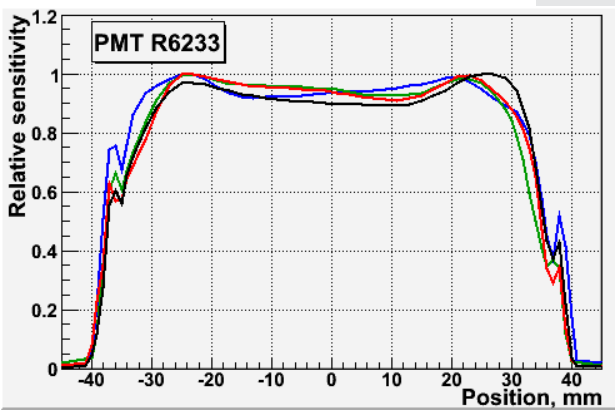
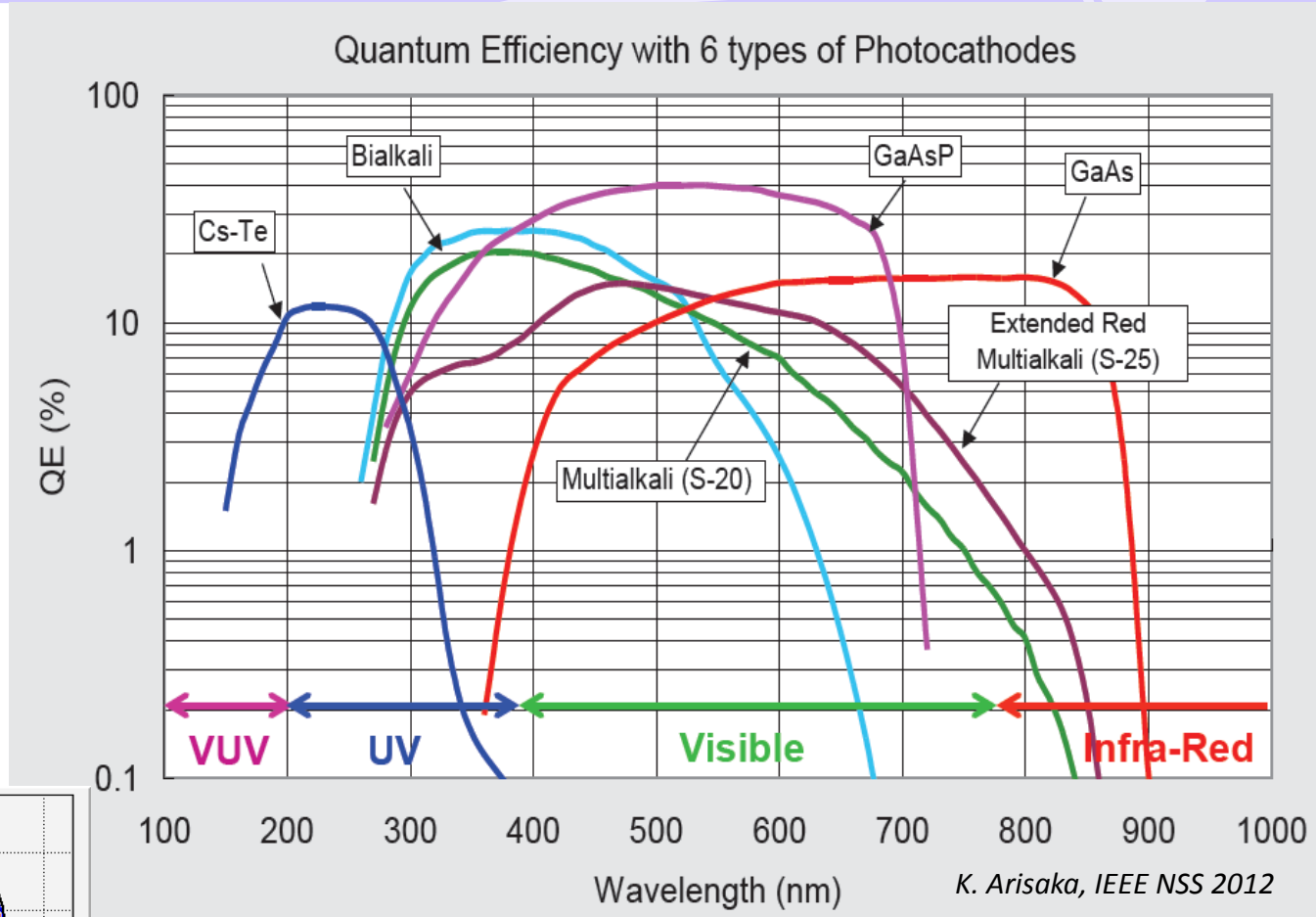
Quantum efficiency Q_ε

$$Q_\varepsilon = (1-R) \frac{P_v}{k} \times \left(\frac{1}{1+1/kL} \right) \times P_s$$

- R : reflexion coefficient
- P_v : exitation proba to vacuum level
- k: full absorption coefficient
- L: p.e mean escape length
- P_e : extraction proba to the PC surface

Photocathode materials:

- alkali metals (Sb, K, Rb, Cs)
- compound semiconductors (GaAsP, GaAs, InGaAs)

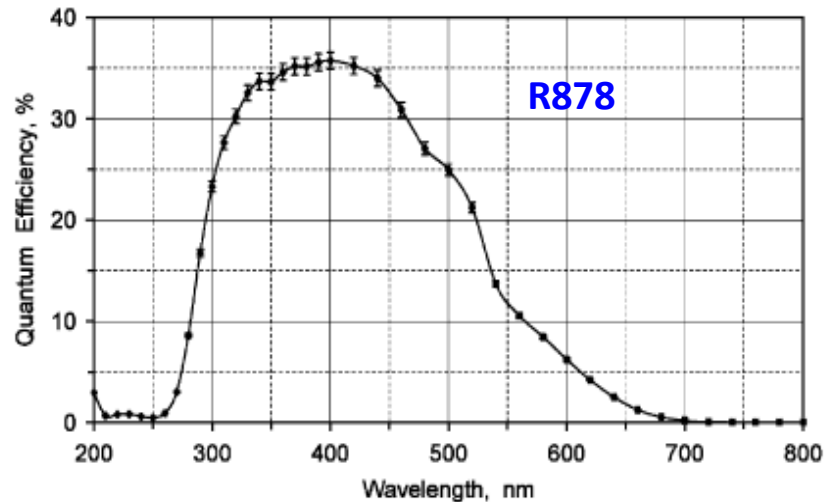


Homogeneity of the photocathode deposition and variations in collection efficiency (depends on the PC geometry)

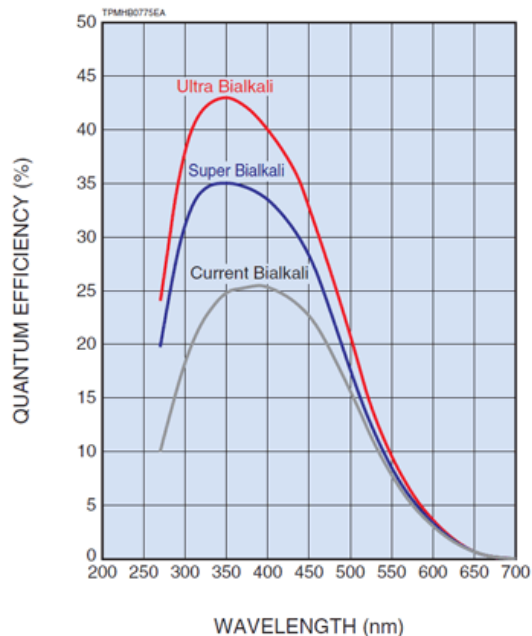
$$Q_{\epsilon} = (1-R) \frac{P_v}{k} \times \left(\frac{1}{1+1/kL} \right) \times P_s$$

↖ reflexion loss
↑ excitation efficiency
↙ loss in the PC
↘ extraction efficiency

reduction of the losses → SBA
 enhancement of the efficiencies → UBA



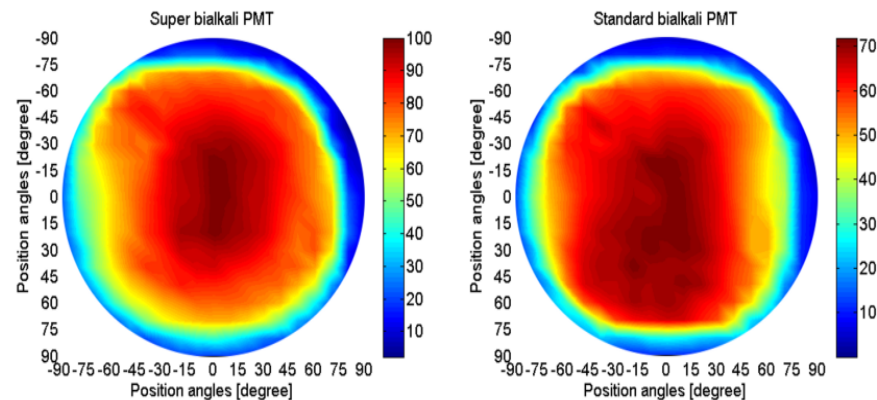
R. Mirzoyan NIMA 567 (2006) 230–232



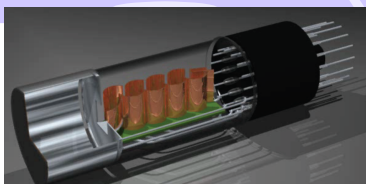
HAMAMATSU, PMT catalogue



Detection efficiency uniformity



E. Leonora, Photodet2012



Photoelectron multiplication: secondary emission of electrons by the dynodes
The HV is supplied through a resistive voltage divider

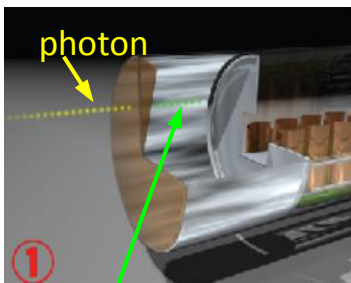
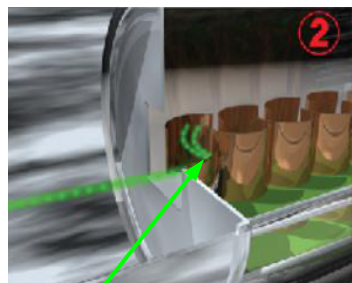
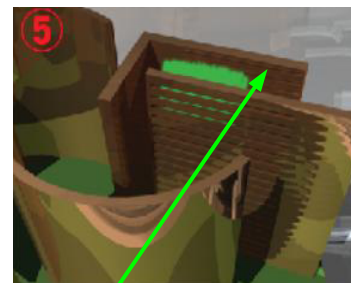
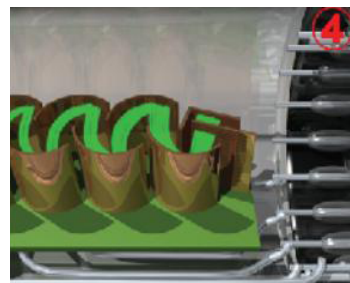
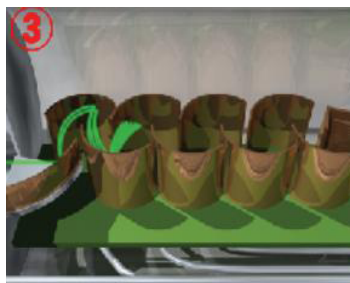


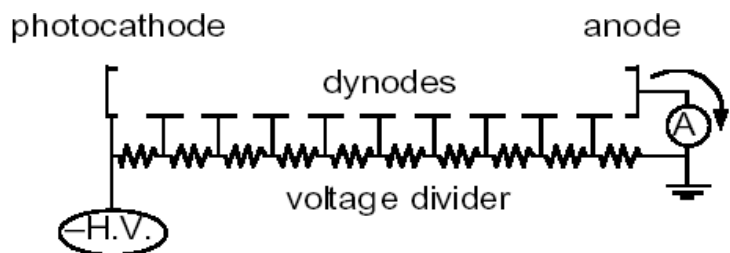
photo-electron



impact on the first dynode
(multiplication coeff : δ_1)



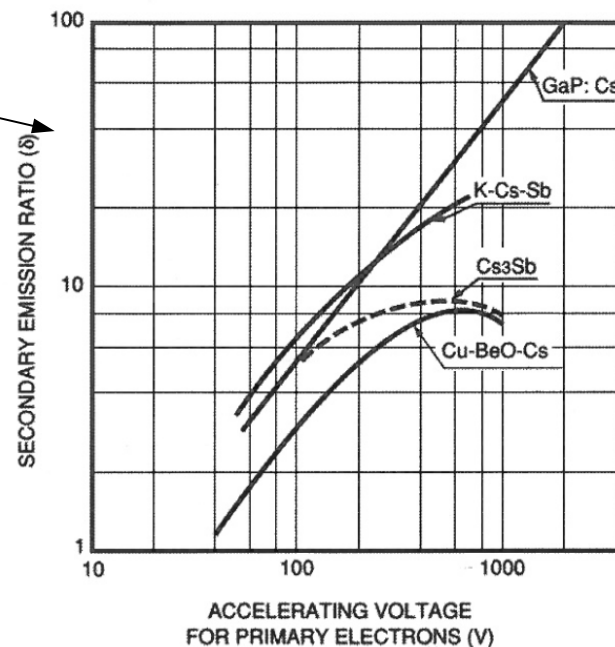
multiplication by n dynodes and signal on the anode



The gain of the PMT depends on the emission coefficient of the dynode (and on the bias voltage) and of their number:

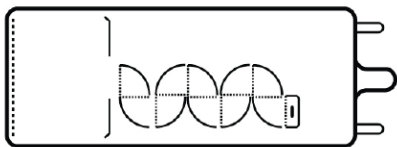
$$G = \delta_1 \times \delta_2 \times \delta_3 \times \dots \times \delta_n$$

$10^5 < G < 10^6$
For $800 < HV < 2000 \text{ V}$



Large variety of dynode types available

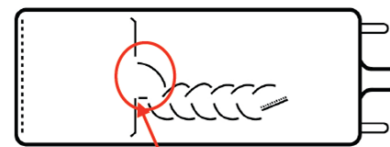
BOX & GRID



large collection area on the first dynode

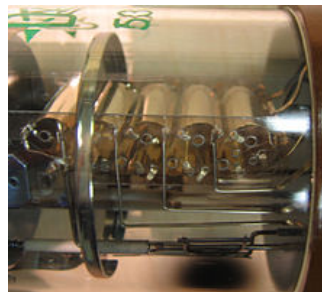
- Good detection efficiency (good CE)
- Slow time response

LINEAR FOCUSED (CC+BOX)

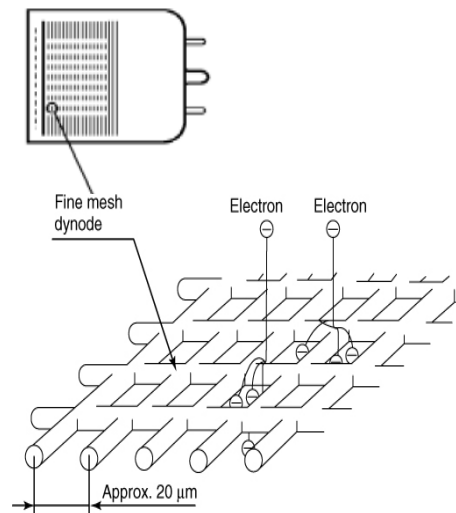


focus of the e- path

- Good output linearity
- Fast time response

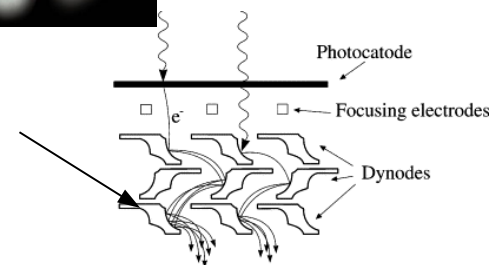
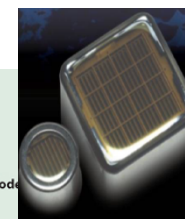
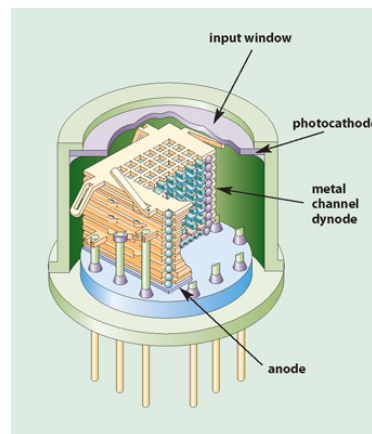


Fine Mesh



- Good output linearity
- High immunity to magnetic fields

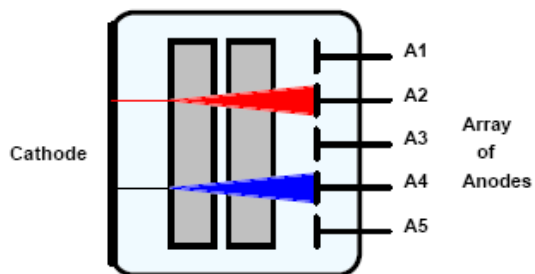
Metal channel



thin dynodes produces by micromachining and precisely stacked

- compact
- Fast time response

Need of space segmentation of the light detection



metal channel dynodes + special anode configuration

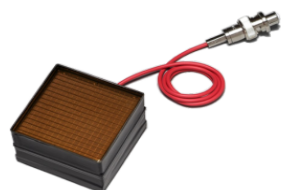
avalanche confined
in a narrow channel

multi-anode design

position sensitive PMT

HAMAMATSU PMT book

Anode Type	Single	Single	Linear (8 ch)	Linear (16 ch)	Linear (32 ch)	Matrix (2 x 2 ch)	Matrix (4 x 4 ch)	Matrix (8 x 8 ch)
Effective Area	$\phi 8$ mm	18 mm x 18 mm	21.6 mm x 2.5 mm	15.8 mm x 16 mm	31.8 mm x 7 mm	18 mm x 18 mm	18.1 mm x 18.1 mm	18.1 mm x 18.1 mm
Effective Area (per channel)	—	—	2 mm x 2.5 mm	0.8 mm x 16 mm	0.8 mm x 7 mm	8.9 mm x 8.9 mm	4.2 mm x 4.2 mm	2 mm x 2 mm



H8500 (8 x 8)



R7600 (8x8)



R11265 (8x8)

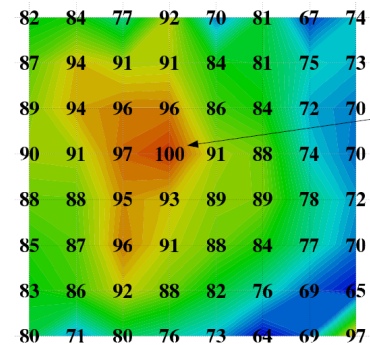


- Compact
- Good timing performances
- Good immunity to magnetic field



- Cross-talk
- Non uniformity across the channels

H8500 response uniformity

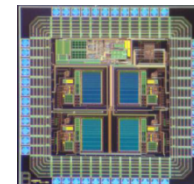
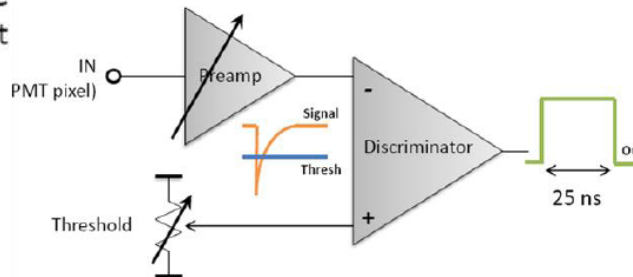


G. Collazuol, SuperB meeting, 2011

CLARO

The CLARO-CMOS is the first prototype of an ASIC for single photon counting with photomultipliers, designed to readout multi-anode PMTs in the upgraded LHCb RICH.

- Each channel has a preamplifier (with settable gain) and a discriminator (with settable threshold)
- This prototype has 4 channels
- No dead time at 40 MHz hit rate
- Power consumption below 1 mW/channel



G. Collazuol, SuperB meeting, 2011

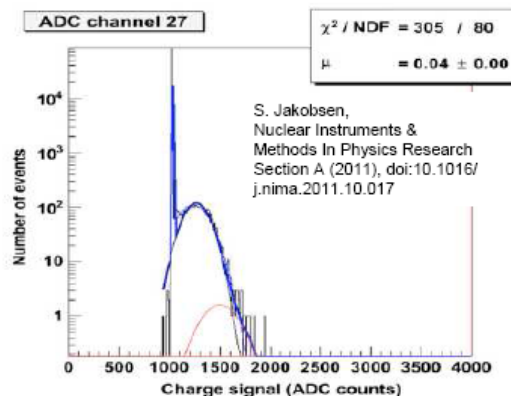
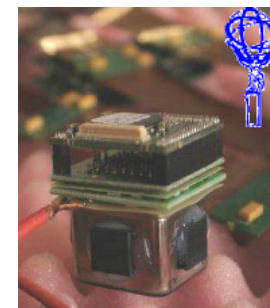
MAROC (Multi Anode Read-Out Chip)

Readout of the MaPMT 64 channels of the ATLAS luminometer

64 channel inputs:

Variable gain current preamps (8 bits/ch.)

- 64 trigger outputs + 2 OR outputs
- 1 mux. analog charge output
- 1 digitized charge output (8, 10 or 12 bits ADC)
- Trigger efficiency= 5fC
- Variable slow shaper (20-100 ns)
- 10 bits DAC as threshold

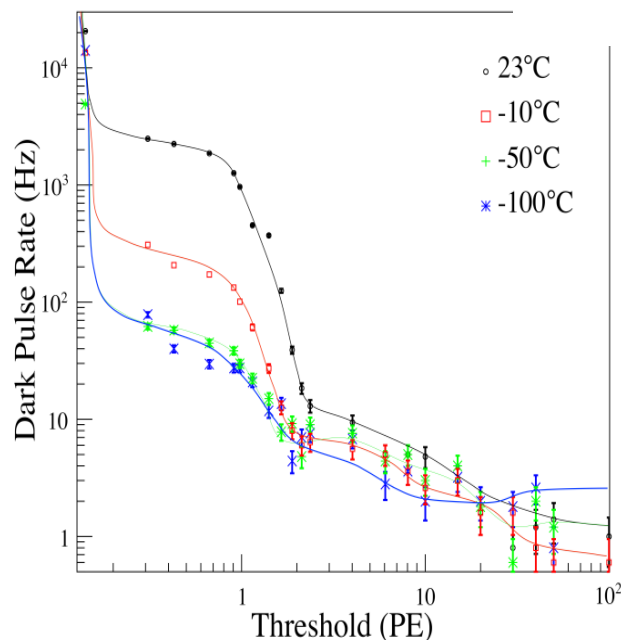
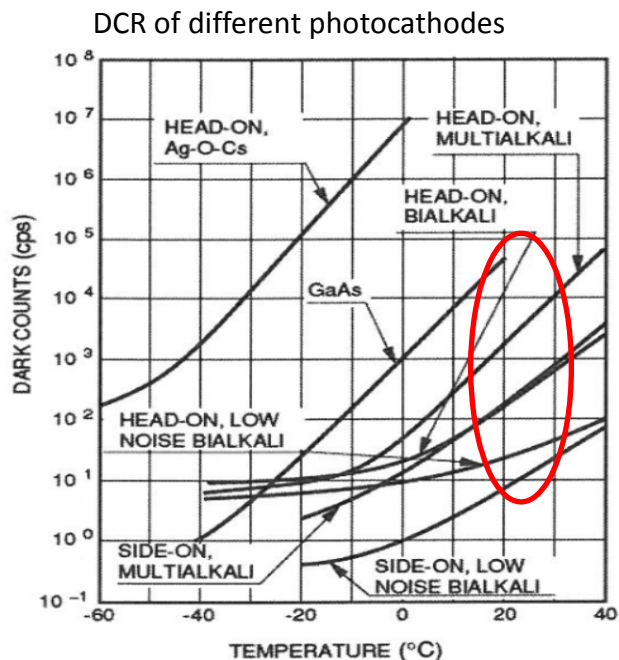
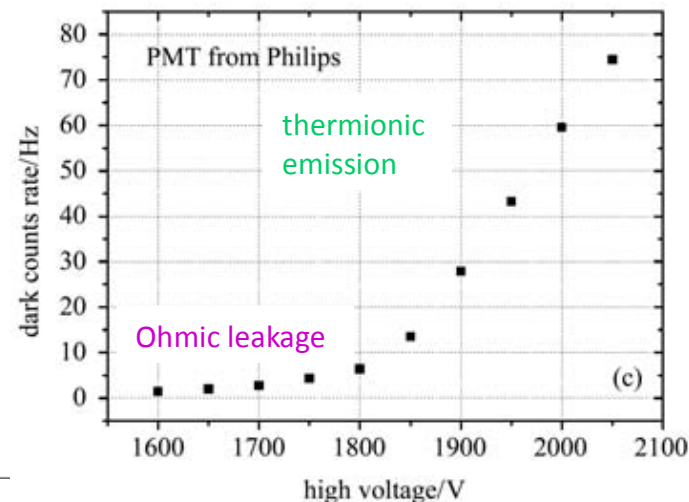


Charge spectrum of one MAPMT channel illuminated by a LED at low light level.

S. Conforti, PhotoDet 2012

Dark current (I_d): current when photomultiplier is operated in complete darkness

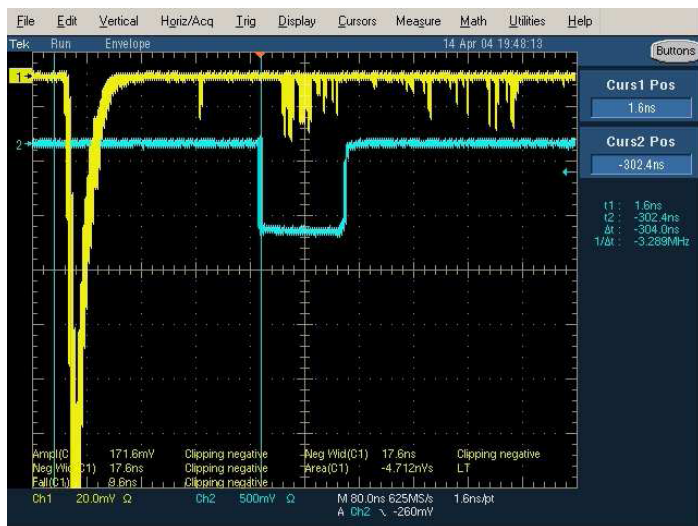
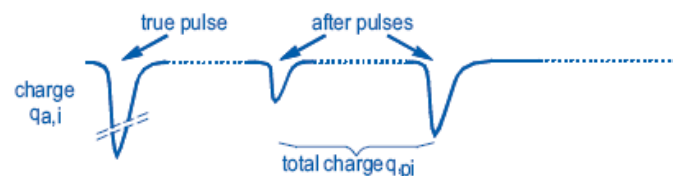
- due to leakage currents between electrodes and insulating surfaces (ohmic leakage)
- depends on the cathode type, the cathode area, and the temperature (thermionic emission)
- is highest for cathodes with high sensitivity at long wavelengths (low work function)
- increases considerably if exposed to daylight



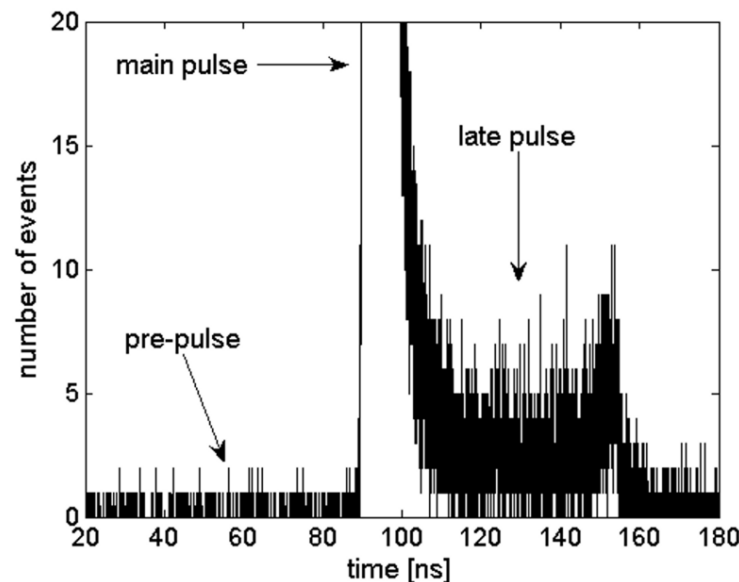
I_d needs to be minimized for low intensities measurements
 → cooling

Afterpulses: small signals, few p.e level, that appear after the main pulse

- short delay afterpulses (up to several tens of ns after the signal) caused by the elastic scattering of the electrons from the first dynode.
- long delay afterpulses (several tens of ns to several μ s after the main pulse) caused by the positive ions which are generated by the ionization of residual gases



Time distributions of late pulses



E. Leonora, VLVnT09

Can be distinguished by the time interval that separates them from the true pulse \rightarrow use of coincidence techniques to minimize their effect

HEP Detector near accelerator (LHC, ILC) : very hostile environment for PMT

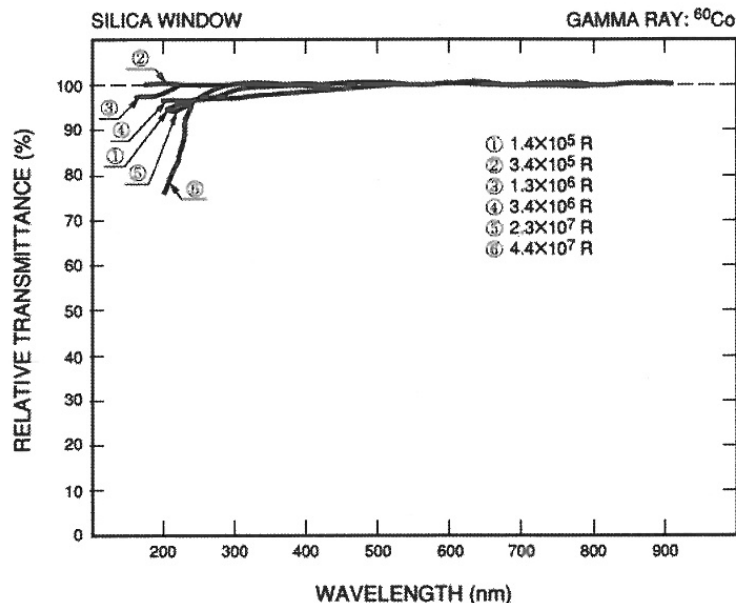
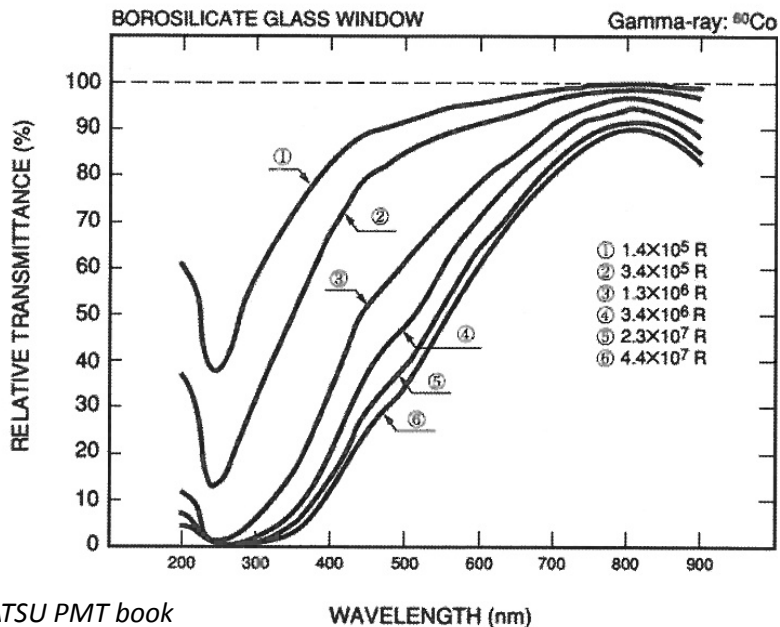


Damages caused by:

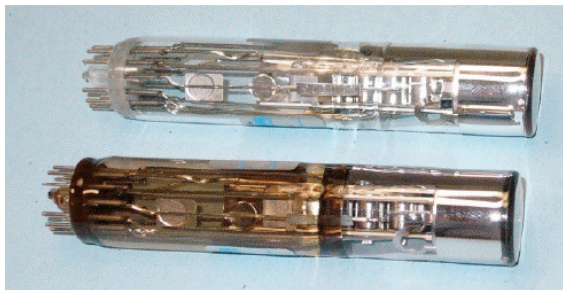
- ☛ ionizing radiation: energy deposited by particles in the detector material (the unit of absorbed dose is Gray (Gy) ==> 1 Gy = 1 J/kg = 100 rad) and by photons from electromagnetic showers
- ☛ neutrons created in hadronic shower, also in the forward shielding of the detectors and in beam collimators



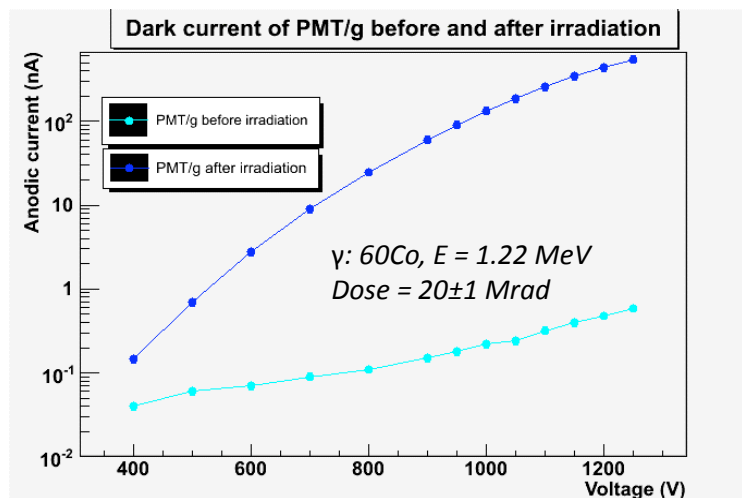
- important deterioration of the window transmittance (Borossilicate glass)
- no effect for visible light with Silica window



- increase of the dark current (scintillation of the glass window)

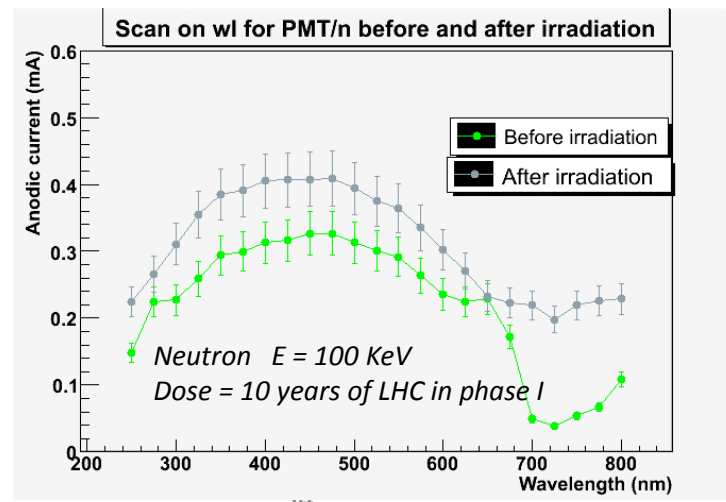
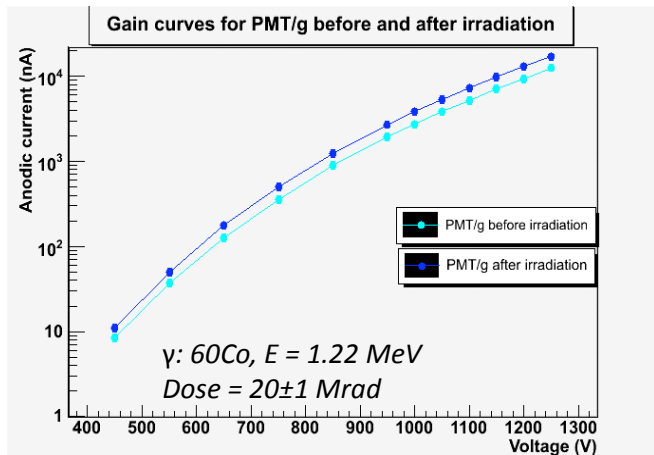


Dark current of PMT R762



A. Sbrizzi LUCID in ATLAS

- no important change of the gain and quantum efficiency



Progress in PMT development

80 years of existence and still in R&D !

some examples ...

Large water Cherenkov and scintillator detectors for long baseline neutrino oscillations, proton decay, supernova and solar **neutrinos experiments**

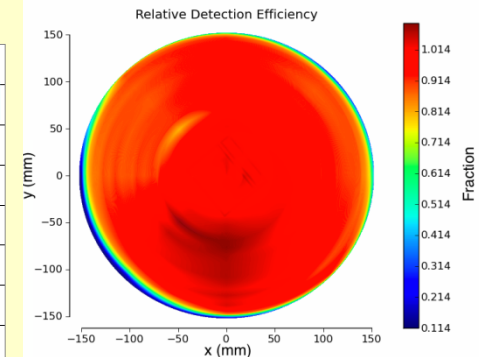
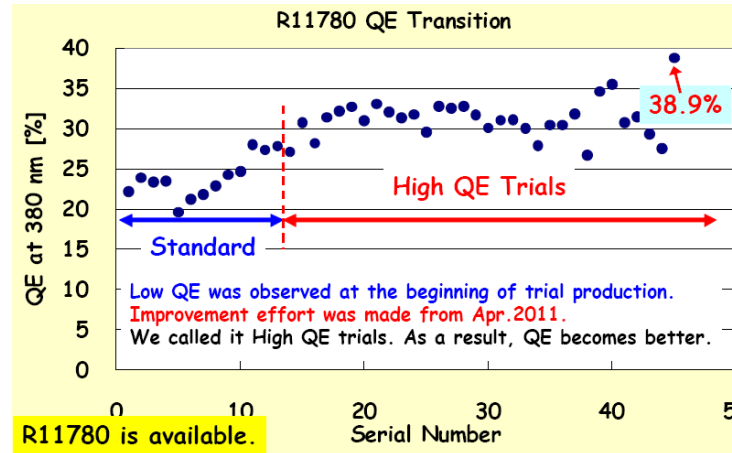
Need for PMT with:

- ✓ large-area
- ✓ high Q_ϵ in UV

R11780 (12-inch)

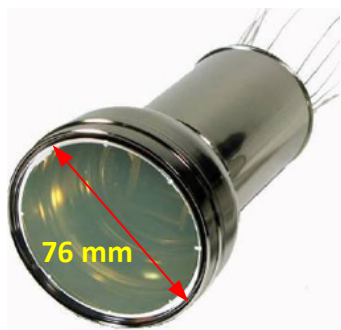


Y. Yoshizawa, Photodet 2012



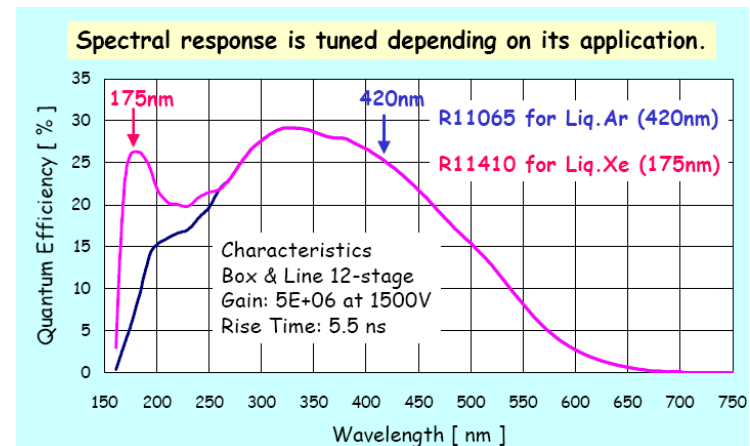
J. Brack, arXiv:1210.2765v2

Scintillation detector for **Dark Matter experiments** (scintillation light from Xe nuclear recoil resulting from the scattering of WIMPs*) → need for Ultra low background PMT working at low temp



3- inch metal bulb PMT

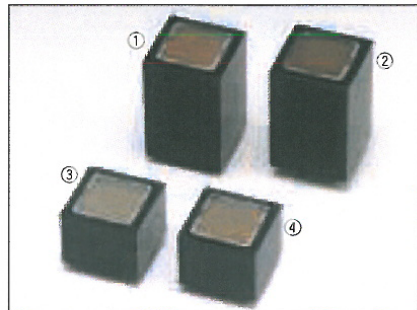
Extremely low radioactivity
Low temp: Liquid Ar(- 186 °C)



Y. Yoshizawa, Photodet 2012

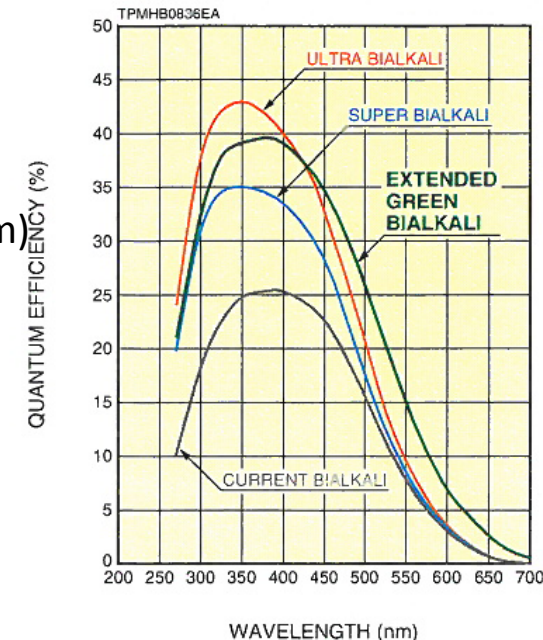
* WIMP: weakly Interacting Massive Particles

PMT with extended green Bialkali photocathode



① H8711-300 ② H7546B-300
③ R7600U-300 ④ R7600U-300-M4

- Extended green bialkali PC ($Q_E = 14\% @ 550\text{ nm}$)
- 2 x 2 multianode
- 4 x 4 multianode
- 8 x 8 multianode



Compact packaging multianode PMTs

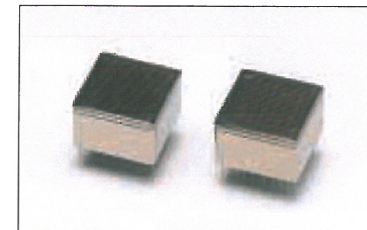
Parameter	H8500C ^② , H8500D ^②	H9500 ^②	NEW R11265-100-M16/M64	Unit
Spectral Response	300 to 650		300 to 650	nm
Transit Time Spread (FWHM)	0.4		0.34 / 0.35	ns
Anode Type	Matrix		Matrix	—
	8 x 8	16 x 16	4 x 4 / 8 x 8	—
Effective Area	49 x 49		23 x 23	mm
Effective Area Ratio ^①	89		77	%

① (Effective Area) / (External Size)

② UV type is also available. Suffix: -03, 185 nm to 650 nm



Left: H8500C, Right: H9500

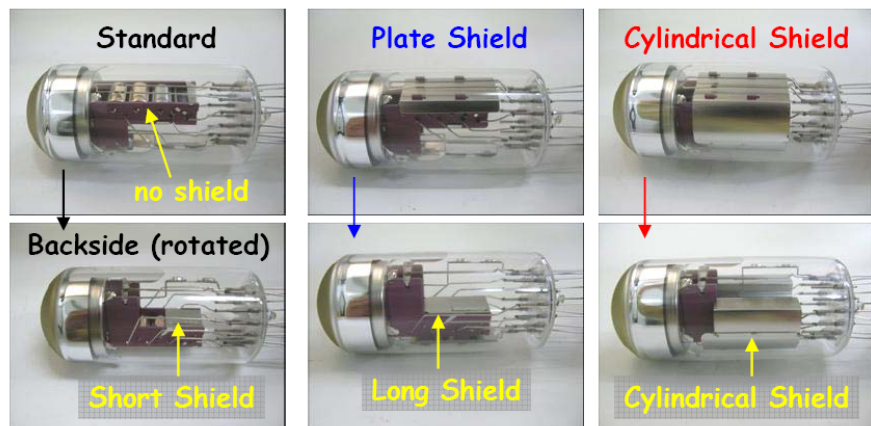


Left: R11265-100-M16, Right: R11265-100-M64

R&D in the structure of the PMT (dynode)

Optimization of Dynode Shield

Dr. Mirzoyan/MPT reported that there is light emission from dynode of R11920-100. We made 2 kinds of trial tubes with different shape of dynode shield and checked the light emission.



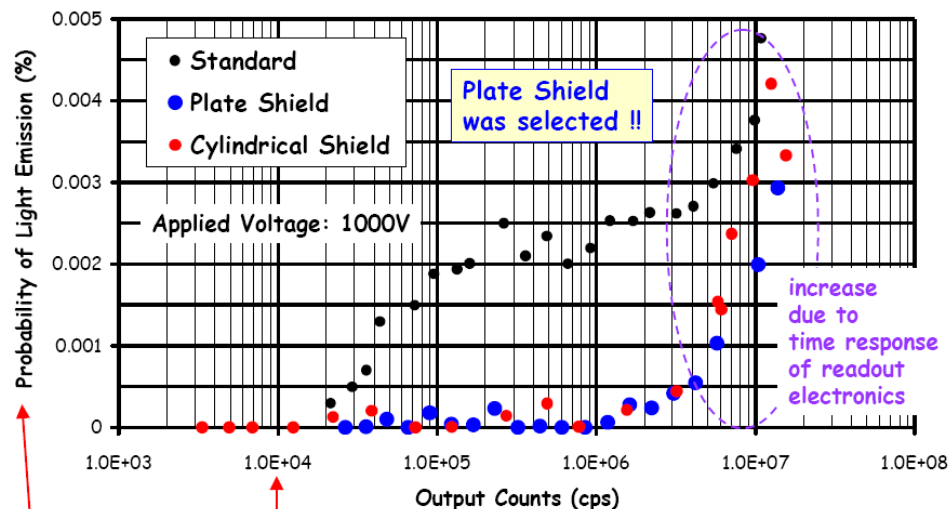
HPK, private communication

Producers and Physicists work together to increase the PMT quality

Lower after-pulse %

	PMT	Voltage	AP/Noise
old	R9420	850V	0.20 %
new	R11920	902V	0.013 %

Light Emission from Dynode

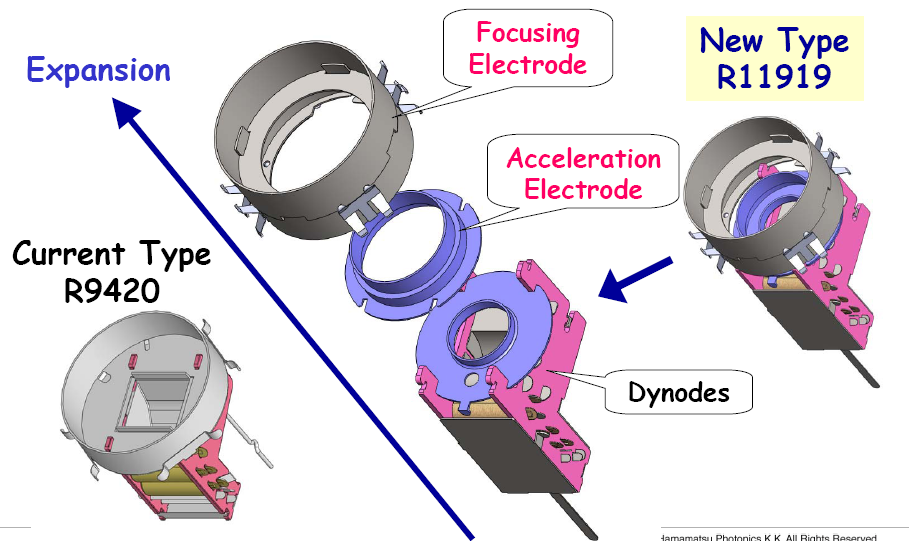


AP/NOISE(%) is normalized at 1.0E+04 output counts.

R&D in the structure of the PMT (electrode)

Comparison of PMT Structure between Current Type and New Type

HAMAMATSU
PHOTON IS OUR BUSINESS



23

HPK, private communication

Hamamatsu Photonics K.K. All Rights Reserved.

Better TTS

R11919 / 1.5-inch FAST PMT

Fast Time Response with Acceleration electrode for TOF-PET and HEP experiments



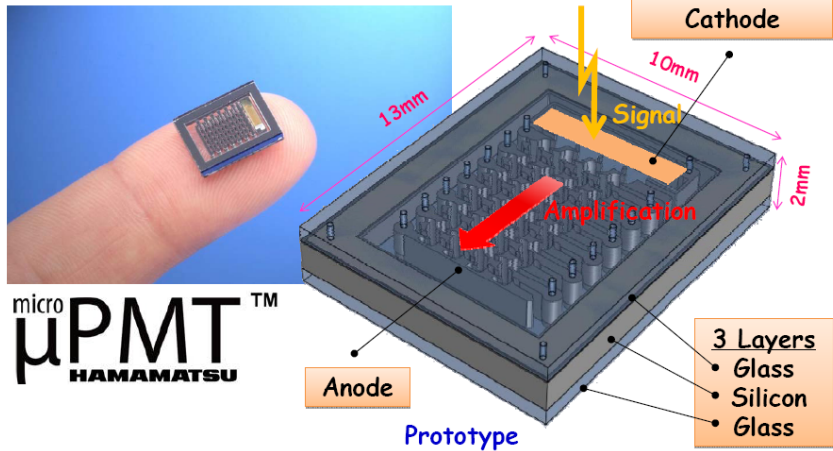
Transit Time Spread = around 270 ps

(R9420 = 550 ps, R11194 = 400 ps)

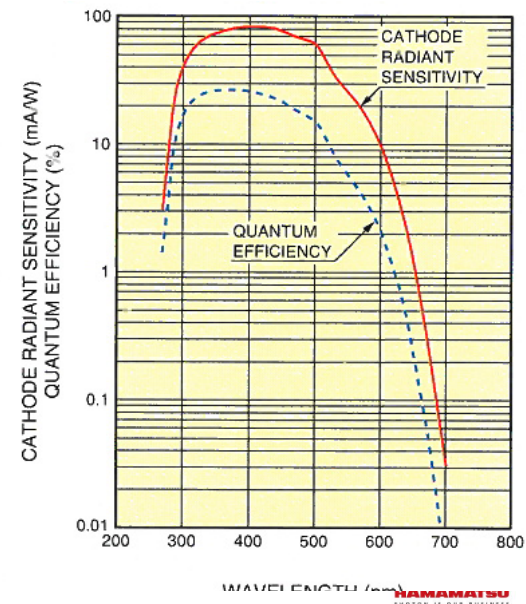
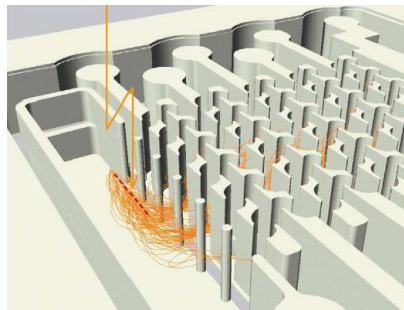
Gain = $1E+06$ (Gain is adjustable by request)

Cathode Blue Sensitivity = around 11

(SBA type could be available in future)

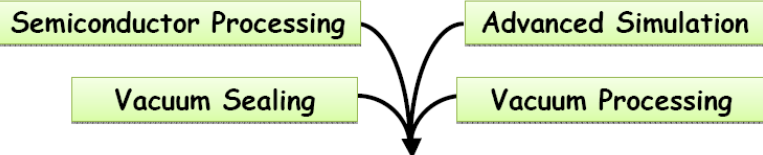


Silicon PMT



Technologies for Micro-PMT

Unification of Key technologies



Photon Sensor with New Concept

Main characteristics

- Effective Area: 3.5 mm x 1 mm
- Quantum Efficiency: 26 % at peak
- Gain (with 12-stage): 1E+06 at ~1000V
- Rise Time: around 1.2 ns
- Single Photon Counting Ability

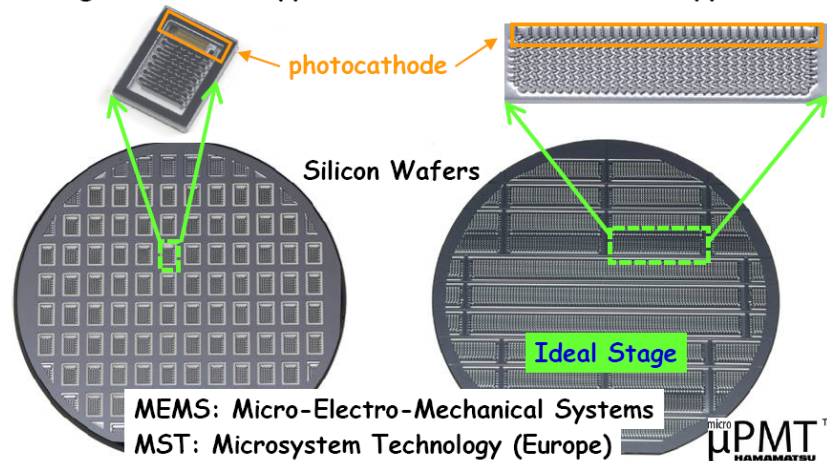
Sample (with assembly) is available.



Micro-PMTs come from Si Wafers !!

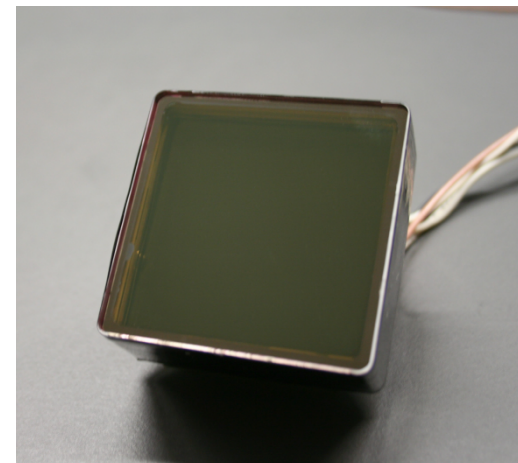
Single Channel Type

Multi Channel Type





BURLE



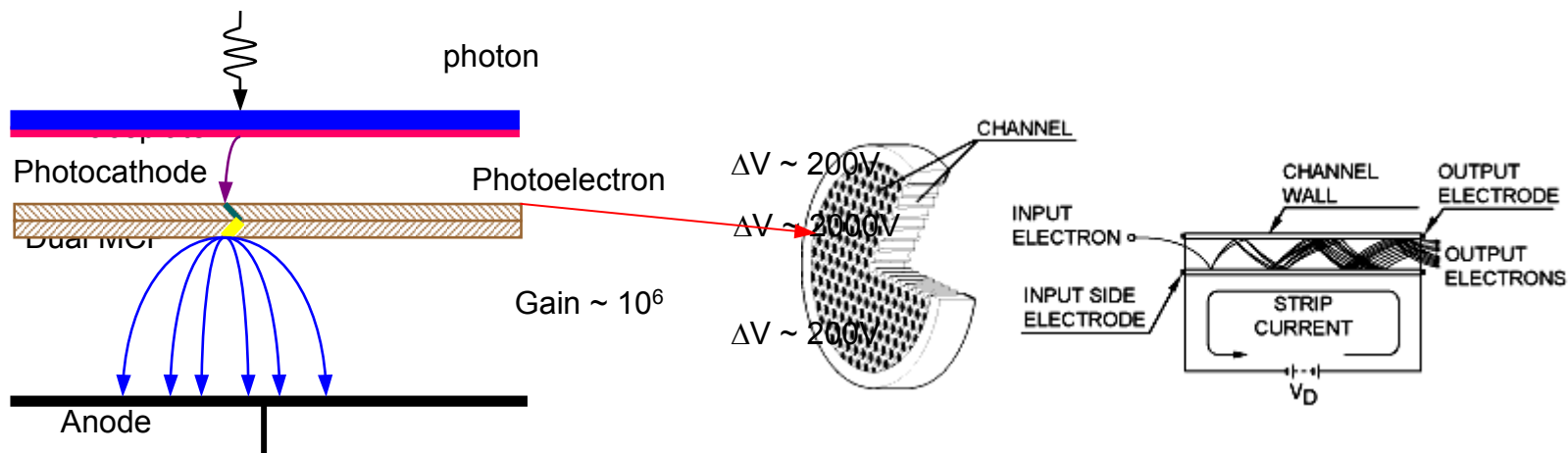
HAMAMATSU
PHOTON IS OUR BUSINESS



R&D in Research Institutes (BINP, Russia –
IEHP, China – LAPP collaboration, USA -, ...)

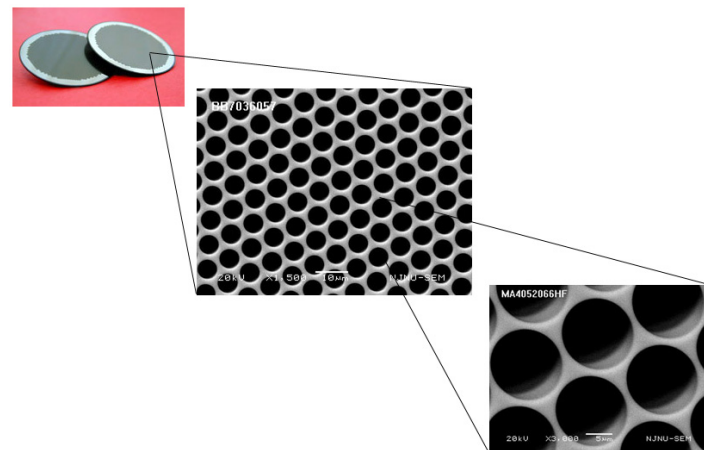


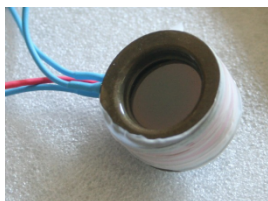
Photodetector multiplication chain = Micro Channel Plate



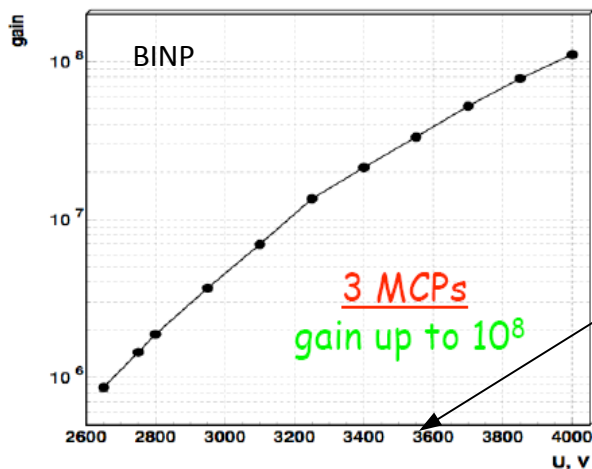
array of holes (10-100 μ m diameter) in a glass plate

- high gain: $\rightarrow 10^7$ with 3 MCP stages
 \rightarrow single photon sensitivity
- very fast time response:
 - \rightarrow signal rise time = 0.3 – 1.0 ns
 - \rightarrow TTS < 50 ps
- quantum efficiency comparable to that of standard PMT
- multi-anode available
- lifetime (QE drops)
- price





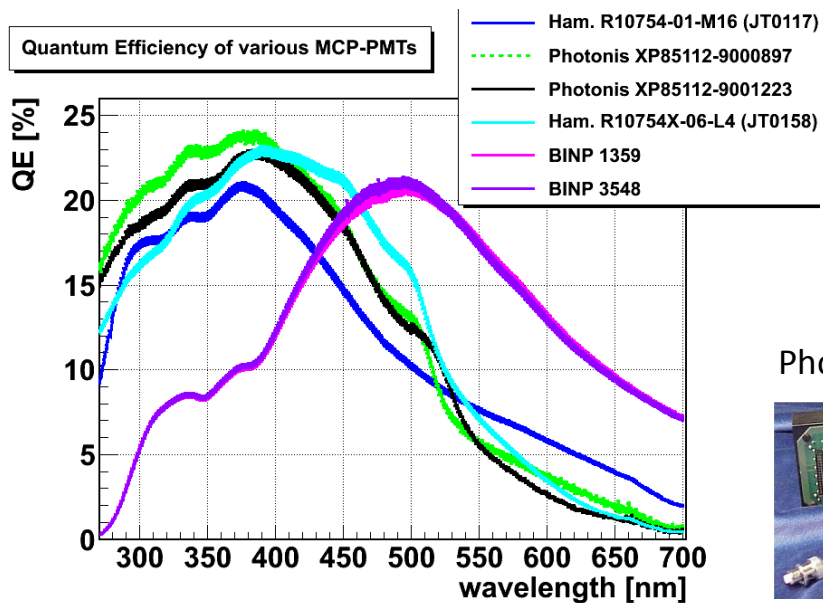
BINP



M. Barnyakov, AFAD 2013

MCP-PMT bias voltage > PMT bias voltage

Quantum Efficiency of various MCP-PMTs

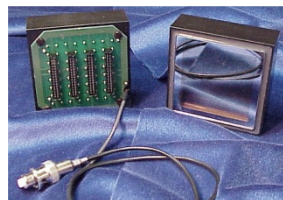


A. Lehmann, Elba Conference 2012

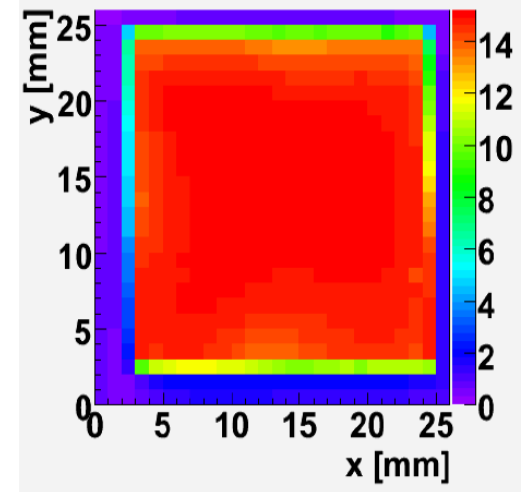


HAMAMATSU

Photonis BURLE



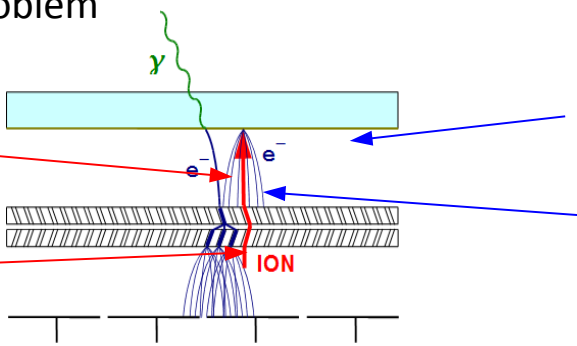
QE homogeneity



T. Inami, TIPP 2011

High photon rate \rightarrow aging problem

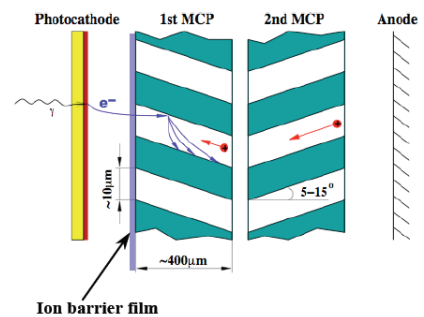
- 2 travel back toward the photocathode
- 1 ionisation of atoms of residual gas



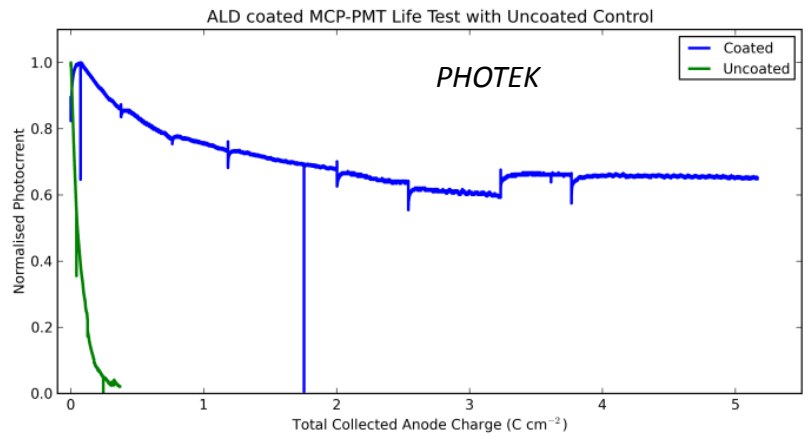
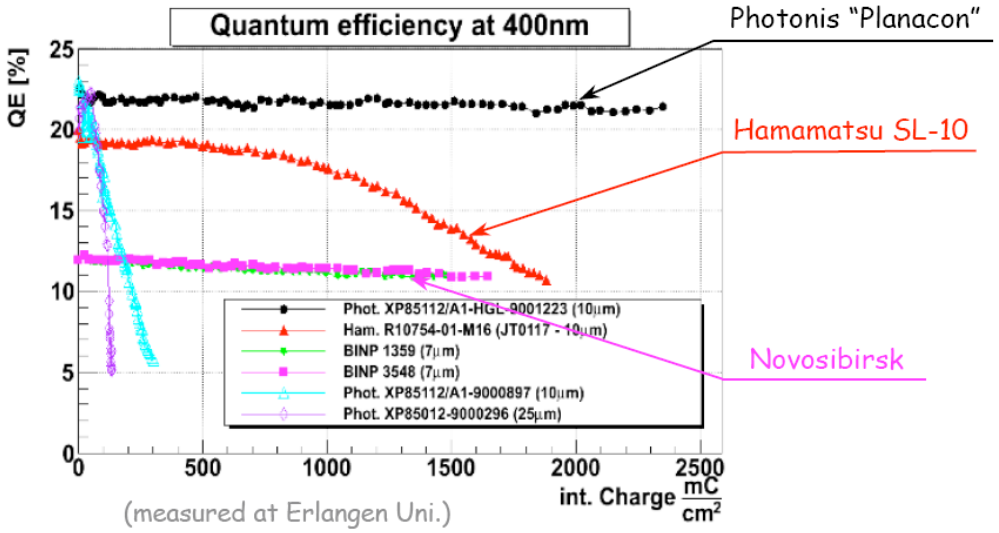
- 3 ion bombardment \rightarrow damages the photocathode \rightarrow reduces the Q ϵ
- 4 production of secondary pulses

Different ways of improvement (depending on the producer):

- Protection layer on the photocathode
- Improvement of the vacuum
- Treatment of the MCP surfaces (atomic layer deposition)
- New photo cathode



A. Lehmann, Elba Conference 2012



T M Conneely, PHOTEK



MCP-PMT time response

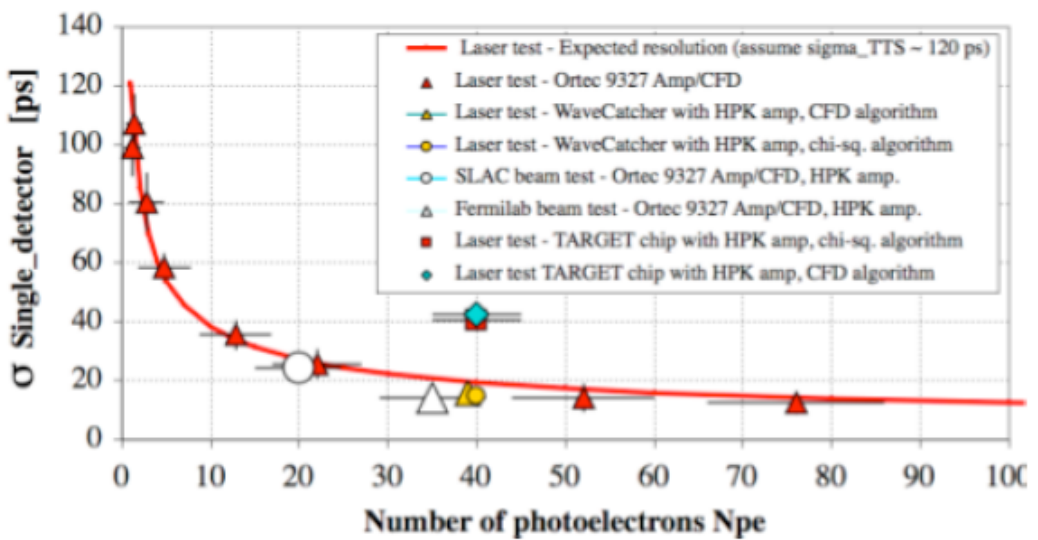


J. Vavra, SLAC-Pub-14279

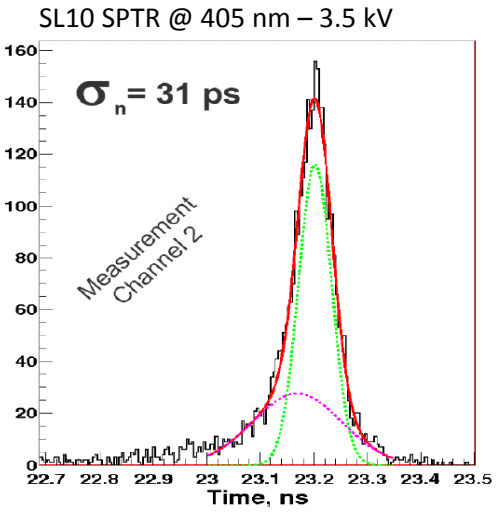
high electric field between PC and MCPin and MCPout and anode → negligible effect of the angle distribution of the p.e

e- transit time in the secondary multiplication process very short

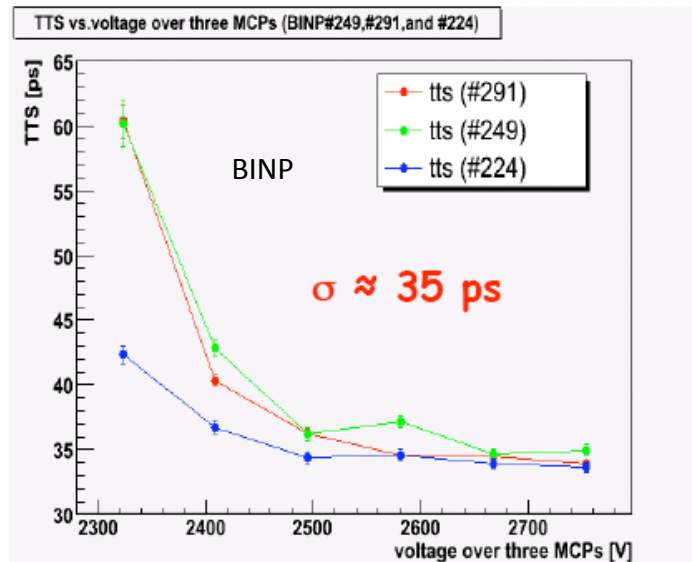
→ very good TTS



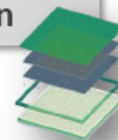
Single Photoelectron Timing resolution



L. Burmistrov, LAL

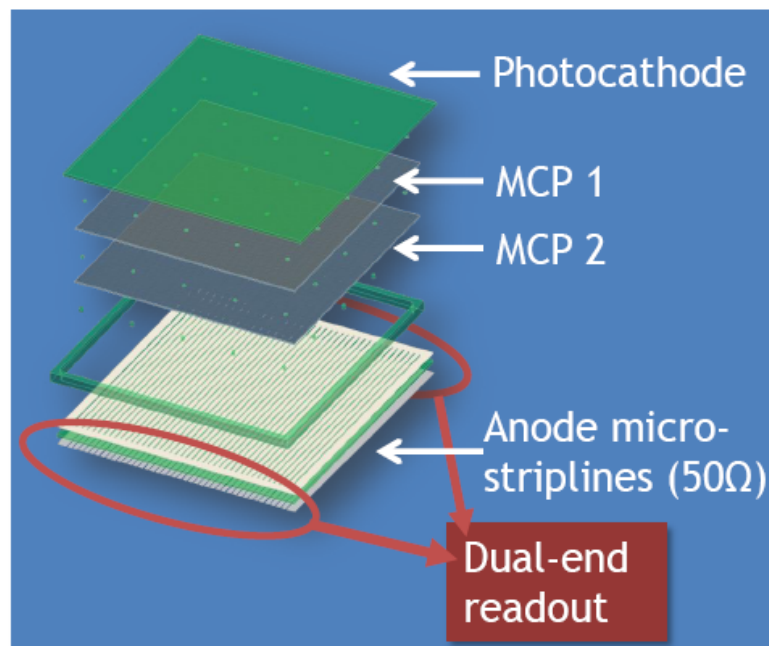
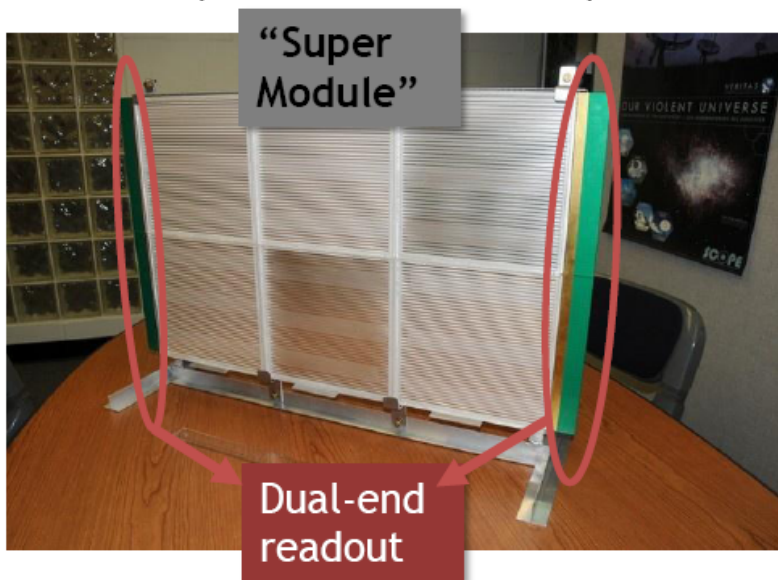


A. Yu. Barnyakov, NIMA 598



The LAPPD project

- Development of large-area, relatively inexpensive Micro-Channel Plate (MCP) photo-detectors
 - 8" x 8" phototubes = 'tile' (large active area)
 - Gain $\geq 10^6$ with two MCP plates
 - Transmission line readout – no pins!
 - Fast pulses + low TTS ~ 30 ps



High photon detection efficiency

+

Single photoelectron Detection

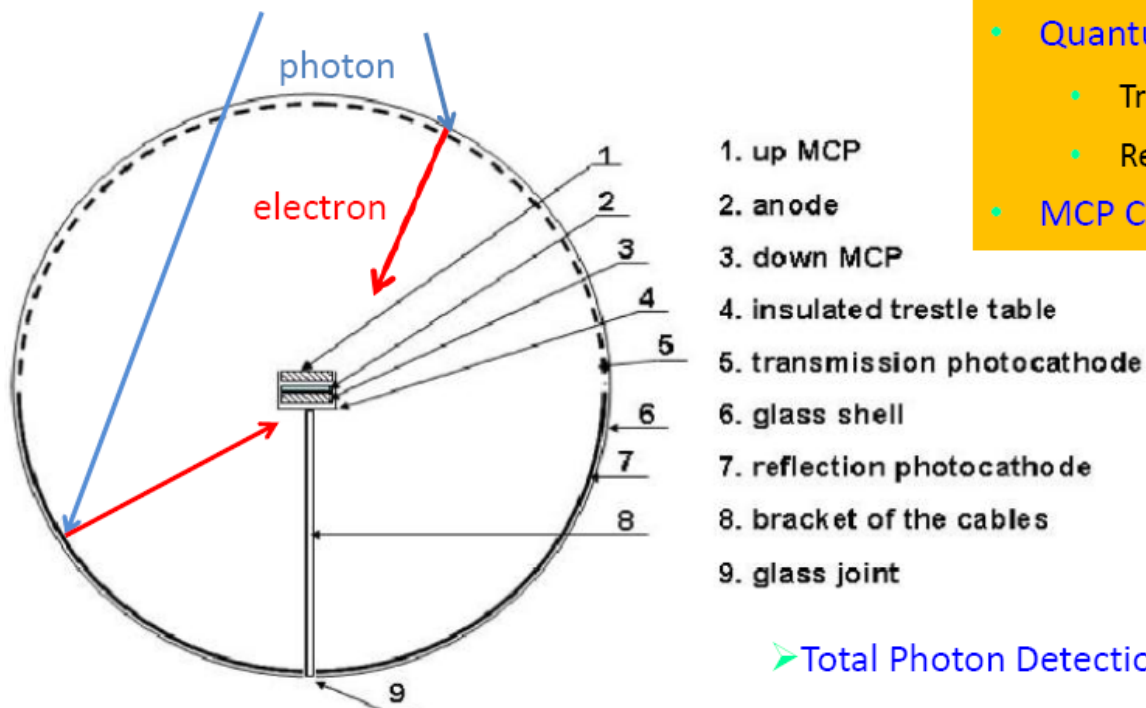
+

Low cost

1) Using two sets of Microchannel plates (MCPs) to replace the dynode chain

2) Using transmission photocathode (front hemisphere) and reflective photocathode (back hemisphere)

} ~ 4π viewing angle!!



1. up MCP
2. anode
3. down MCP
4. insulated trestle table
5. transmission photocathode
6. glass shell
7. reflection photocathode
8. bracket of the cables
9. glass joint

• Quantum Efficiency:

- Transmission photocathode: 20%
- Reflection photocathode: 40%

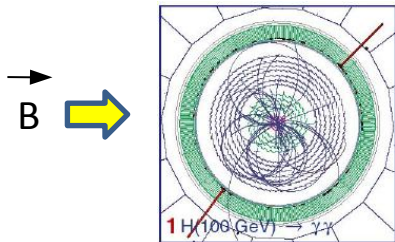
• MCP Collection Efficiency: 60%



➤ Total Photon Detection Efficiency: ~30%

2012/6/13 Photon Detection Efficiency: 14% → 30% ; × ~2 at least !

★ earth magnetic field = 30-60 mT



curves the trajectory of charges particles



separate the particles



easier analysis



reduce the detector size



reduce the detector price

PMT

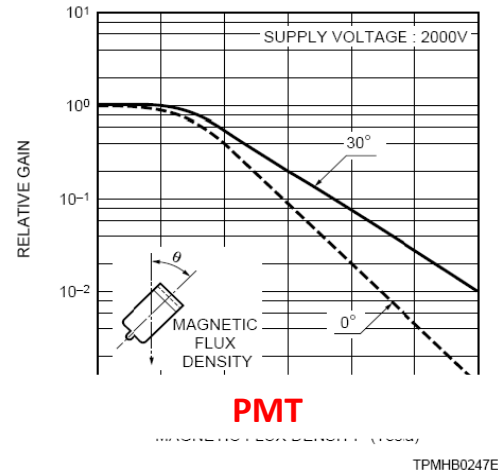
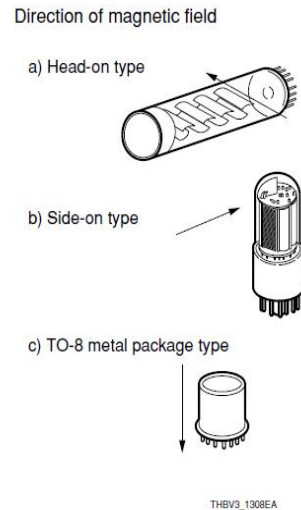
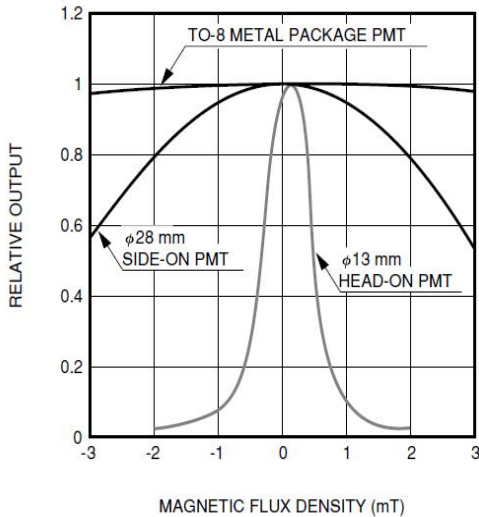
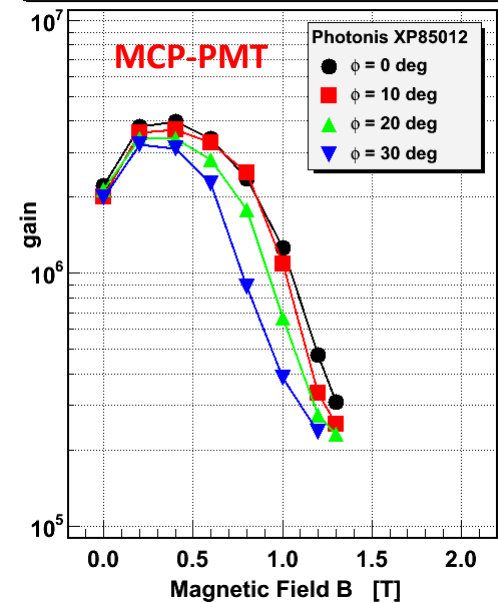


Figure 6-25: Gain vs. magnetic flux density

Gain Dependence on Tilt Angle ϕ



Albert Lehmann RICH 2010

Figure 13-8: Magnetic characteristics of typical photomultiplier tubes

HAMAMATSU PMT book

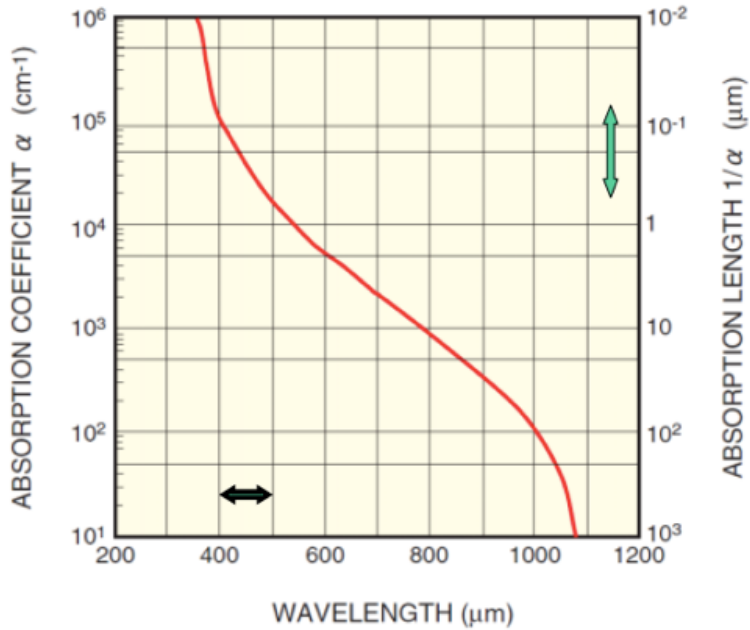
PMT very sensitive to magnetic field → shielding required (μ metal)

A decorative vertical element on the left side of the slide, consisting of numerous thin, overlapping lines in various colors (red, orange, yellow, green, blue, purple) that create a shimmering, fiber-optic-like effect.

Silicon Photo Multiplier



Internal photoelectric effect in Si



Beer-Lambert law $I(\lambda, z) = I(\lambda)e^{-\alpha(\lambda)z}$

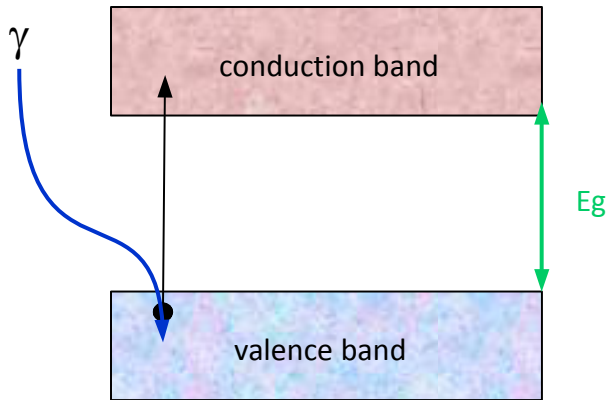
$I(\lambda)$: initial photon flux

$I(\lambda, z)$: photon flux on the distance z from SiPM surface

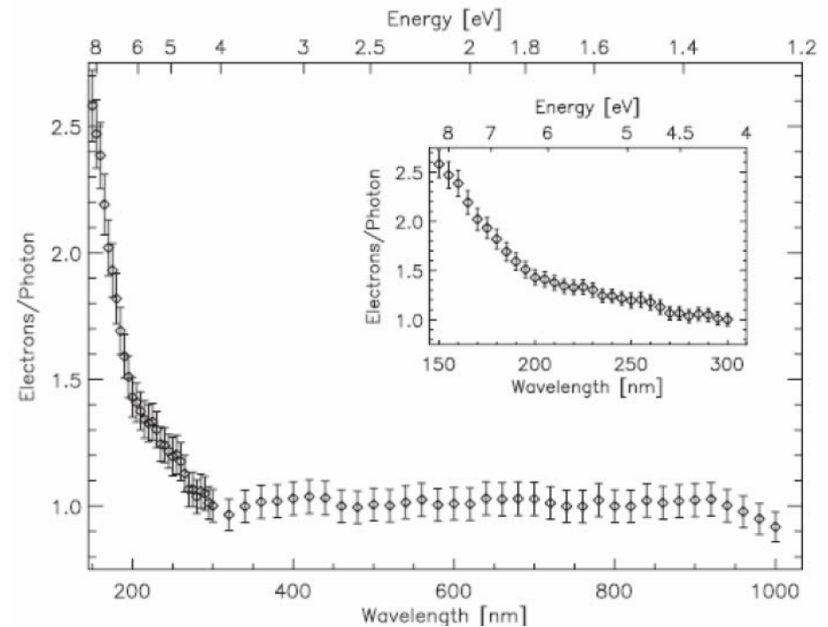
$\alpha(\lambda)$: optical absorption coefficient

z : penetrated thickness in Si

Number of electron / incident photon as a function of λ

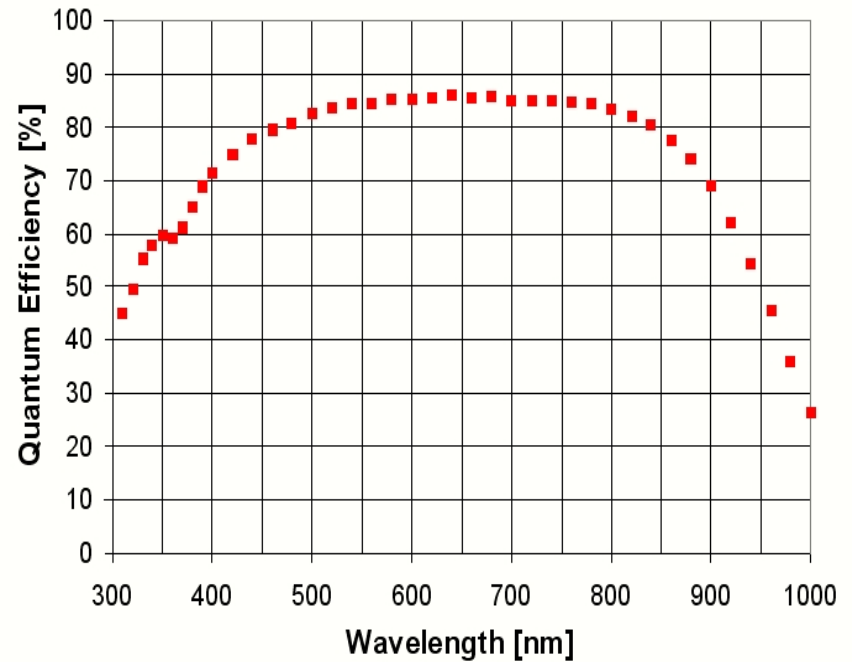
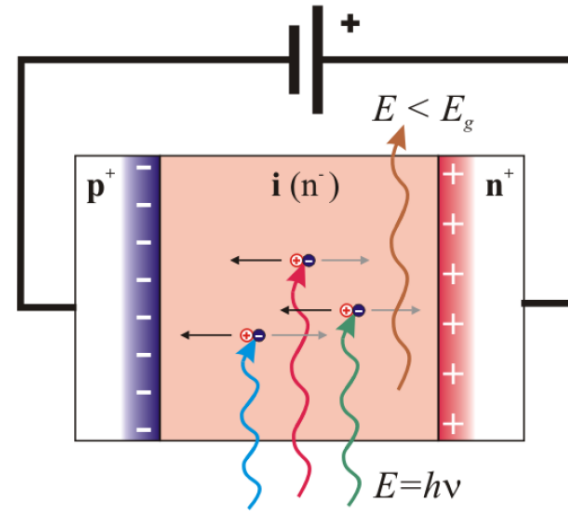
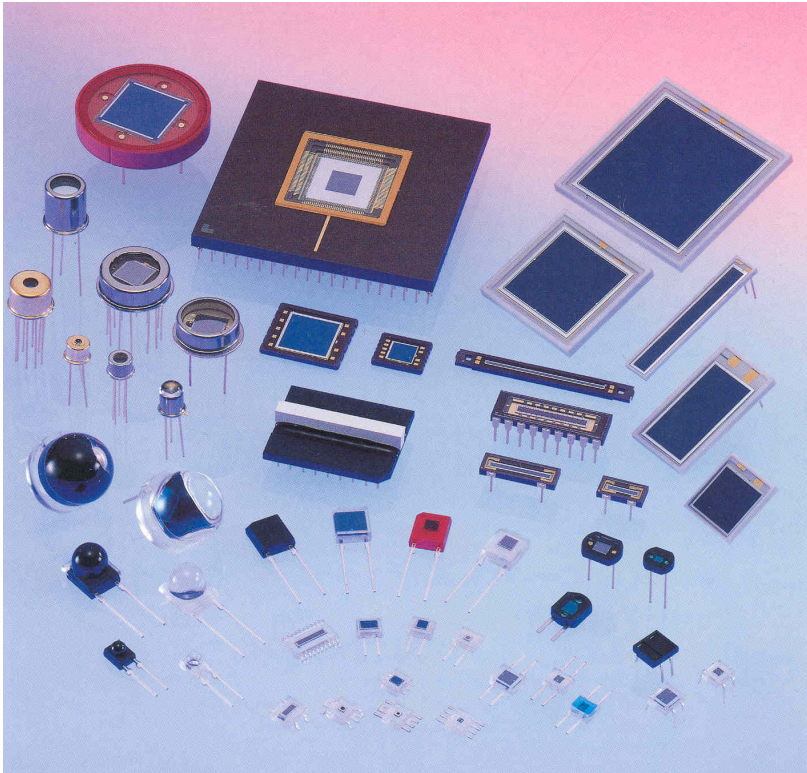


Band gap (T=300K) = 1.12 eV (~1100 nm)





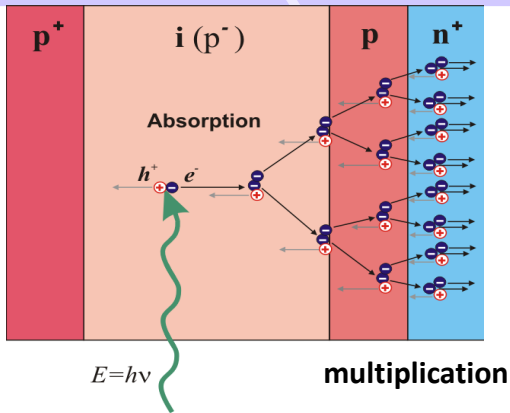
The Pin photodiode



➤ p layer very thin ($< 1 \mu\text{m}$)

➤ high QE (80% @ 700nm)

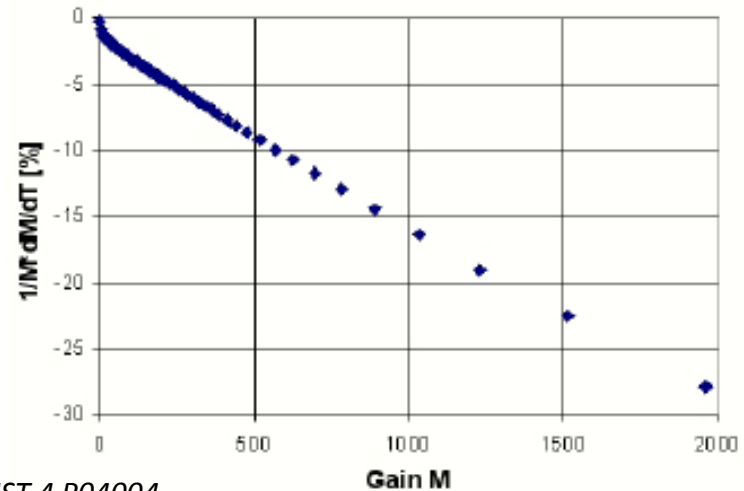
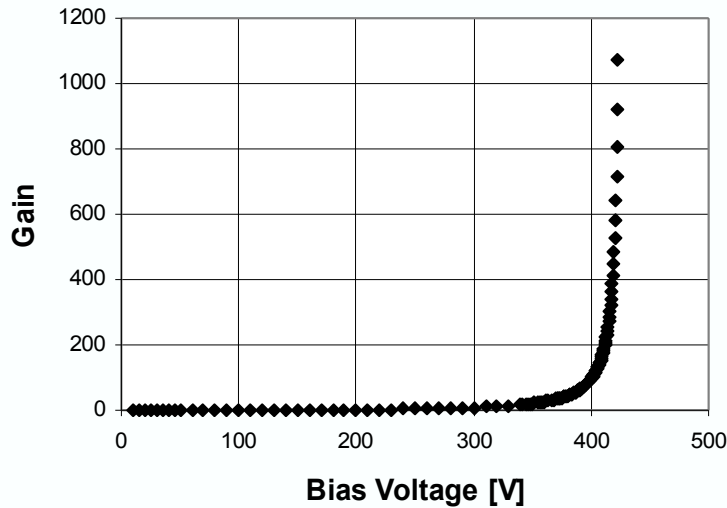
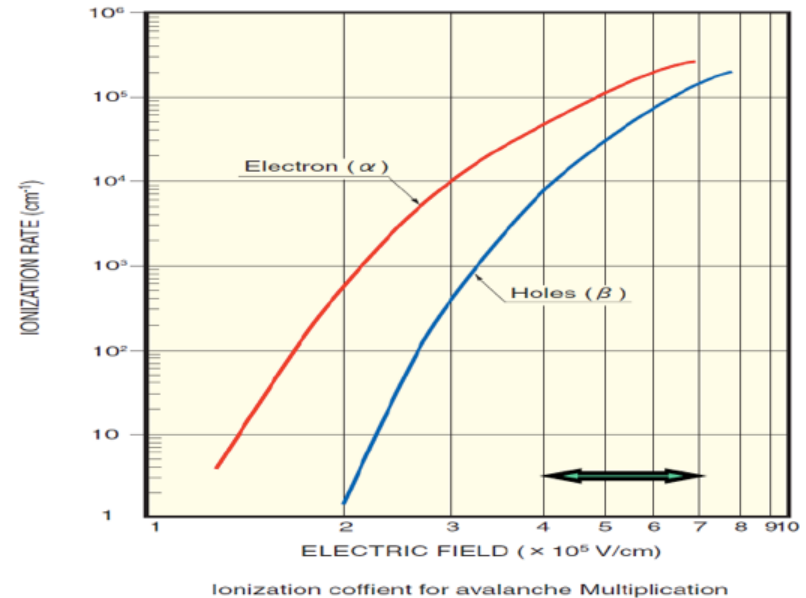
➤ Gain = 1



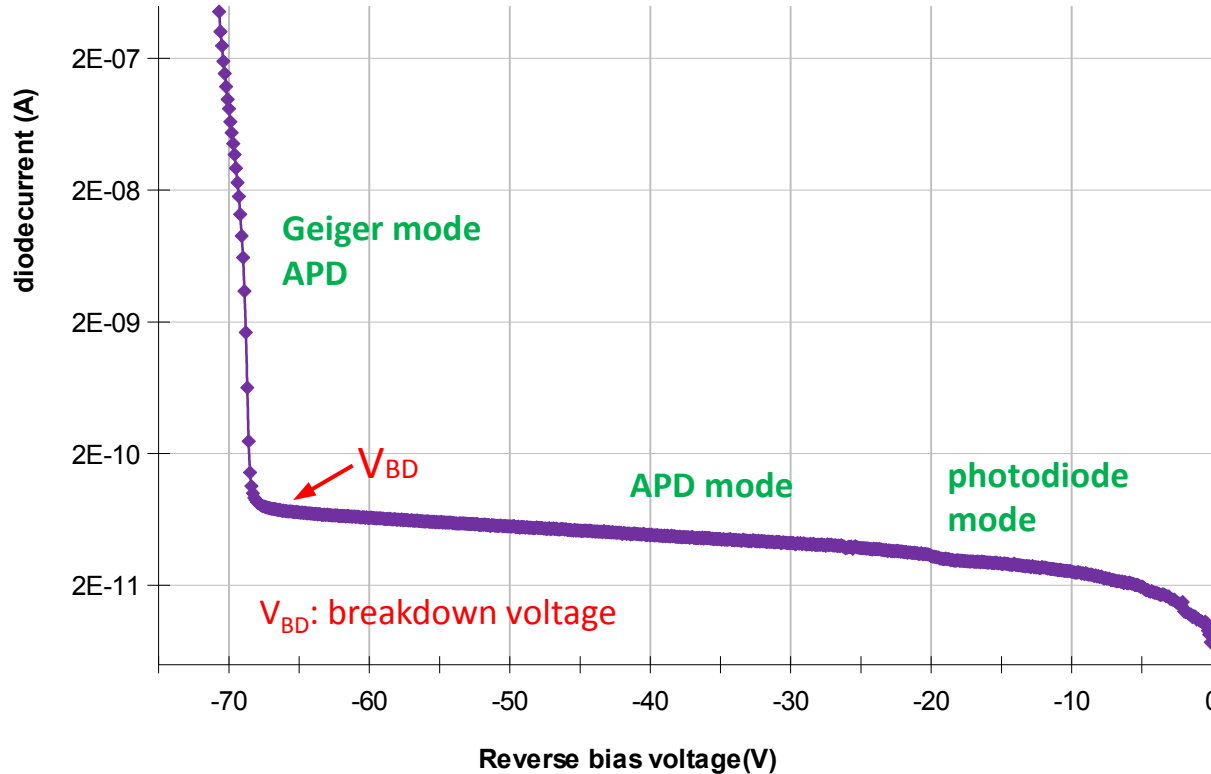
Bias voltage : few 100 V

- high QE (80% @ 700nm)
- Gain = 50 – 100
- high variation with temp. and bias voltage : $\Delta G = 3.1\%/V$ and $-2.4\%/K$

Ionization coefficients α for electrons and β for holes

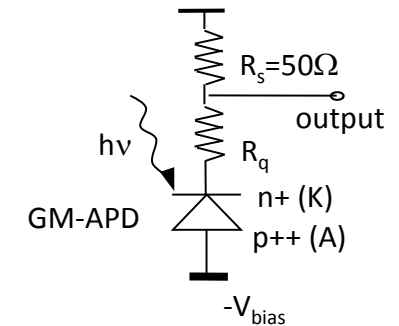
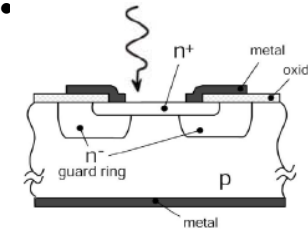


D. Renker, 2009 JINST 4 P04004



Geiger mode -APD

- $V_{bias} > V_{BD}$
- $G \Rightarrow \infty$
- single photon level

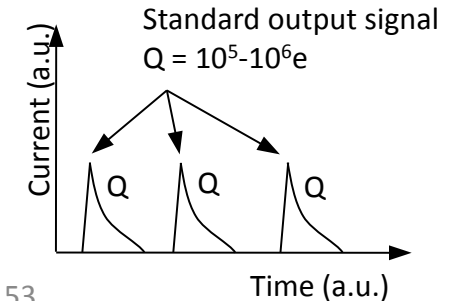


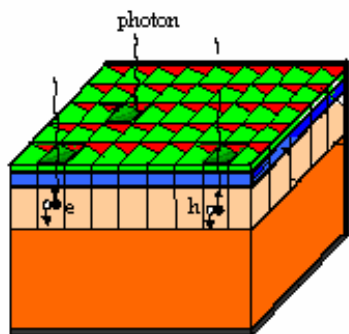
Photodiode

- $0 < V_{bias} < V_{APD}$ (few volts)
- $G = 1$
- Operate at high light level (few hundreds of photons)

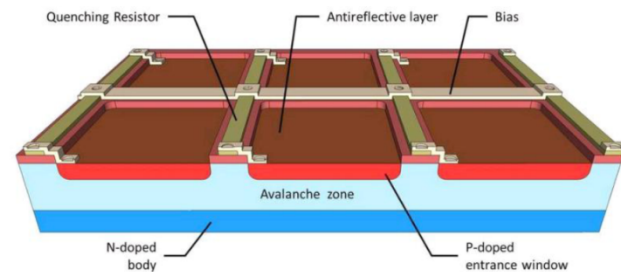
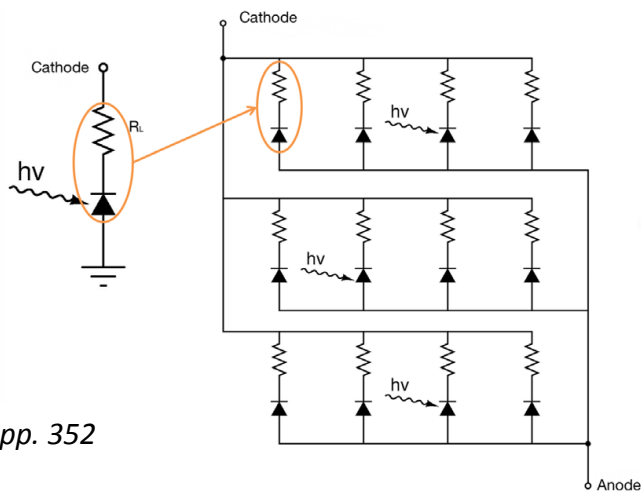
APD

- $V_{APD} < V_{bias} < V_{BD}$
- $G = M$ (50 - 100)
- Linear-mode operation



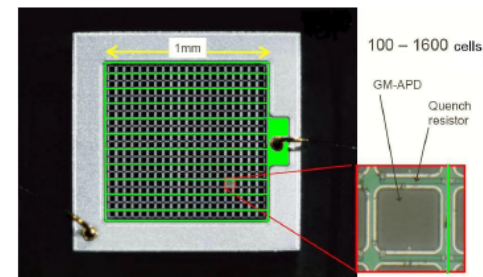


- # Microcells
- # Q.Elements
- n+
- p
- p+



Valeri Saveliev, ISBN 978-953-7619-76-3, pp. 352

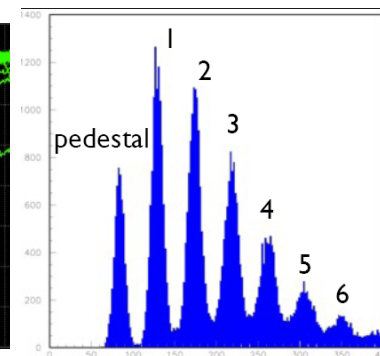
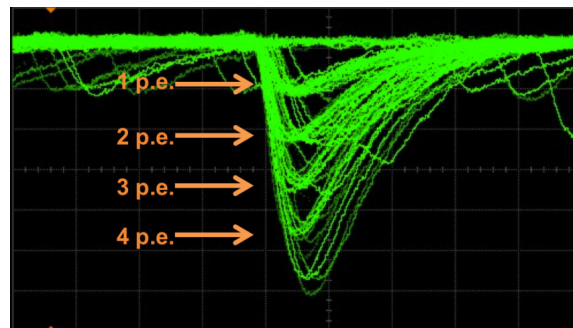
- ✓ GM-APDs (pixel) connected in parallel (few hundreds/mm²)
- ✓ Each cell is reverse biased above breakdown
- ✓ Self quenching of the Geiger breakdown by individual serial resistors



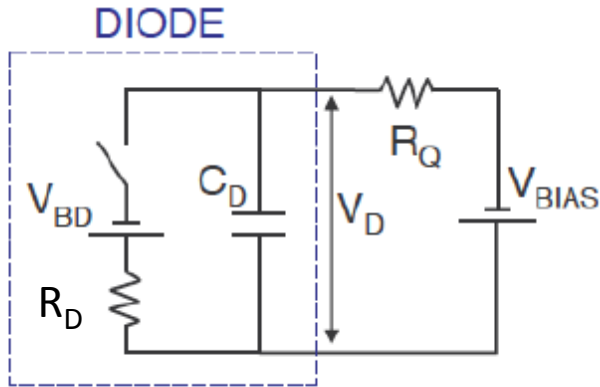
Each element is independent and gives the same signal when fired by a photon



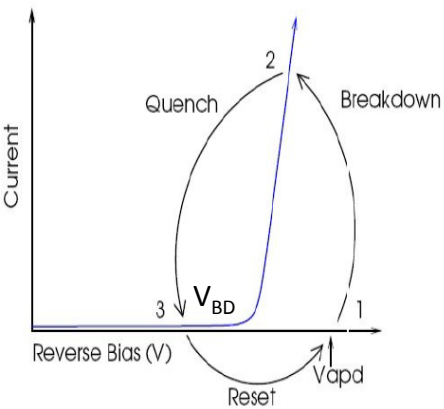
output charge is proportional to the number of incident photons



G. Bisogni, RESMDD10



V_{BD} : breakdown voltage
 R_Q : quenching resistance
 R_D : diode resistance
 C_D : diode capacitance
 V_{BIAS} : bias voltage

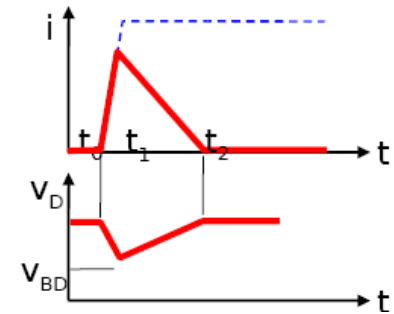


1 → 2 : avalanche triggered, switch closed
 C_D discharges to V_{BD} with the time constant $\tau = R_D \times C_D$
 asymptotic growth of the current

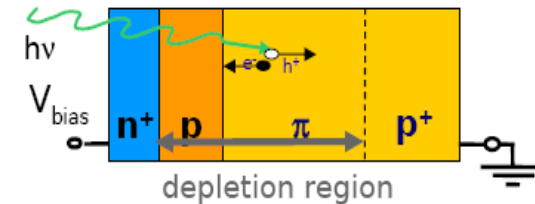
2 → 3 : avalanche quenched, switch open
 capacitance charged until no current flowing with the time constant $\tau' = R_Q \times C_D$

3 → 1 : reset of the system. The carrier traversing the high-field region triggers the avalanche

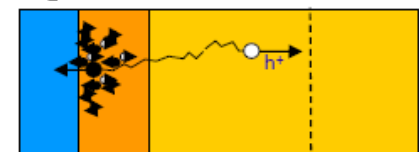
Time sequence



$t=0$: carrier initiates the avalanche

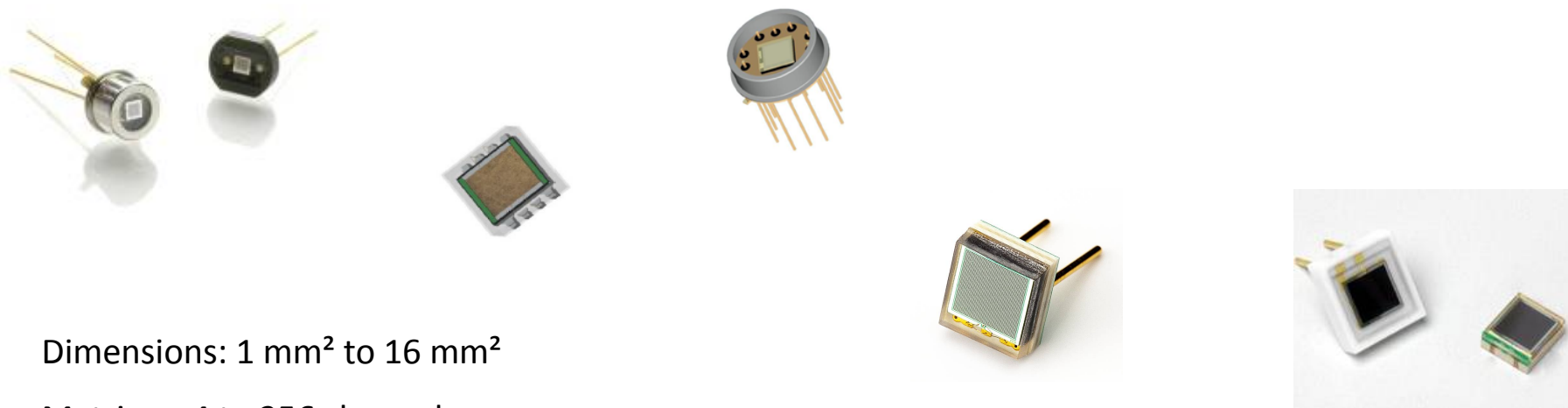


$0 < t < t_1$: avalanche spreading



$t_1 < t$: self-sustaining current limited by series R

G. Collazuol, LIGHT11

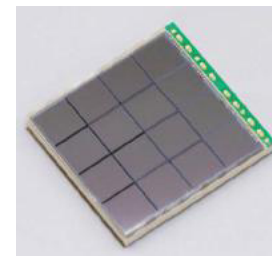
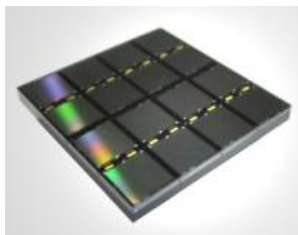
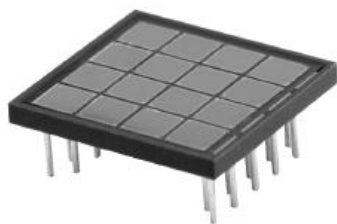


Dimensions: 1 mm² to 16 mm²

Matrixes: 4 to 256 channels

Pixel size: 15 μm, 25, ..., 100 μm

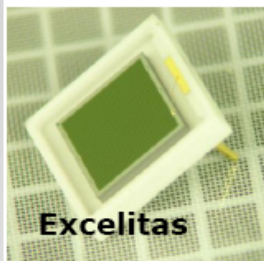
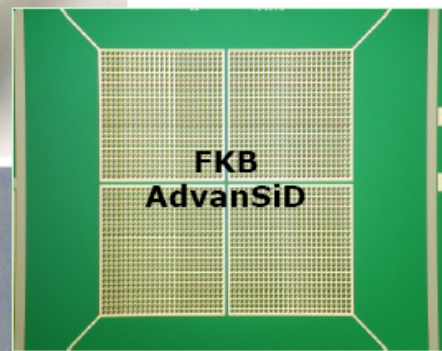
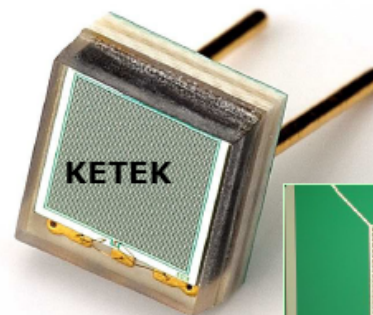
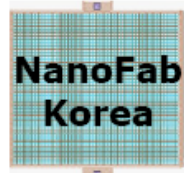
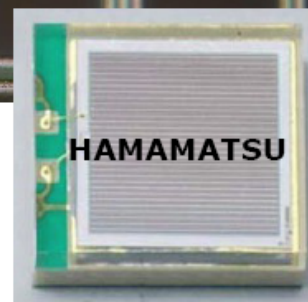
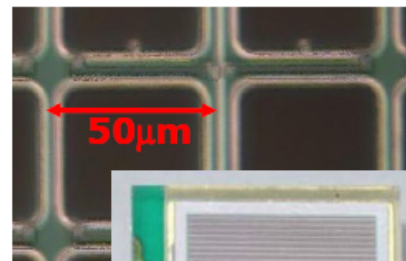
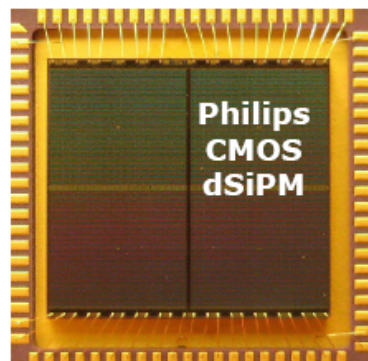
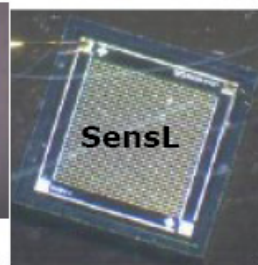
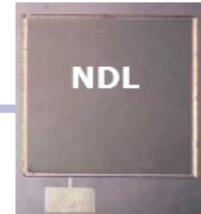
Packaging: metal (TO8), ceramic, plastic, with pins, surface mount type, matrix (wire bonding, TSV (Through Silicon Via))



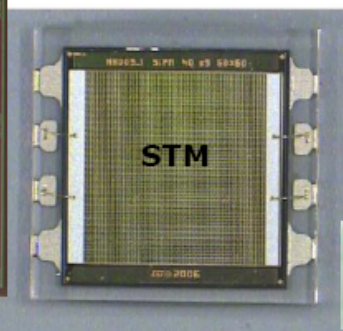
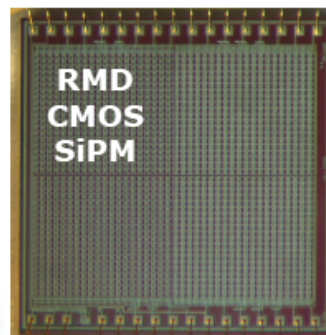
Producers of SiPMs

Many institutes/companies are involved in SiPM development/production:

- **CPTA**, Moscow, Russia
- **MePhi/Pulsar Enterprise**, Moscow, Russia
- **Zecotek**, Vancouver, Canada
- **Hamamatsu HPK**, Hamamatsu, Japan
- **FBK-AdvanSiD**, Trento, Italy
- **ST Microelectronics**, Catania, Italy
- **Amplification Technologies** Orlando, USA
- **SensL**, Cork, Ireland
- **MPI-HLL**, Munich, Germany
- **RMD**, Boston, USA
- **Philips**, Aachen, Germany
- **Excelitas tech.** (formerly Perkin-Elmer)
- **KETEK**, Munich, Germany
- **National Nano Fab Center**, Korea
- **Novel Device Laboratory (NDL)**, Beijing, China
- **E2V**
- **CSEM**



Amplification Technologies (DAPD)



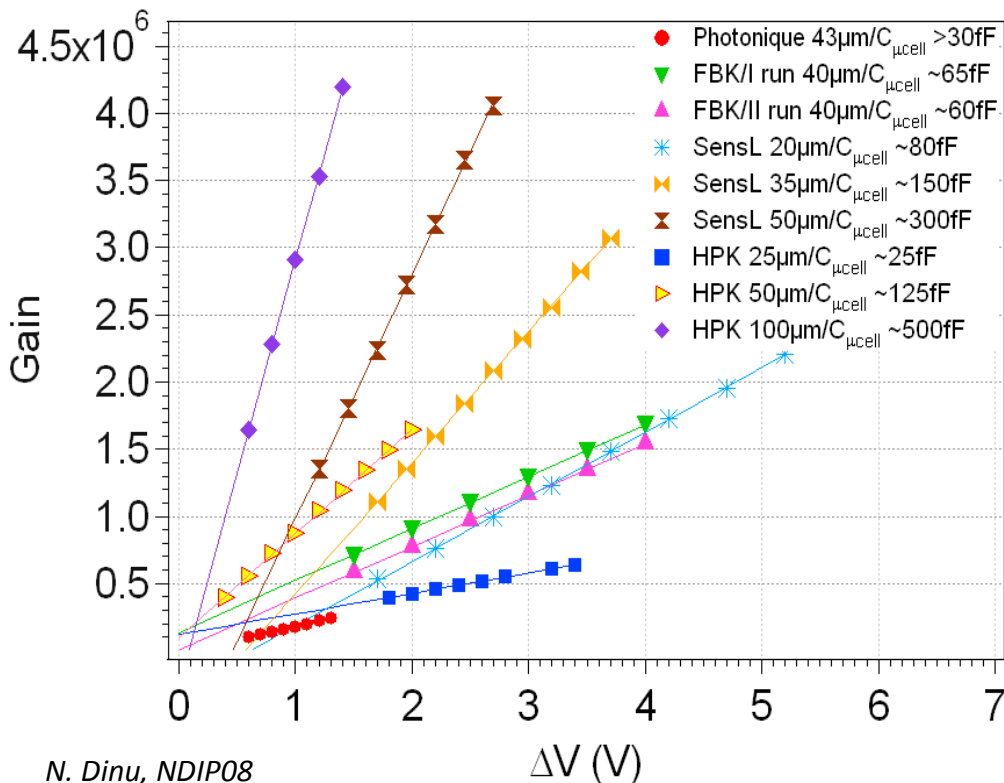
G.Collazuol - PhotoDet 2012

many names like Silicon PM (SiPM), Geiger APD (G-APD), Metal Resistive layer Semiconductor (MRS-APD), Multi Photon Pixel Counter (MPPC), SiPM, SPM,... **SiPM is by now the most used name**

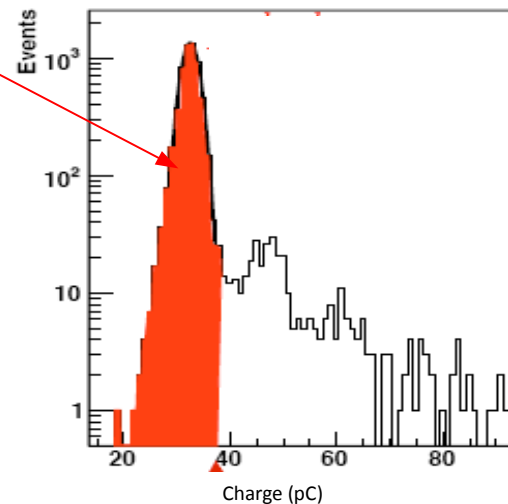
Defined as the charge developed in one pixel by a primary carrier

$$\text{Gain} = \frac{Q_{\text{pixel}}}{e} = \frac{C_{\text{pixel}} \times (V_{\text{bias}} - V_{\text{BD}})}{e}$$

Gain of 1 mm² SiPM (25°C)



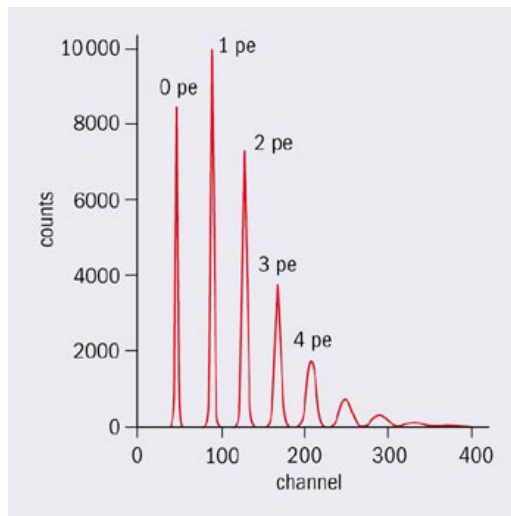
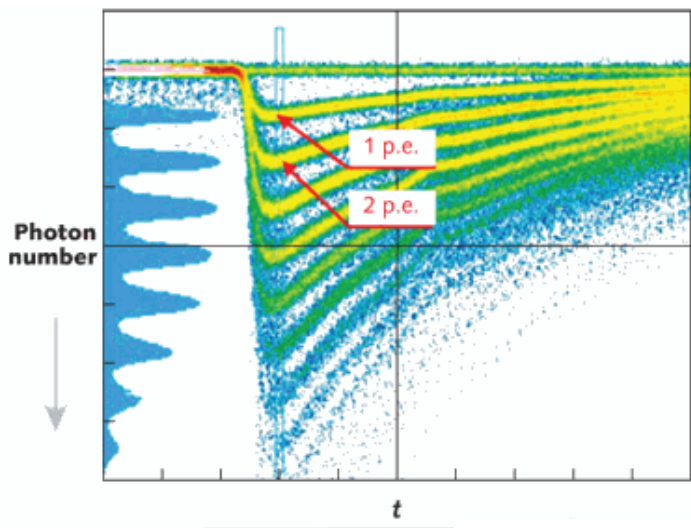
N. Dinu, NDIP08



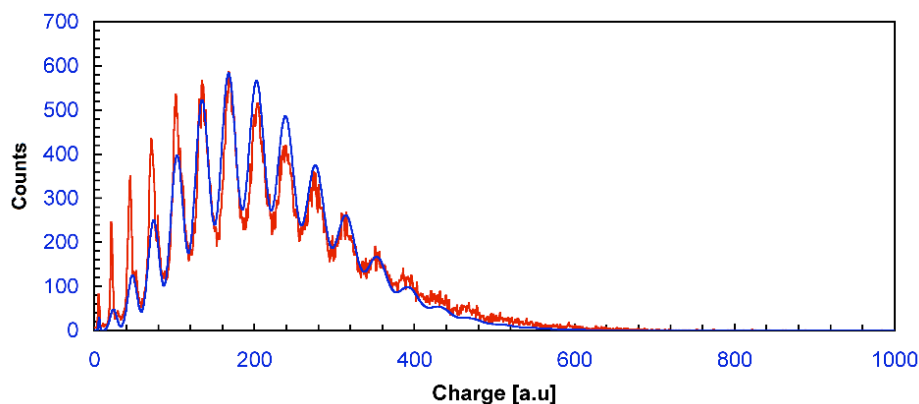
$10^4 < \text{Gain} < 10^6$

- linear increase of the gain with V_{bias}
- slope of the linear fit of G as a function of V_{bias}
→ pixel capacitance (tens to hundreds of fF)
- increase of the gain with the pixel dimensions

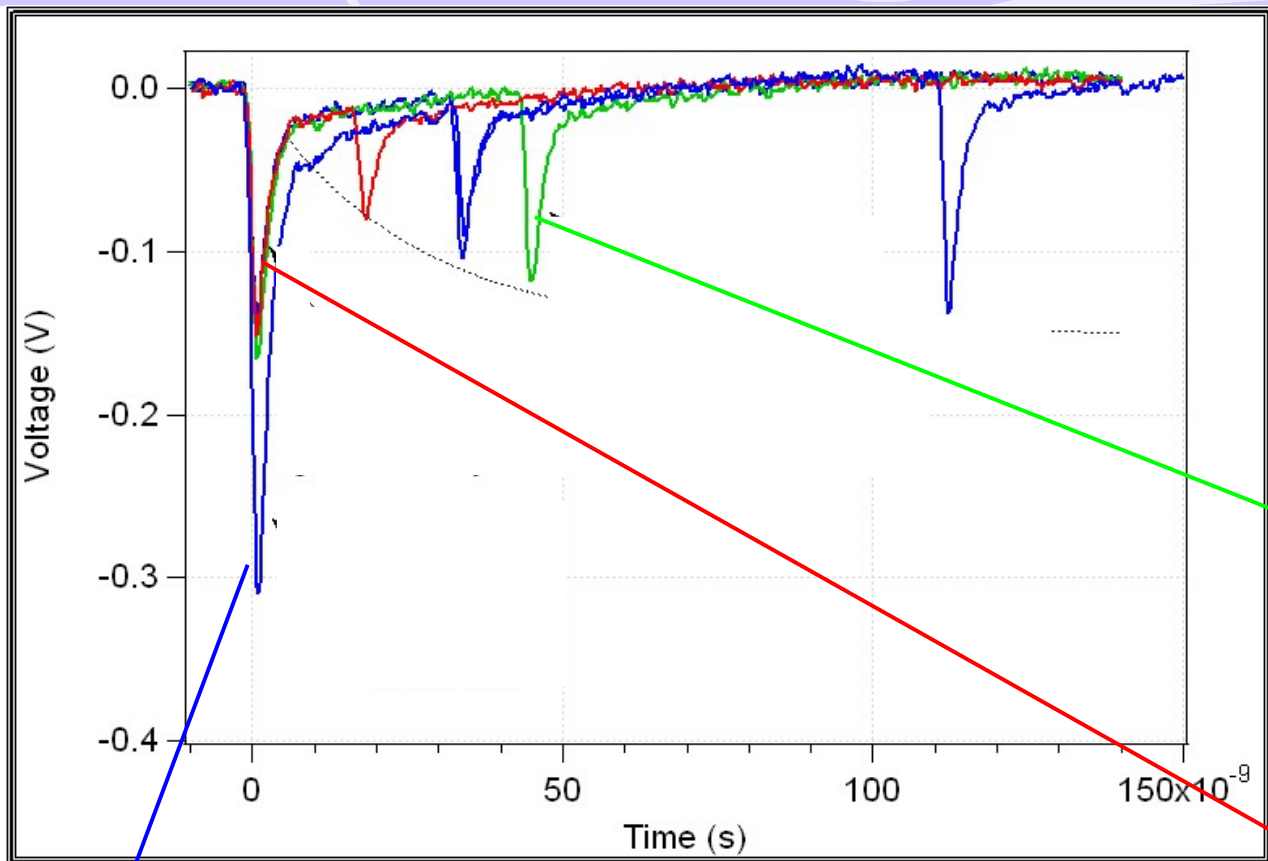
The resolution of SiPM allowed very precise analysis of the detecting photon flux up to single photon



100c-69.7V-1.0%



Single photons are well separated in a wide range



Cross-talk : amplitude = 2 p.e

avalanche in one pixel → proba that a photon triggers another avalanche in a neighboring pixel without delay

After-pulses

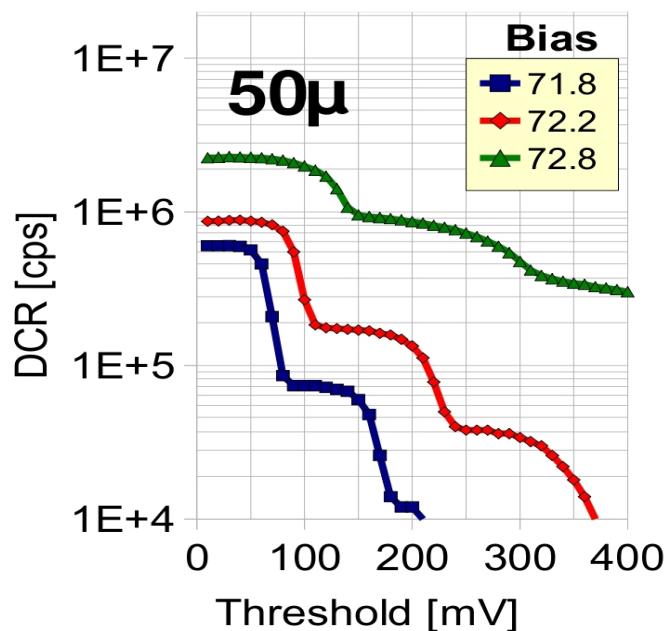
carriers trapped during the avalanche can produce delayed secondary pulses

Dark counts

pulses triggered by non-photo-generated carriers (thermal / tunneling generation in the bulk or in the surface depleted region around the junction)

Breakdown triggered by thermally generated carriers → dark counts with a rate of 80 kHz to several MHz /mm² at 25°C when the threshold is set to half of the one photon amplitude.

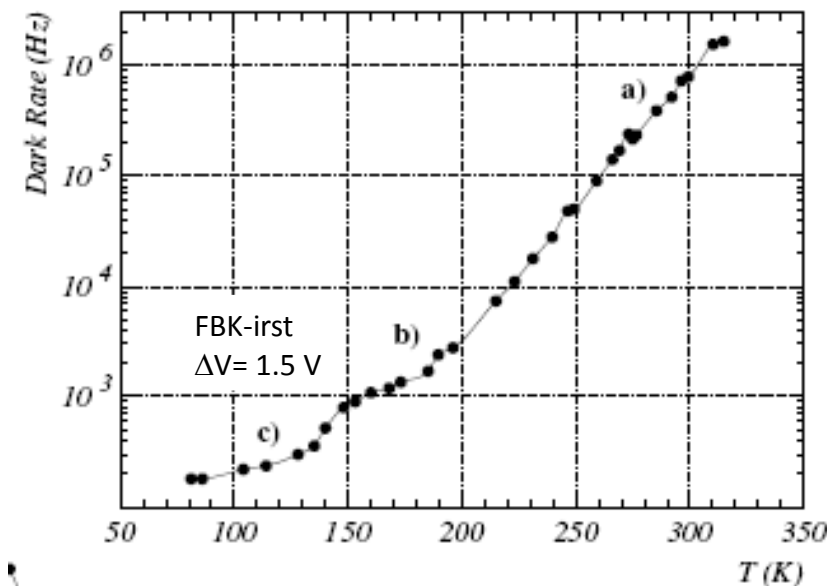
Dark Count vs. Threshold



S. Gundacker, PhotoDet 2012

The dark count rate falls rapidly with increasing threshold with steps that depend on the crosstalk probability

Variation with temperature

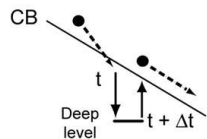


G.Collazuol, NIMA 628

Best way to decrease the Dark Count rate:

- ✓ operate the SiPM at lower gain
- ✓ cooling (factor 2 reduction of the dark counts every 8°C)

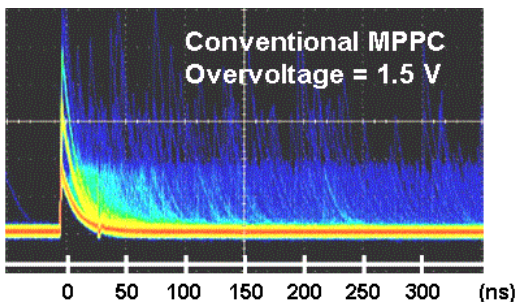
Breakdown → plasma → filling of the traps



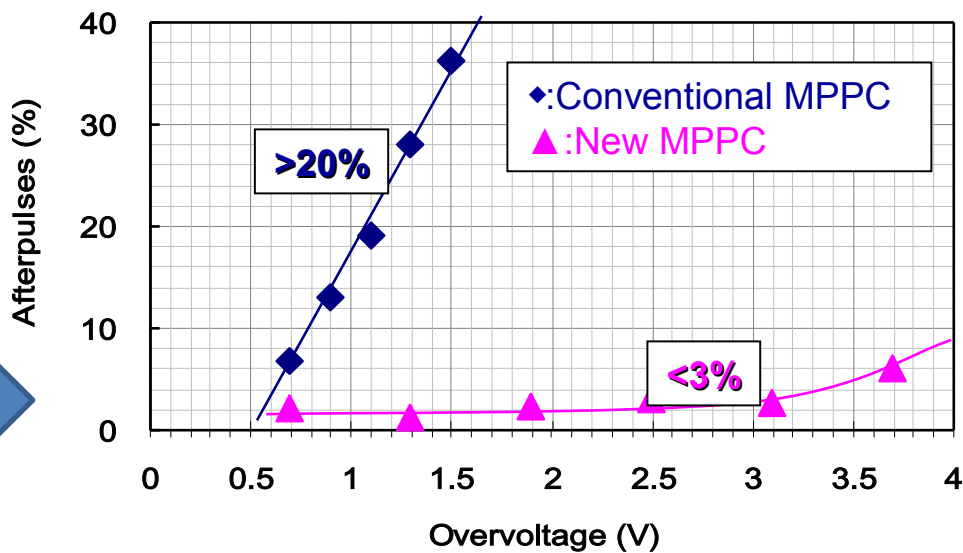
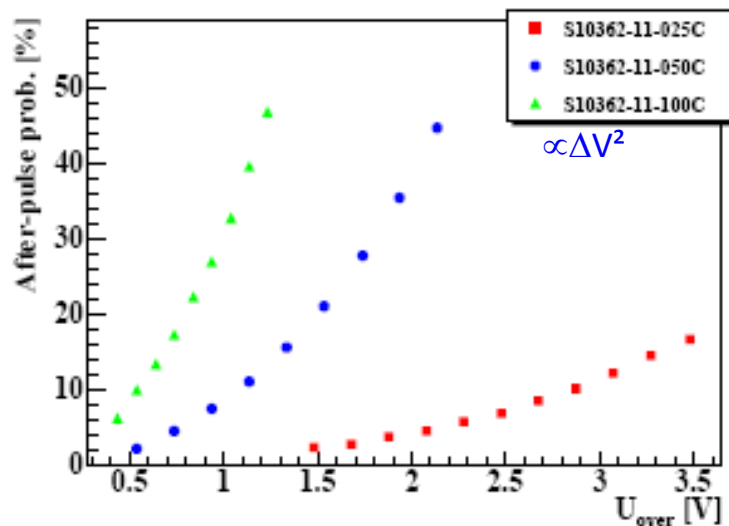
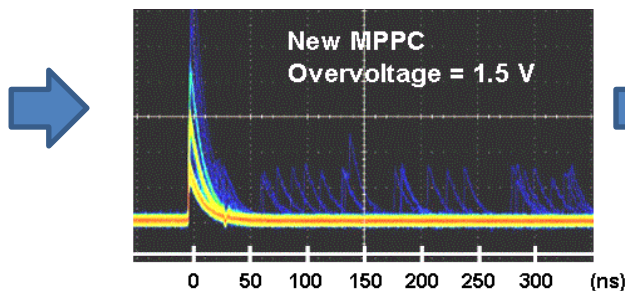
trapping + delayed release → afterpulse

$$P_{\text{afterpulse}}(t) = P_{\text{trig}} \times P_{\text{capture}} \frac{e^{-t/\tau}}{\tau}$$

P_{capture} : trap capture proba
 P_{trig} : avalanche triggering proba
 τ : trap lifetime

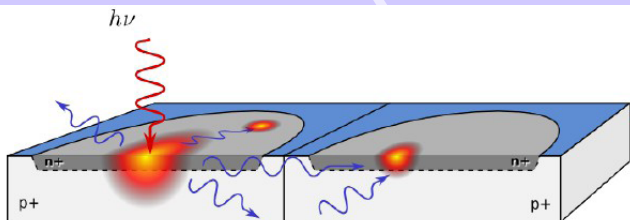


Minimization of the trap levels

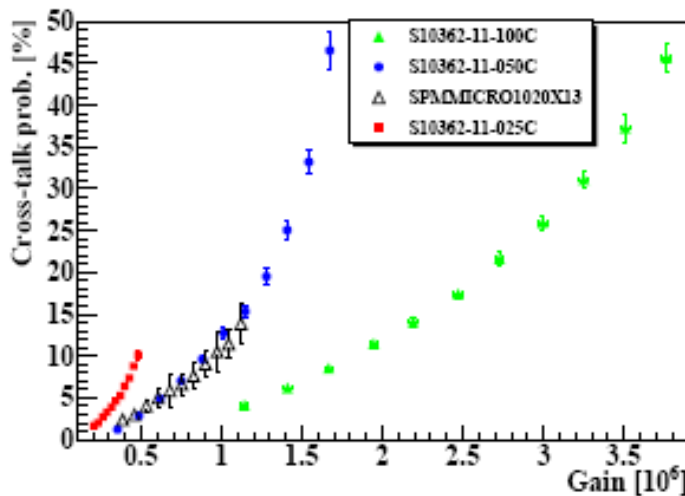


P. Eckert, arXiv:1003.6071v2

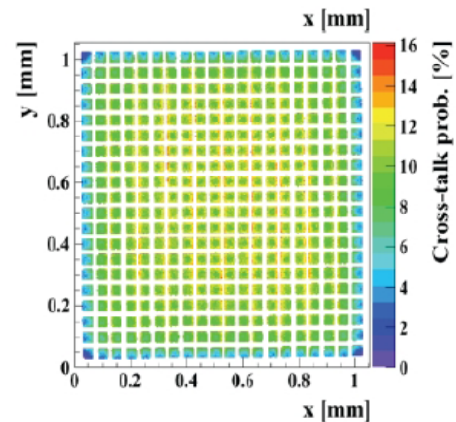
HPK, private communication



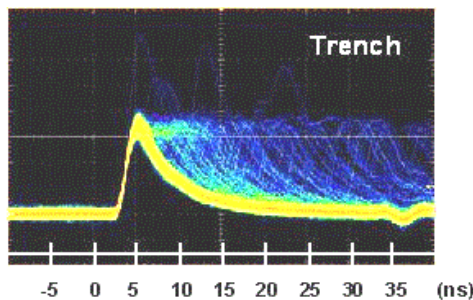
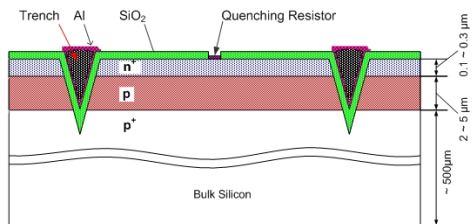
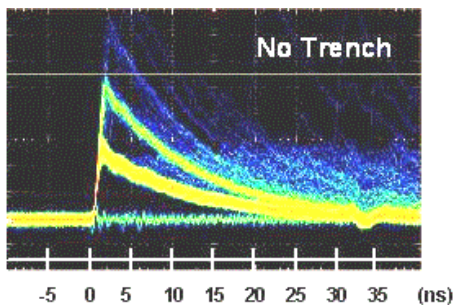
An avalanche in one pixel may produce an optical photon which can trigger another avalanche in a neighboring pixel without delay: probability $3 \cdot 10^{-5}$ / carrier to emit photons with $E > 1.12$ eV



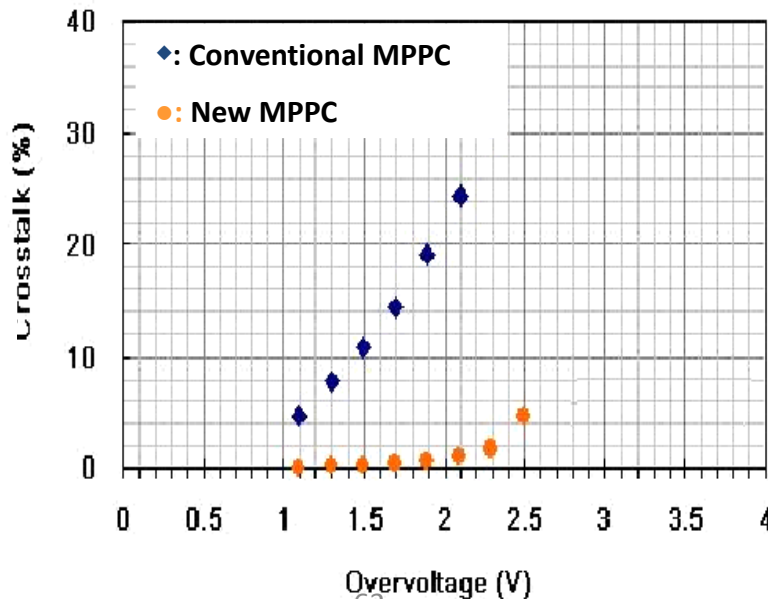
P. Eckert, arXiv:1003.6071v2



A. Tadday, SiPM Workshop DESY 2012



Trenches between pixels



HPK, private communication

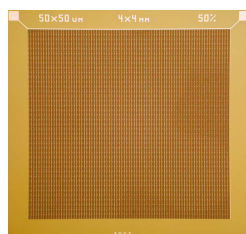
Large SiPMs: large sensitive area but high DCR ...



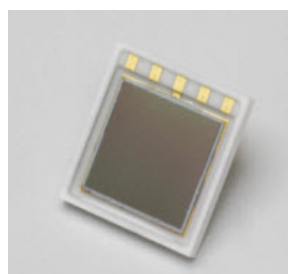
ZECOTEK MAPD-3N



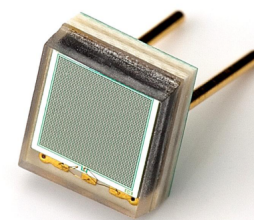
ASD-SiPM4S



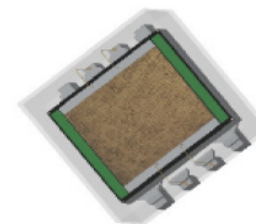
HAMAMATSU S10985



KETEK PM3350



STMicroelectronics



Producer	Reference	Area (mm ²)	PDE max @ 25 °C *	Dark Count Rate (Hz) @ 25°C *	Gain *
ZECOTEK	MAPD-3N	3 x 3	30% @ 480 nm	$9 \cdot 10^5 - 9 \cdot 10^6$	10^5
FBK - AdvanSiD	ASD-SiPM4S	4 x 4	30% @ 480 nm	$5.5 \cdot 10^7 - 9.5 \cdot 10^7$	$4.8 \cdot 10^6$
HAMAMATSU	S10985-50C	6 x 6	50% @ 440 nm (includes afterpulses & crosstalk)	$6 \cdot 10^6 - 10 \cdot 10^6$	$7.5 \cdot 10^5$
KETEK	PM3350	3 x 3	40% @ 420 nm	$4 \cdot 10^6$	$2 \cdot 10^6$
STMicroelectronics	SPM35AN	3,5 x 3,5	16% @ 420 nm	$7.5 \cdot 10^6$	$3.2 \cdot 10^6$

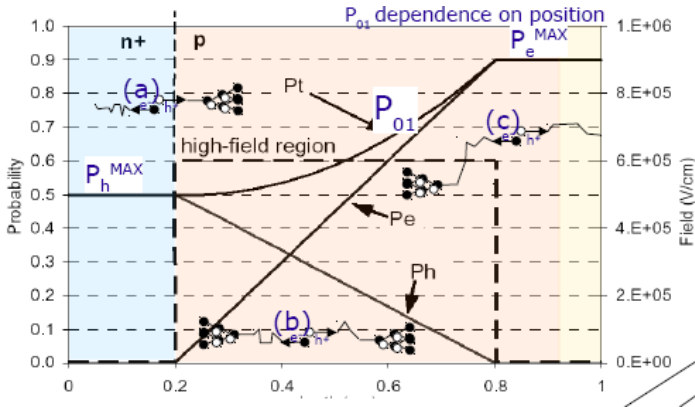
* datasheet data

Ongoing R&D to increase the active area at KETEK, AdvanSiD, Excelitas (6 x 6 mm²)

Other solution to get larger area : connection of several channels of a matrix



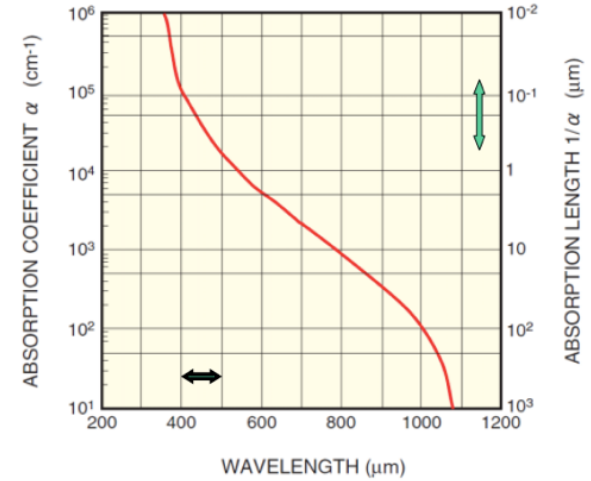
Sensitivity : Photo Detection Efficiency (PDE)



W.Oldham, IEEE TED (1972)

Q_ε: carrier Photo-generation

probability for a photon to generate a carrier that reaches the high field region in a pixel



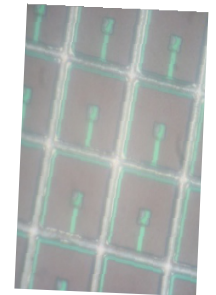
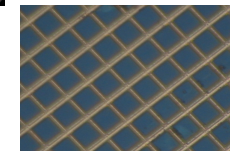
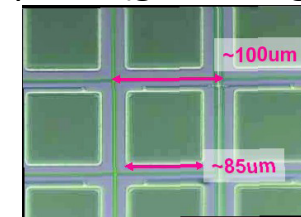
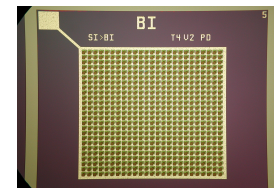
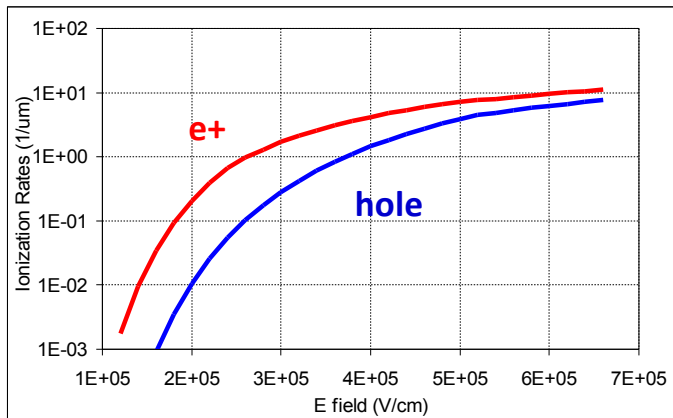
$$PDE = Q_{\epsilon} \cdot P_{trig} \cdot \epsilon_{geom}$$

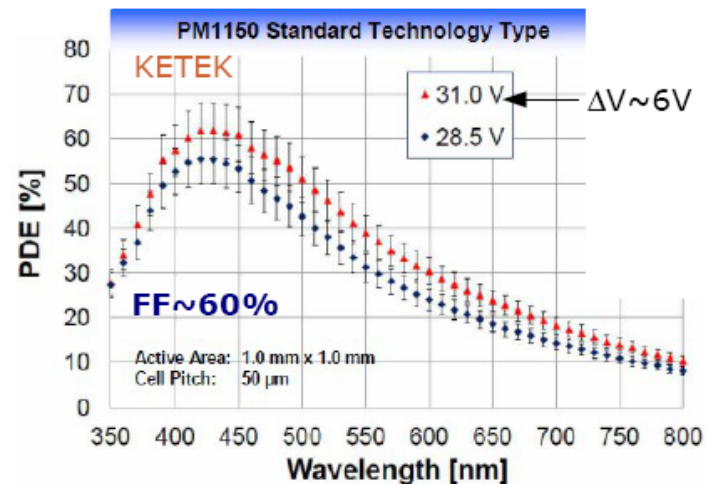
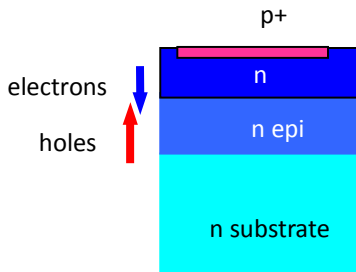
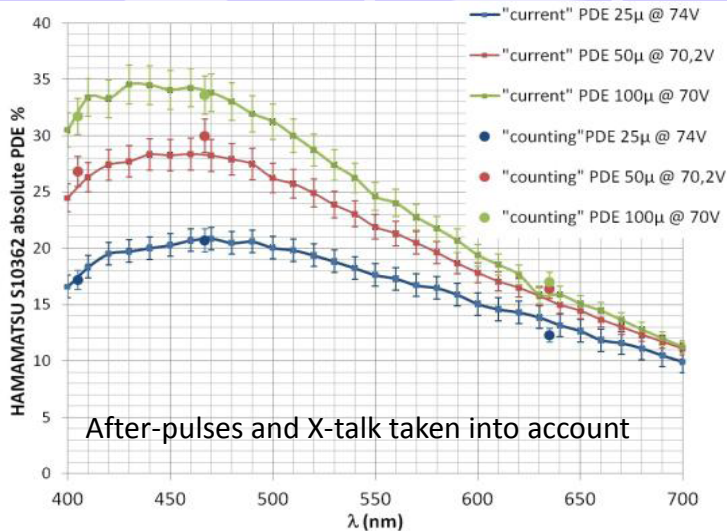
P_{trig} : avalanche triggering

probability for a carrier traversing the high-field to generate the avalanche

ε_{geom} : geometrical Fill Factor

fraction of dead area due to structures between the pixels (guard rings, trenches)

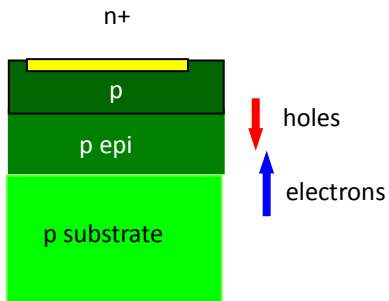
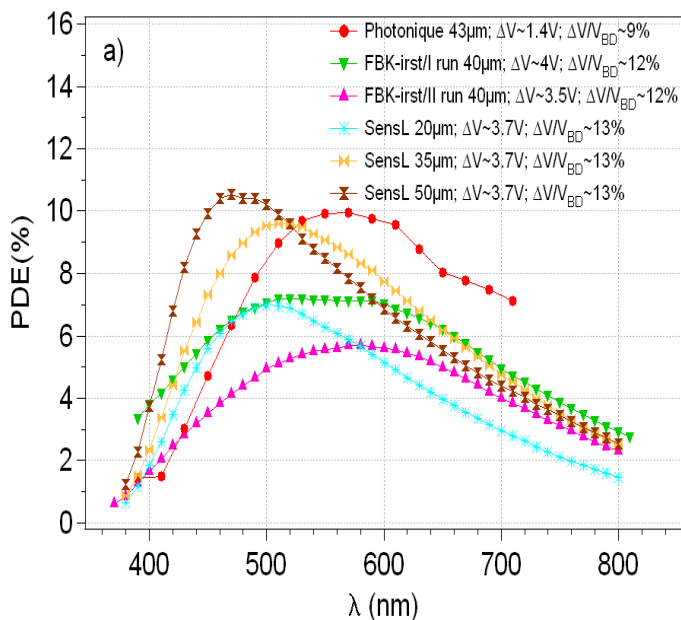




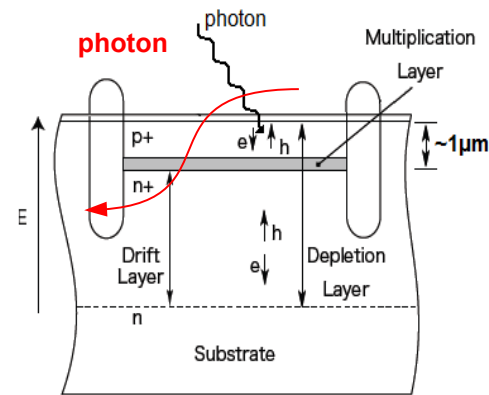
F. Wiest - AIDA 2012

V. Chaumat, PoS(PhotoDet 2012)058

PDE shape is dependent of the structure:
p-on-n is more blue sensitive than n-on-p
(e- trigger avalanches at short λ)



N. Dinu, NIMA A 610 (2009)



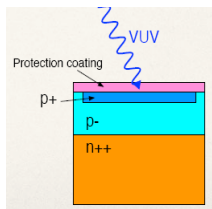
Otte, PD09

Almost no detection of the UV light → limitation of the suitability of SiPMs for Noble-gas detectors

PDE for VUV is ≈ 0 for commercial devices because of the low transmission for VUV of the sensitive layer due to:



Possible solutions:



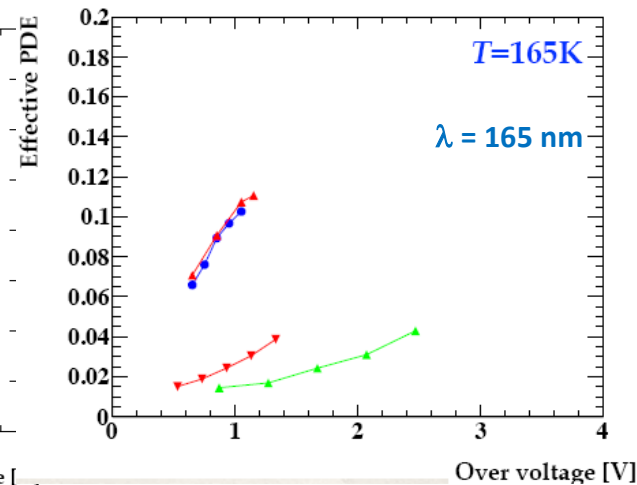
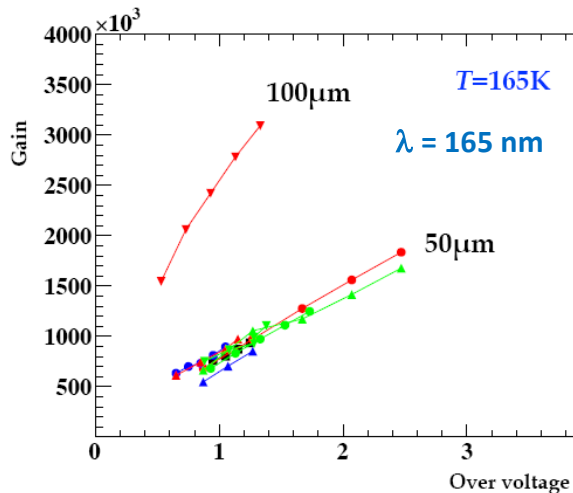
- ❖ protection coating (epoxy resin/silicon rubber)
- ❖ insensitive layer (p+ contact layer with \sim zero field)
- ❖ absorption length in Si for VUV photon: $\sim 5\text{nm}$
- ❖ high reflectivity for VUV on Si surface

- ❖ Remove protection coating
- ❖ Thinner p+ contact layer
- ❖ Optimize reflection/refractive index on sensor surface

HAMAMATSU

UV-enhanced MPPC under development (collaboration between Hamamatsu, ICEPP and KEK) : removal of the protection coating and optimization of the MPPC parameters → currently sensor size: $3 \times 3\text{mm}^2$ (cell size = $50\ \mu\text{m}$)

- ❖ PDE (165 nm) = 10 % (best sample)
- ❖ Gain $\approx 10^6$ @ 165 K
- ❖ DCR = 0 @ 165 K
- ❖ large $R_q \rightarrow$ long tail ($\approx 150\ \text{ns}$)



W. Ootani, PhotoDet2012

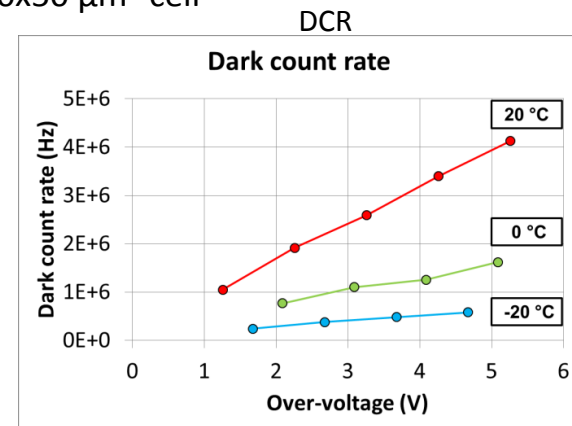
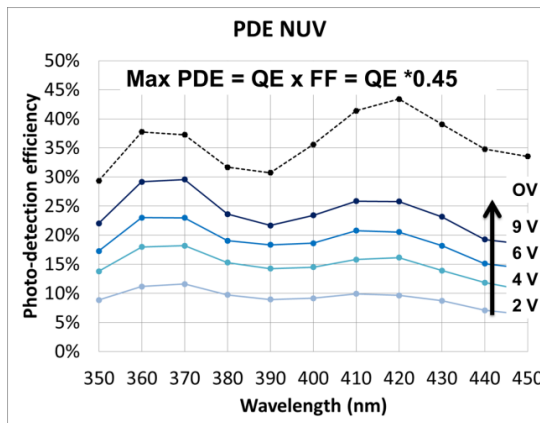
FBK NUV-SiPM (Near-UV SiPM)

1x1mm² 50x50 μm² cell

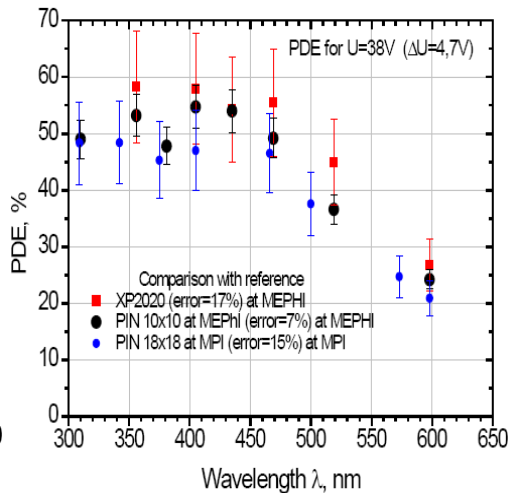
Designs available: 1x1, 2x2, 3x3, 4x4mm²

Results (FBK measurements):

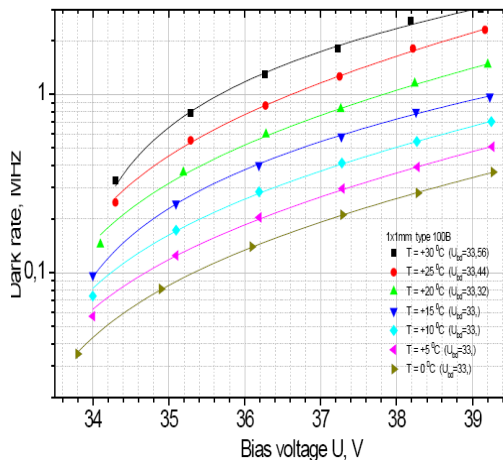
- ✿ PDE (350 nm) = 30 % (FF = 45 %)
- ✿ DCR = 200 kHz @ 20°C (ΔV = 5V)



A. Ferri, NIMA 718

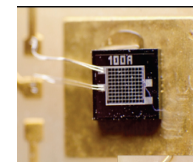


E. Popova,
PhotoDet2012



E. Popova, NDIP2011

Excelitas



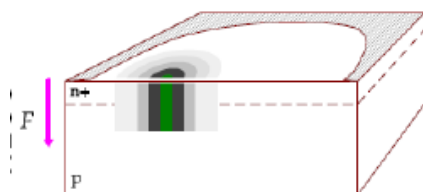
Collaboration between Excelitas, MEPHI and MPI : 1x1 mm² (cell size = 100 μm)

- ✿ PDE (350 nm) = 50 %
- ✿ DCR = 800 kHz @ 20 °C (ΔV = 4V)

Ongoing R&D to improve the PDE in the VUV + large area (> 10 mm²)

active layer very thin
 breakdown development fast → good timing properties expected
 big amplitude of the signal

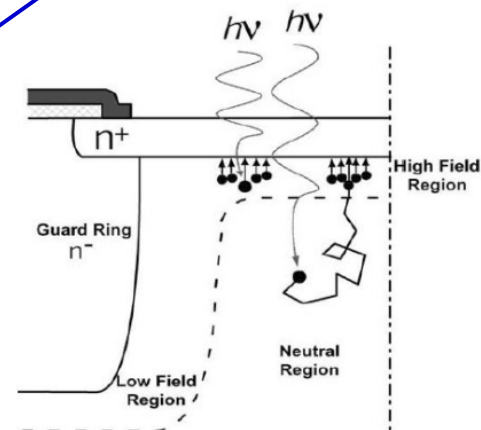
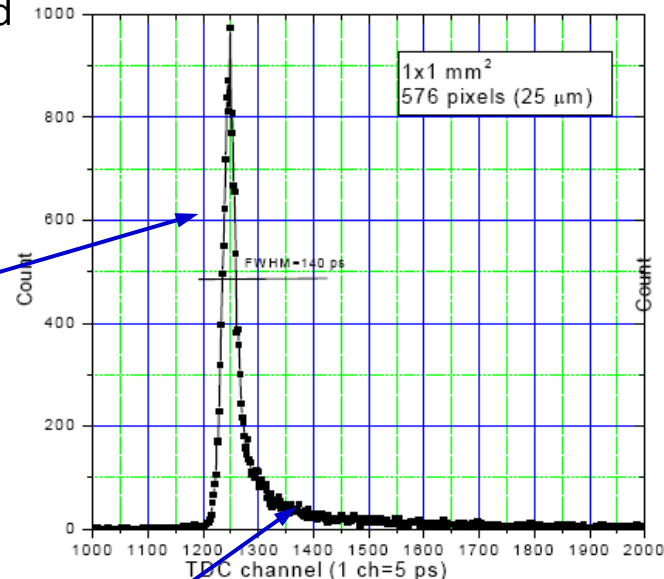
fast component of Gaussian shape with $50 \text{ ps} < \sigma < 150 \text{ ps}$
 The fluctuation are due to the variance of the transverse diffusion speed and the variance of transverse position of photo-generation.



Transverse multiplication

slow component: minor non Gaussian tail with time scale of several ns due to minority carriers, photo-generated in the neutral regions beneath the depletion layer that reach the junction by diffusion.

Time spread distribution

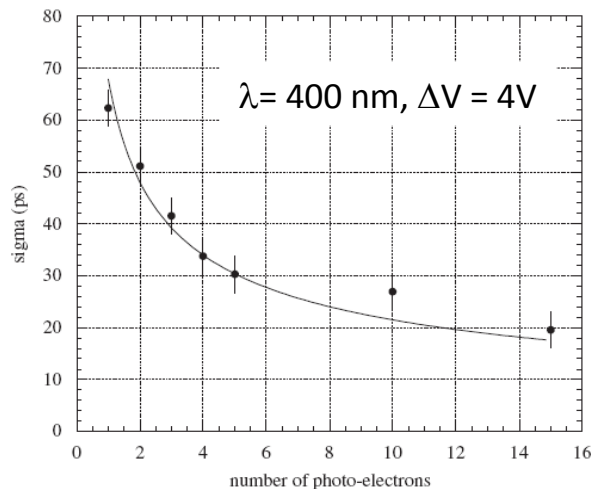




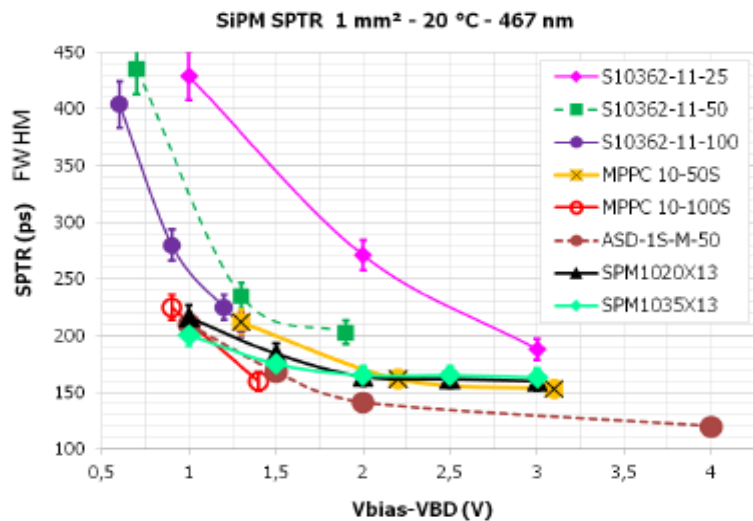
Time response of SiPMs



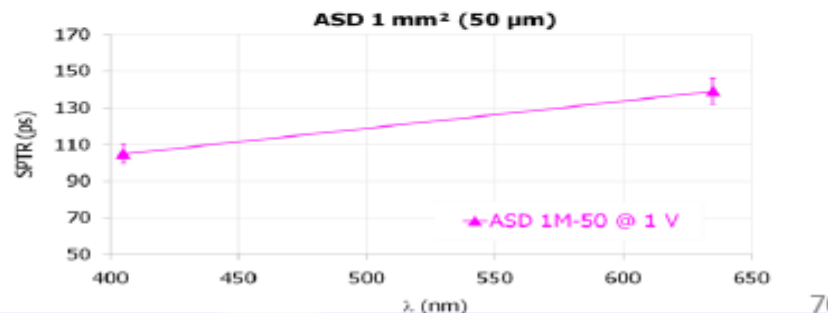
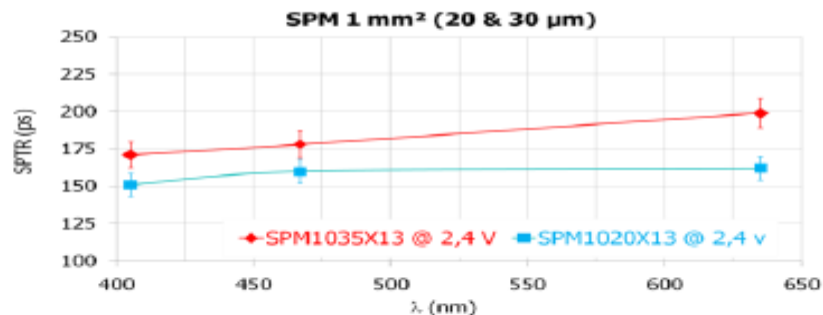
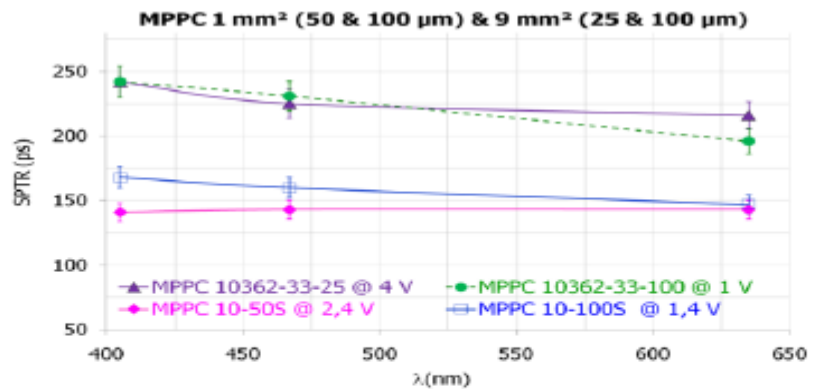
Timing resolution as a function of the incident number of photons



Single Photoelectron Timing resolution



SPTR (FWHM) as a function of λ



2 or more photons in 1 cell look exactly like 1 single photon

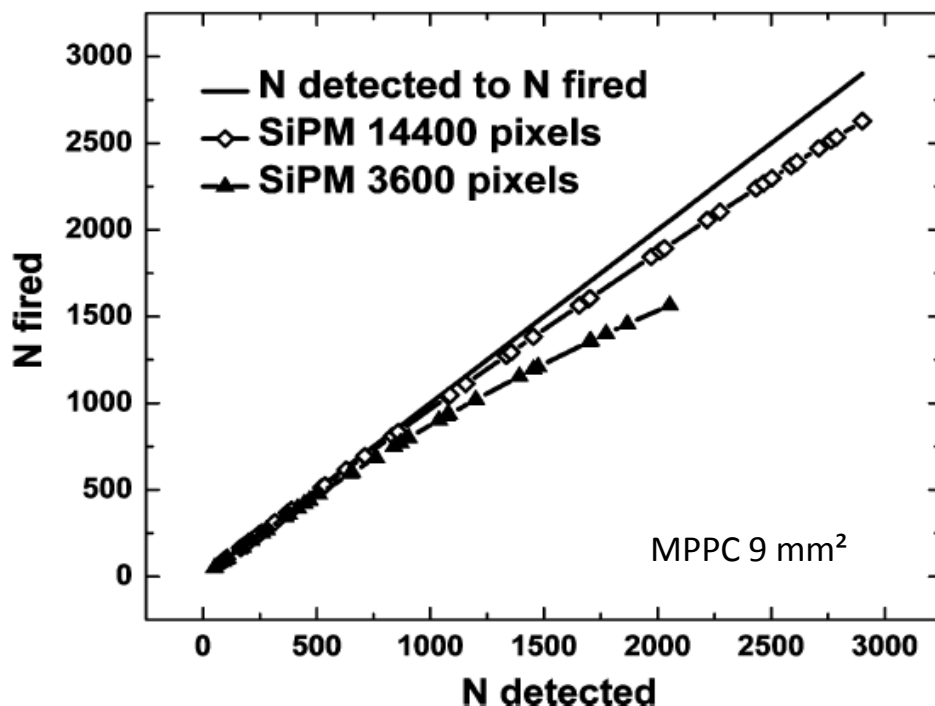
$$N_{firedcells} = N_{total} \cdot \left(1 - e^{-\frac{N_{photon} \cdot PDE}{N_{total}}}\right)$$

$N_{firedcells}$: number of excited pixels

N_{total} : total number of pixels

N_{photon} : number of incident photons in a pulse

Output signal: proportional to the number of fired cells as long as $N_{photon} \times PDE \ll N_{total}$



The saturation is a limiting factor for the use of SiPM where large dynamic range of signal (5000 – 10000 photons/pulse) has to be detected (calorimetry)

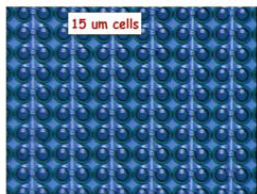


Saturation: solution = large dynamic range

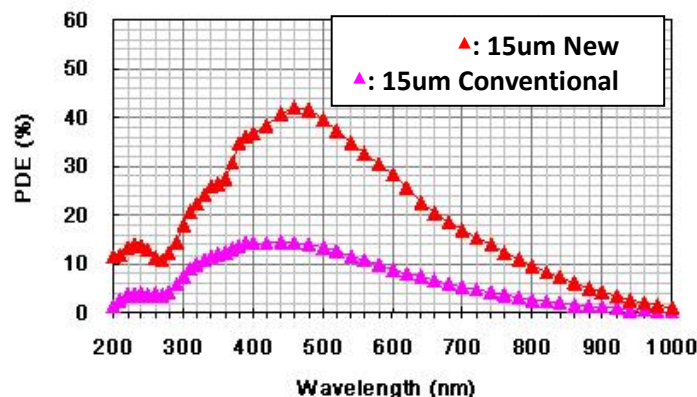


large dynamic range in Calorimetry or PET → high density SiPM : device with more than 1000 cells/mm²

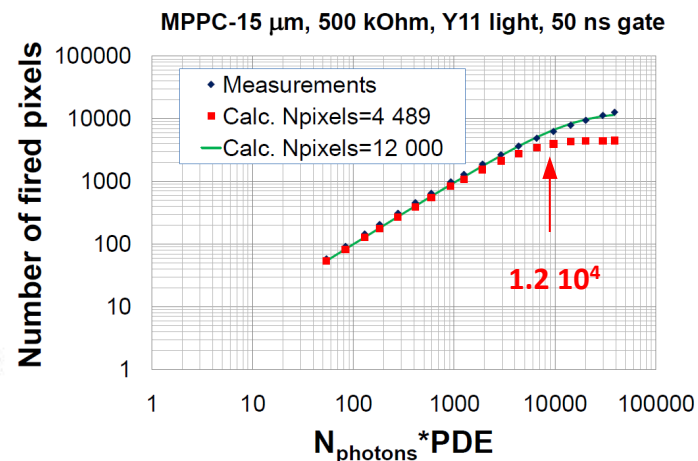
HAMAMATSU



1 mm²
4489 cells
cell size : 15 μm
gain = 2 · 10⁵



HPK, private communication

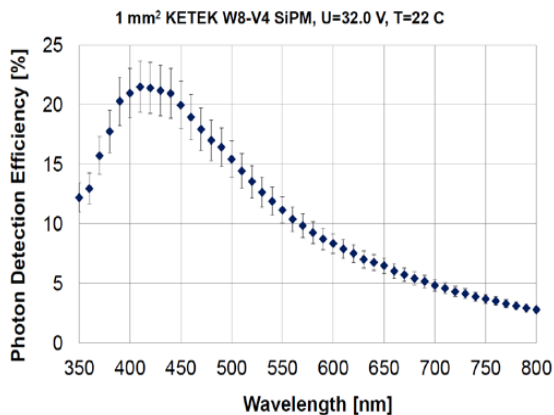


Y. Musienko, NDIP-2011

fast cell recovery time (~4ns) → the linearity for Y11 (WLS fiber) light of 4489 cells/mm² MPPC corresponds to a SiPM with ~ 12000 cells/mm²

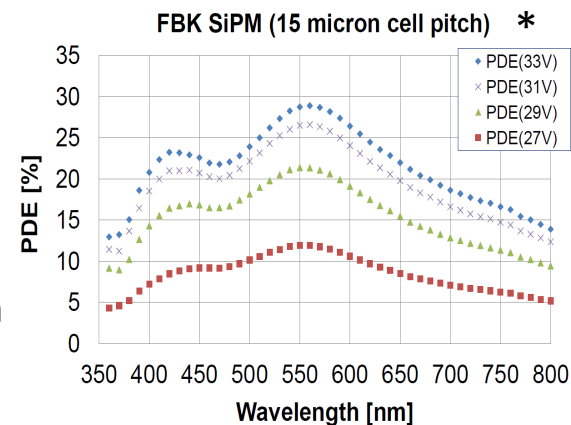
KETEK

1 mm²
4489 cells
cell size : 15 μm
gain = 0.7 · 10⁶
recovery time = 8 ns



FBK

RGB-SiPM-HD
2.2 x 2.2 mm²
4404 cells
cell size : 15 μm



* measurements by Y.Musienko @ CERN

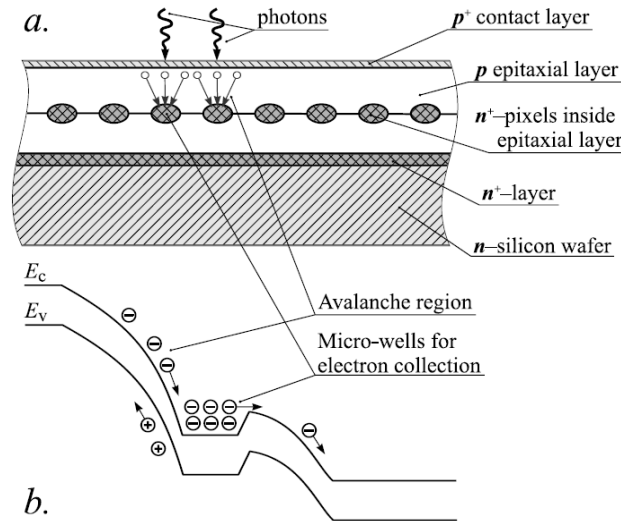


Saturation: solution= very large dynamic range



ZECOTEK

Special design: both the matrix of avalanche regions and the individual passive quenching elements are created inside the Si substrate with a special field distribution of the inner electric field



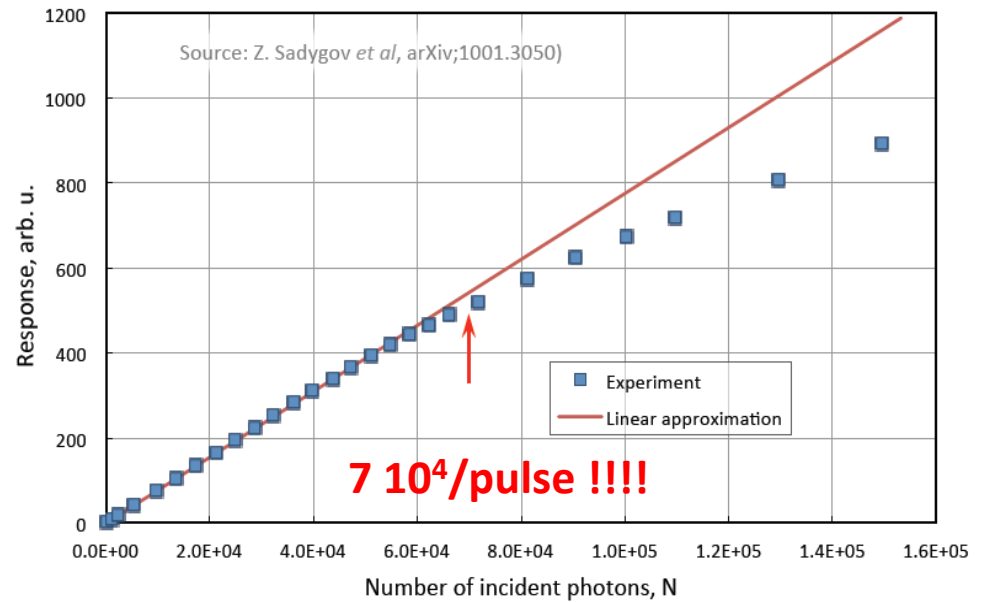
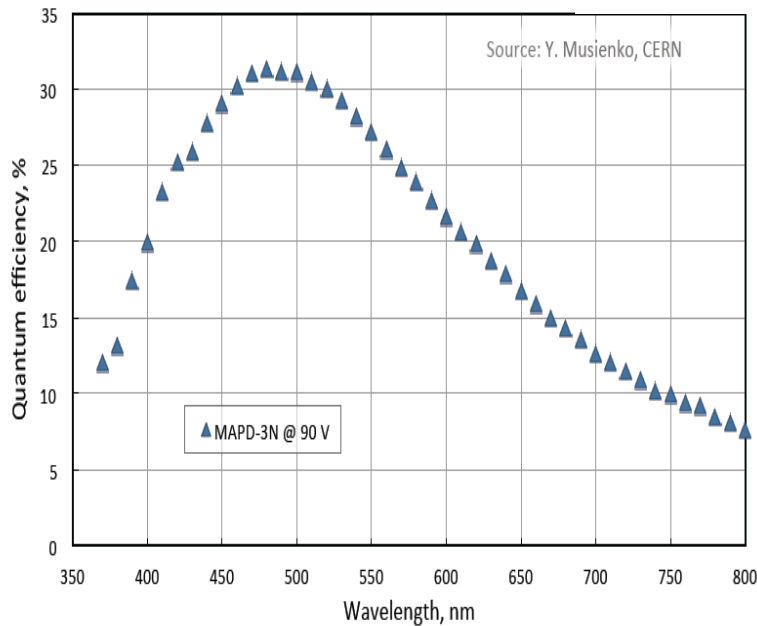
MAPD-3N

3 x 3 mm²

135000 cells (15000/mm²)

gain = 10⁵

slow cell recovery time : 300 μ s



protons / neutrons

bulk damages caused by lattice defects

γ -rays

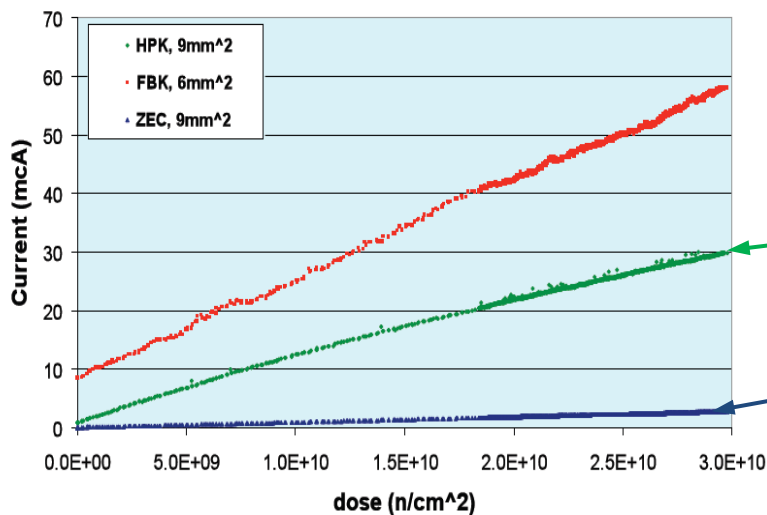
creation of trapped charges near the Si-insulator interface

Radiation hardness, an issue for photodetector in Calorimeters

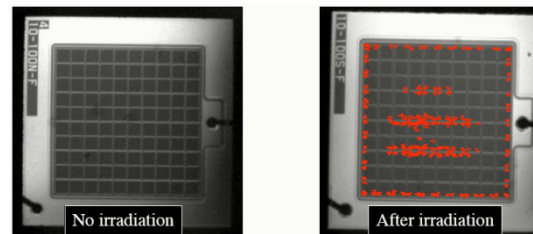
- increase of the DCR
- change of the breakdown voltage
- change of the gain and PDE dependence as a function of bias voltage

- ❖ limitation of the low light detection capability
- ❖ destruction of the device

1Mev Neutron dose vs leakage current



Y. Musienko, LHC on the March workshop 2011



HAMAMATSU have developed new MPPC more resistant to irradiation

MAPD have a good behavior under irradiation but its recovery time is long (300 μ s)



Radiation-hardness of SiPMs (2)

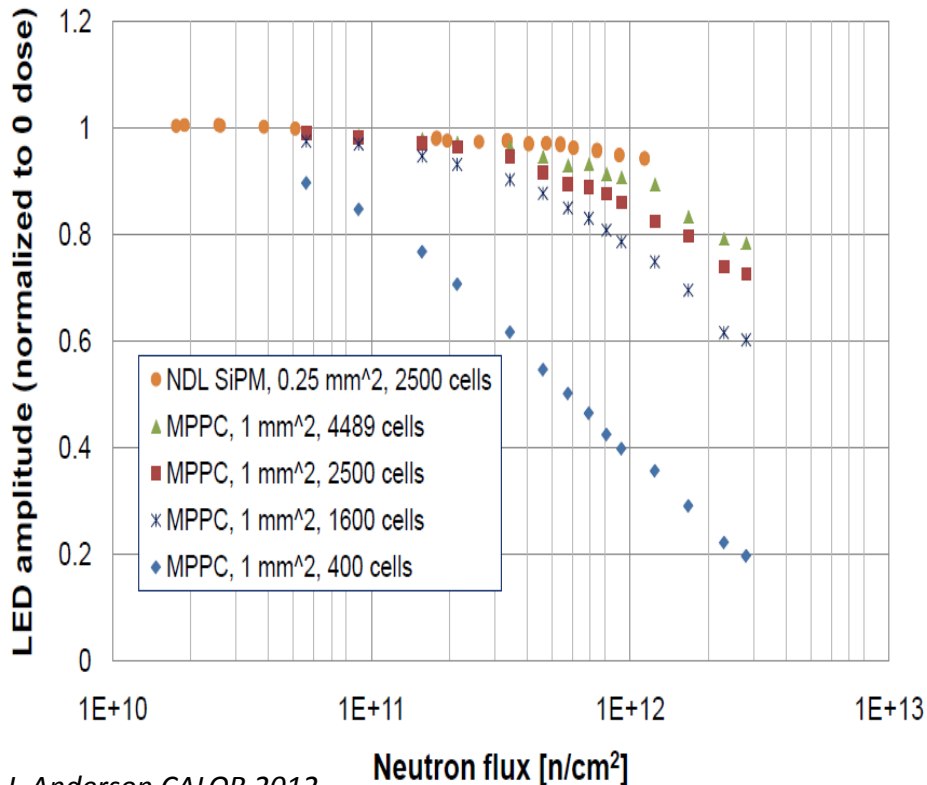


HAMAMATSU and NDL developed new devices :

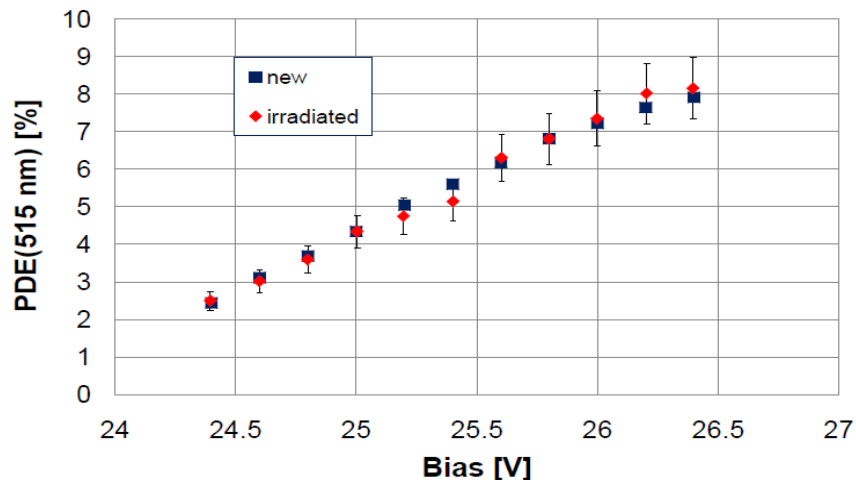
- 15 μm cell size MPPC (1 mm^2)
- 10 μm cell size NDL (0.25 mm^2) SiPM

which **survived 10^{13} n/cm² 1 MeV equivalent neutron flux** (10^8 n/cm² 3 years ago)

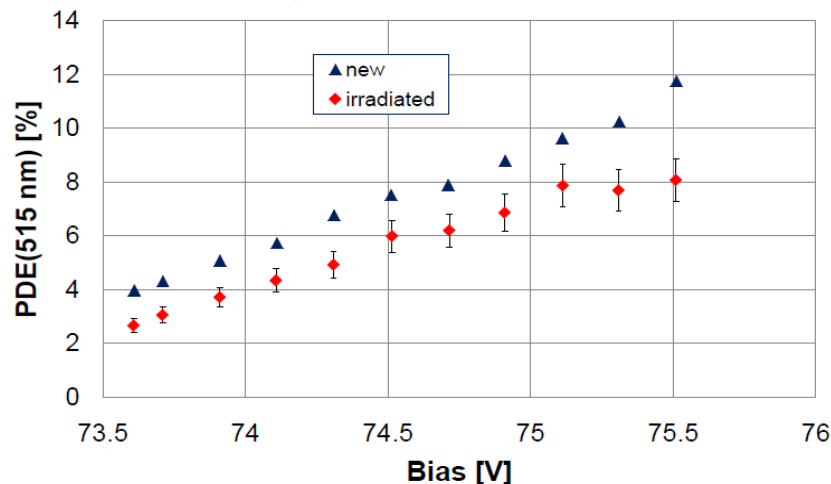
LED vs. Flux ($R_L=3$ kOhm, no bias correction, non-annealed)



NDL SiPM after 1E13 neutrons/cm², T=22 C



15 μm MPPC after 1E13 neutrons/cm²

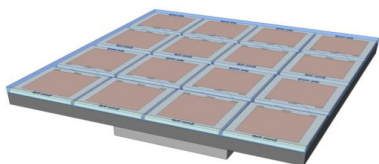


Y. Musienko, NDIP 2011

Segmentation of the light detection + need of larger active area → SiPM matrix

FBK

ASD-SiPM4S-P-4x4T-50



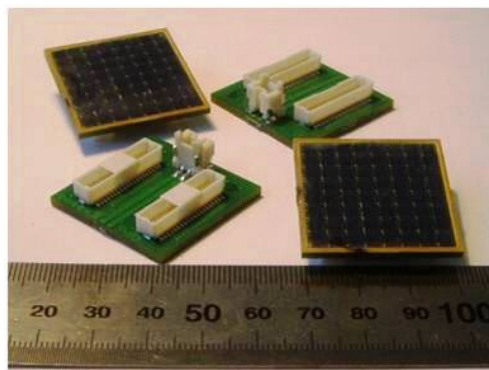
4x4 channels

1 channel = $4 \times 4 \text{ mm}^2$

6400 cells ($50 \times 50 \mu\text{m}^2$)

/channel

Zecotek



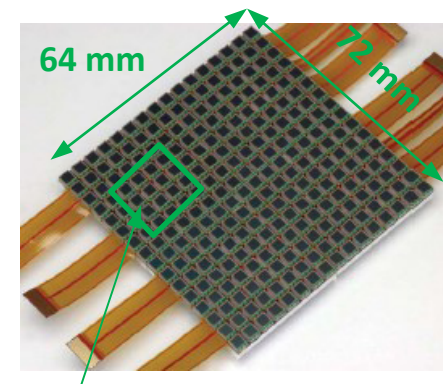
8x8 channels

1 channel = $3 \times 3 \text{ mm}^2$

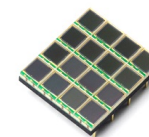
15000 cells /channel

HAMAMATSU

S11834-3388DF



S11064-025



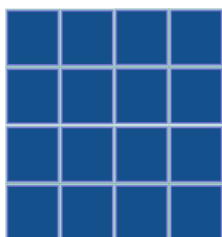
4x4 channels

1 channel = $3 \times 3 \text{ mm}^2$

14400 cells ($25 \times 25 \mu\text{m}^2$) /channel

Excelitas

Ketek

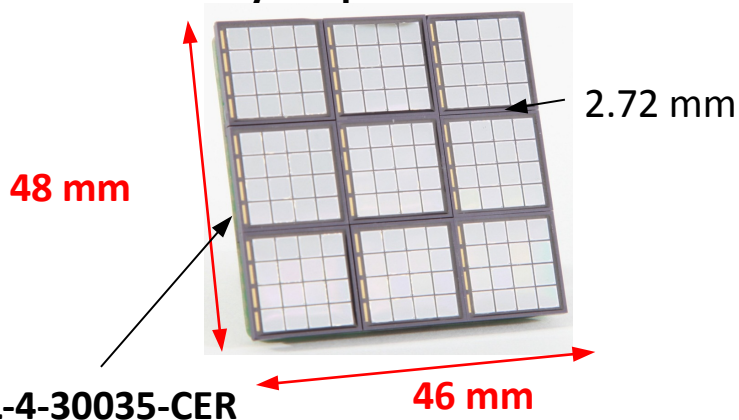


R&D in progress

**Matrixes of 16 channels
with 3×3 or $6 \times 6 \text{ mm}^2$**

Sensl

ArraySL-4p9-30035



SL-4-30035-CER

4x4 channels

1 channel = $3 \times 3 \text{ mm}^2$

4774 cells ($35 \times 35 \mu\text{m}^2$) /channel

ArraySM-8



8x8 channels

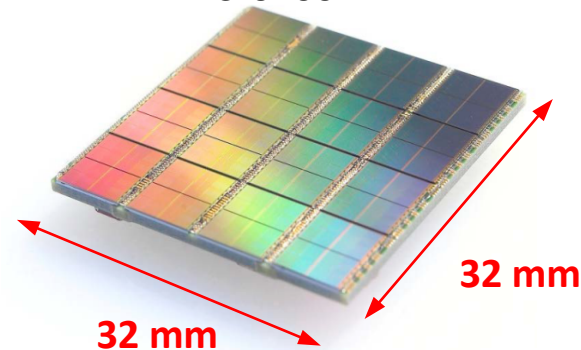
1 channel = $6 \times 6 \text{ mm}^2$

18980 cells /channel

new surface mount package

Philips Digital Photon Counting

DLS-6400-22-44



8x8 channels

1 channel = $3.9 \times 3.2 \text{ mm}^2$

6396 cells ($59 \times 32 \mu\text{m}^2$) /channel

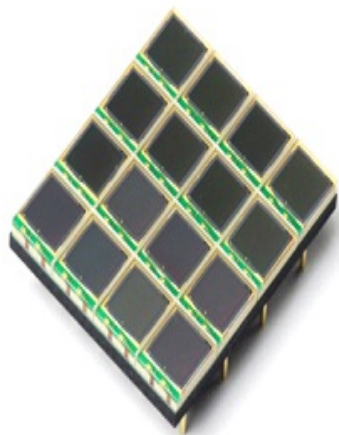
Electronics embedded

Requirements for the SiPM matrixes:

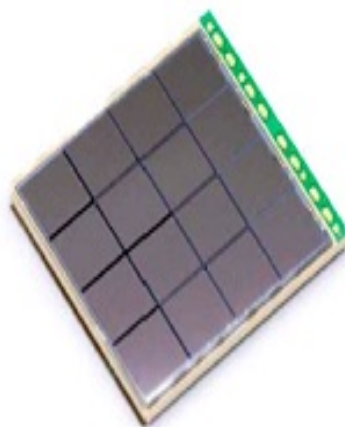
- improvement of the spatial resolution and PDE
- simplification of the assembly for the building of detectors with large surface

Important effort on the packaging + development of monolithic SiPM matrices (all the channels are on the same substrate)

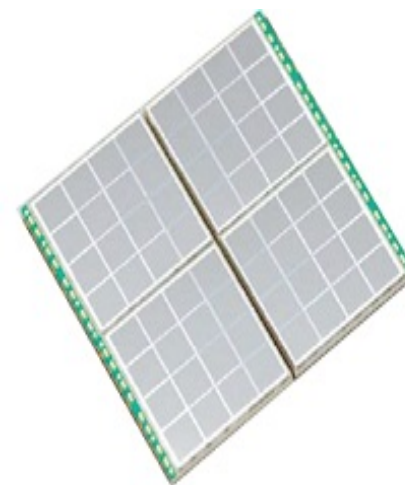
Discrete Array



Monolithic Array



3-side buttable Tiling

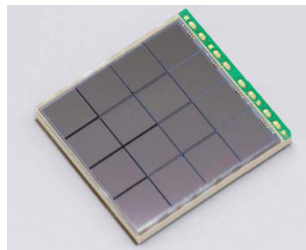


HAMAMATSU

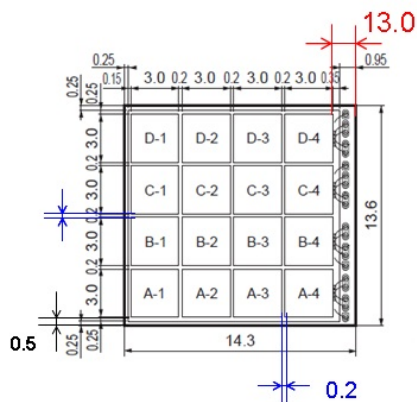
4x4 channels

1 channel = 3x3 mm²

3600 cells (50x50 μm²)/channel



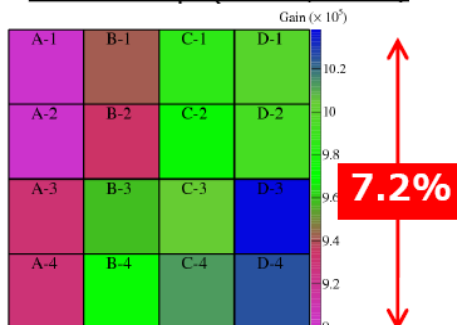
S11828-3344



3 sides tileable

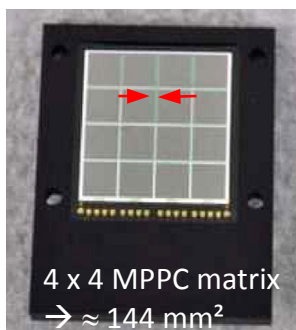
1 cathode – 16 anodes

Gain map (71.9V, 0 °C)



ave. gain = 9.7×10^5

Kato et al, NIMA 638 (2011) 83–91

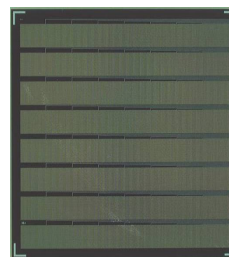


4 x 4 MPPC matrix
→ ≈ 144 mm²

S10985 - 36x36 mm²

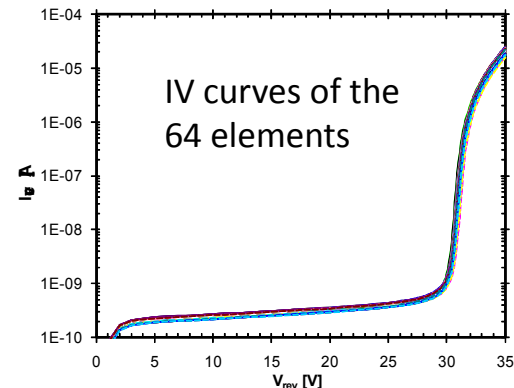
57600 cells

FBK



8 x 8 channels

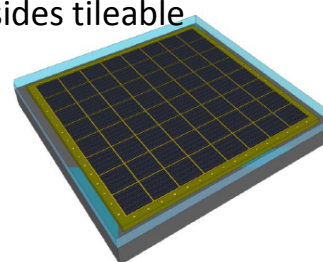
DASiPM2 project



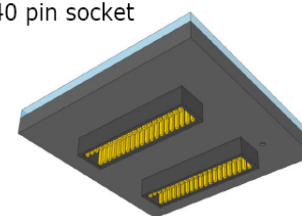
Marcatili et al, NIMA 659 (2011) 494–498

Ongoing R&D at AdvanSiD to improve the performances

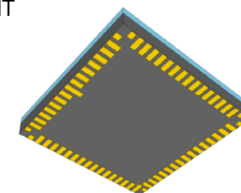
4 sides tileable



40 pin socket



SMT



64 channels

1.5x1.5 mm² SiPMs (pixels)

C. Piemonte, private communication

HAMAMATSU development: another way to improve the fill factor and therefore the PDE

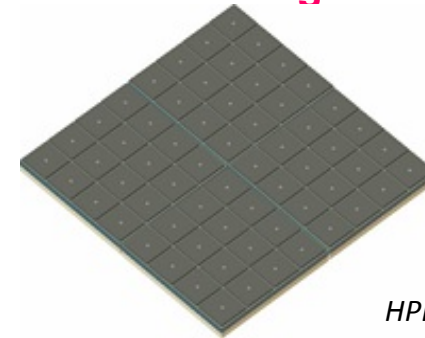
Through Silicon Via Technology

Discrete Array

NEW June 2013



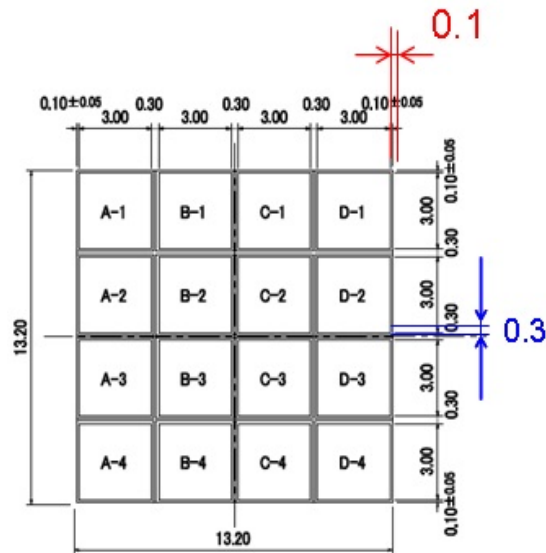
4-side buttable Tiling



HPK, private communication

8x8 channels

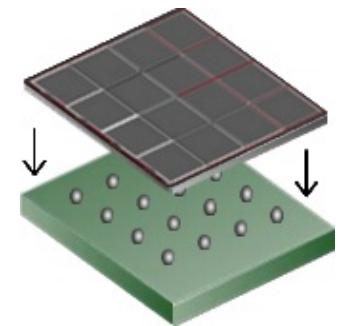
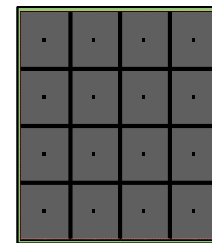
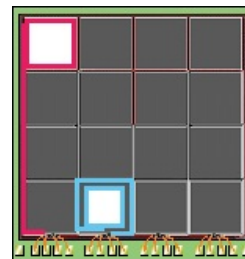
1 channel = 3x3 mm²



*Non-resin protection type

with wire bonding (traces to the bonding pads)

⇒ with TSV

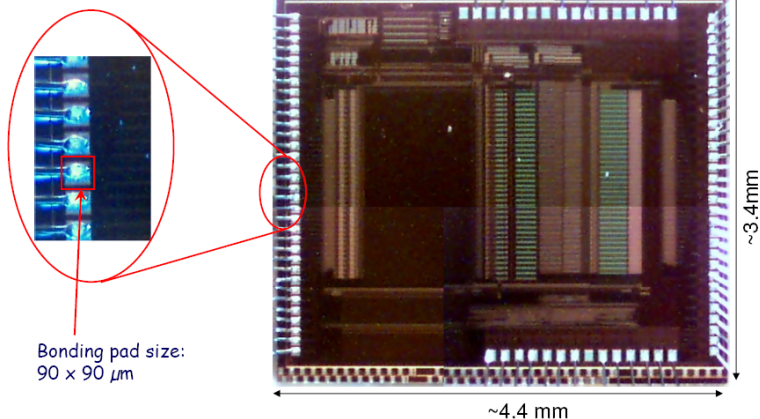


should have a better PDE and timing resolution

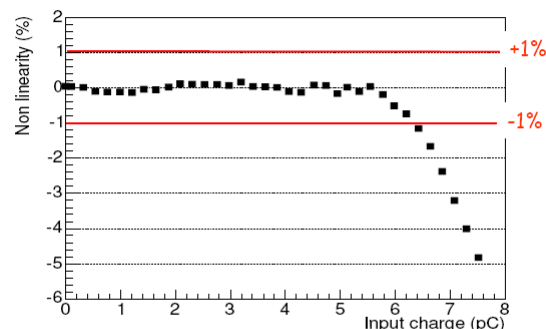
Chip Name	Measured quantity	Application	Input configuration	Technology
FLC_SiPM	Pulse charge	ILC Analog HCAL	Current input	CMOS 0,8 μm
MAROC	Pulse charge, trigger	ATLAS luminometer	Current input	SiGe 0,35 μm
SPIROC	Pulse charge, trigger, time	ILC HCAL	Current input	SiGe 0,35 μm
NINO	Trigger, pulse width	ALICE TOF	Differential input	CMOS 0,25 μm
PETA	Pulse charge, trigger, time	PET	Differential input	CMOS 0,18 μm
BASIC	Pulse height, trigger	PET	Current input	CMOS 0,35 μm
SPIDER (VATA64-HDR16)	Pulse height, trigger, time	SPIDER RICH	Current input	
RAPSODI	Pulse height, trigger	SNOOPER	Current input	CMOS 0,35 μm

W. Kucevitz, SiPM workshop CERN 2010

Chip **VATA64-HDR16** developed for SiPM applied in Ring Imaging Cherenkov Detector of SPIDER (Space Particle IDentifiER) Experiment: 64 channels, low noise, large dynamic range



Linearity better than 1% up to $\sim 6 \text{ pC}$

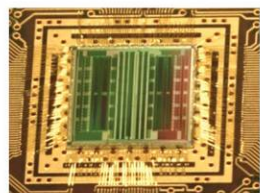


RMS noise $\sim 0.5 \text{ fC}$ (ASIC only)
 $\sim 0.85 \text{ fC}$ (with board)

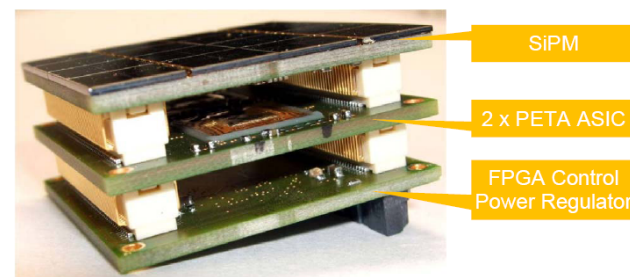
Dynamic range $\sim 1000 \text{ MIP}$

P.S.Marrocchesi

PETA: (Position-Energy-Time-ASIC) chip was developed within FP7 EU Project HIPERIMAGE



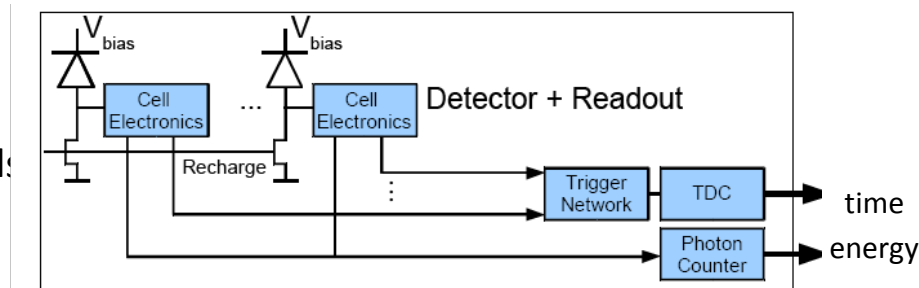
- Amplification (differential voltage amp.)
- Discrimination (per channel threshold trim)
- Time Stamping (50ps bins)
- Integration (self gated, program. int. time)
- Digitization (~ 8 Bit resolution)
- All digital readout (LVDS handshake)
- Self triggered, asynchronous operation



W. Shen, Heidelberg Detector Workshop 2010

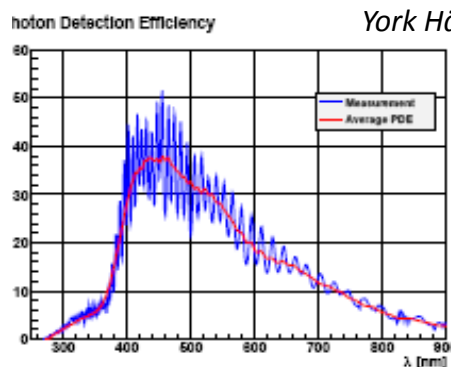
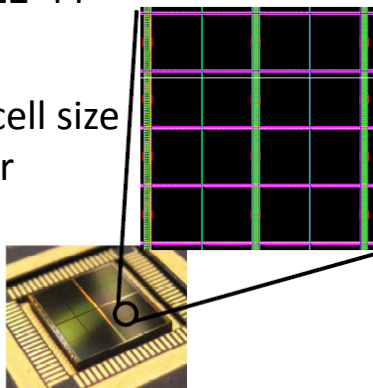
Array of G-APDs integrated in a standard CMOS process. The signal from each pixel is digitized and the information is processed on chip:

- time of first fired pixel is measured
- number of fired pixels is counted
- active control is used to recharge fired cells



DLS-3200-22-44

- 3200 cells
- 59 x 64 μm^2 cell size
- 78% fill-factor



York Hämisch, TIPP 2011

- *afterpulsing* $\sim 0.1\%$ (20 °C)
- *DCR* = 100 kHz/mm² (20 °C)
- *temperature sensitivity* $\sim 0.33\%/^{\circ}\text{C}$
- *timing resolution (SPTR)* = 60 ps (FWHM)
- *recovery time* : 10 – 40 ns

T. Frach, 2012 JINST 7 C01112

Drawbacks:

➤ requires a dedicated readout provided by Philips (can be an advantage when you do not want to develop your own electronics !)

➤ dead space around the sensor ?



Opened question:

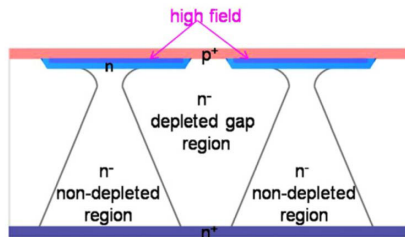
what about the radiation hardness of this device ?

New techno: SiPMs with bulk integrated resistors

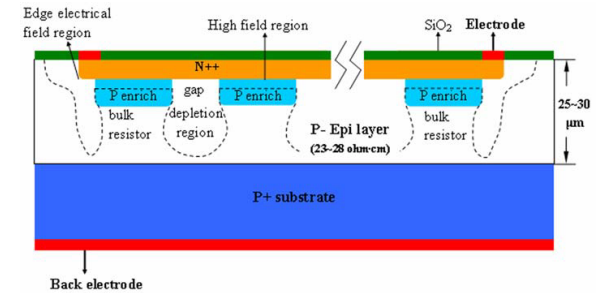


Using of Silicon bulk as a quenching resistor instead of a polysilicon structure on top of the detector

MPI



NDL

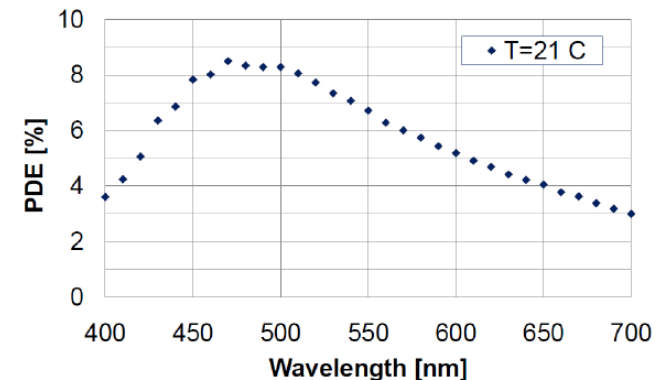


Advantages

- simple fabrication process
- no obstacles in entrance window
- possible high geometrical fill-factor
- possibility of antireflective coating
- possible high cell density

- 0.5 × 0.5 mm² cell size : 10 μm
- 10000 cells/mm²
- DCR = 9 MHz/mm² (21 °C)
- Gain = 1.2 10⁵ (21 °C)
- PDE (475 nm) = 8 %
- recovery time : 4.8 ns

SiPM (U=26.5 V, 2 500 cells, 0.25 mm²)

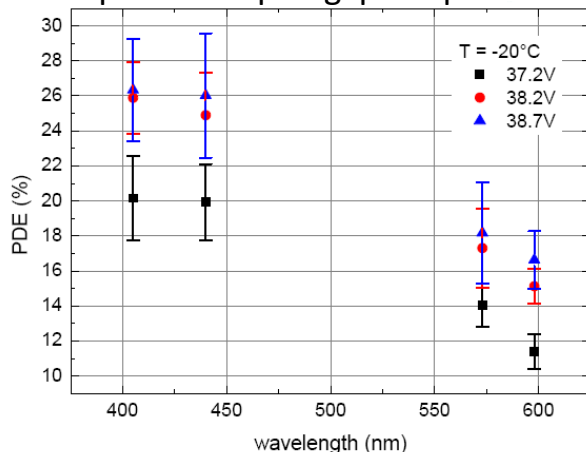


H. Dejun, NDIP2011

84

- Fill factor= 71.6%
- Cross-talk=15%
- DCR= 10 MHz/mm² (27 °C)
- PDE (440 nm) = 20 %

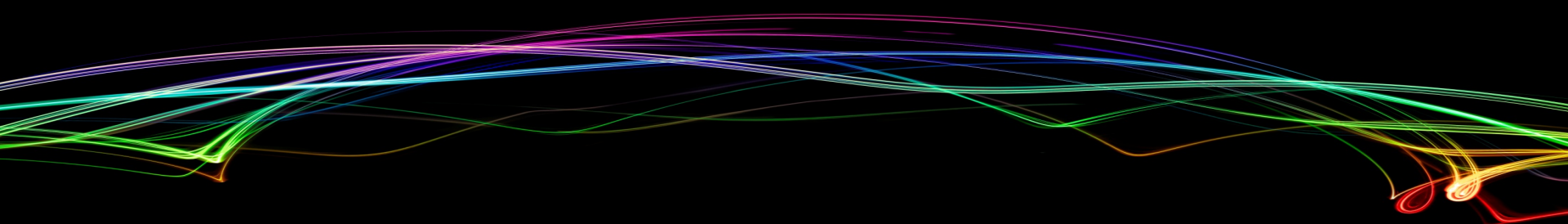
pitch = 130μm gap = 20μm



Promising results

R&D on going at MPI and NDL to improve the structure and the performances

C. Jendrysik, 12th Pisa Meeting on Advanced Detectors, 2012



Conclusion

**Quick comparison between PMT, MCP-PMT
and SIPM**



PMT	<ul style="list-style-type: none"> ▪ High gain (10^6) with 1000 – 2000 V ▪ Low noise ▪ High quantum efficiency (35 % in blue) ▪ Large area ($> 10000 \text{ mm}^2$) ▪ Large number of configurations ▪ Commercial products since 70 years 	<ul style="list-style-type: none"> ▪ Non linearity ▪ Response uniformity ▪ Affected by magnetic field ▪ Long-term stability ▪ Fragility ▪ Only 2 producers on the market
MCP-PMT	<ul style="list-style-type: none"> ➤ High gain (10^7) ➤ High quantum efficiency (20 %) ➤ Very good timing properties (SPTR = 30 ps) 	<ul style="list-style-type: none"> ➤ Affected by magnetic field ➤ Fragility ➤ Cost
SiPM	<ul style="list-style-type: none"> • High gain (10^5-10^6) with low voltage ($< 100 \text{ V}$) • Single photo detection • Good timing resolution (SPTR = 50 ps) • Insensitivity to magnetic field (up to 7 T) • High photon detection efficiency (35 % in blue) • Mechanically robust • A lot of R&D and different producers • Low cost mass production possible (ex: T2K) 	<ul style="list-style-type: none"> • High dark count rate @ room temperature for large device ($\geq 9 \text{ mm}^2$) • High temperature dependence of the breakdown voltage, the gain • Small devices • Few geometrical configurations available



Lectures and Revues :

- **EDIT 2011 school @ CERN**
- **Vacuum based photodetector**, IEEE NSS 2012, **Katsushi Arisaka**
- **PhotoDet 2012 workshop**, LAL Orsay: The SiPM Physics and Technology - a Review , **Gianmaria Collazuol**
- **SiPM workshop**, 16.02.2011, CERN: State of the art in SiPM's, **Yuri Musienko**

Reference articles:

- **Photomultipliers** from S. Donati
- **Silicon Photomultiplier - New Era of Photon Detection** from Valeri Saveliev
- **Advances in solid state photon detectors** from D. Renker and E. Lorenz
- **Silicon Photo Multipliers Detectors Operating in Geiger Regime: an Unlimited Device for Future Applications** from G. Barbarino, R. de Asmundis, G. a De Rosa, C. M Mollo, S. Russo and D. Vivolo

Books:

- ❖ **Hamamatsu PMT Handbook**
- ❖ **Burle PMT book**

Articles and presentations:

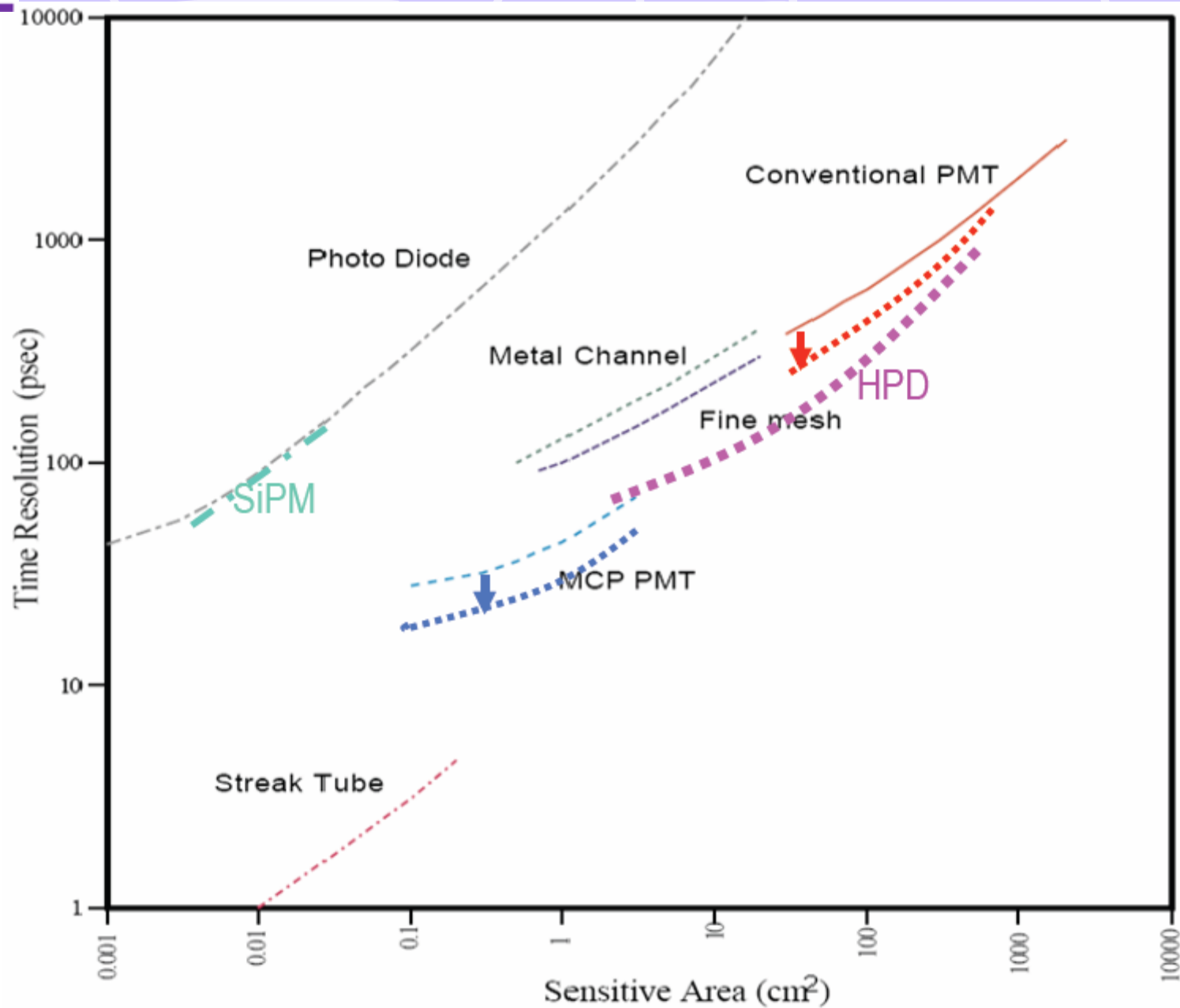
All quoted under the figures and plots of this presentation (my apologies if I forgot some of them)

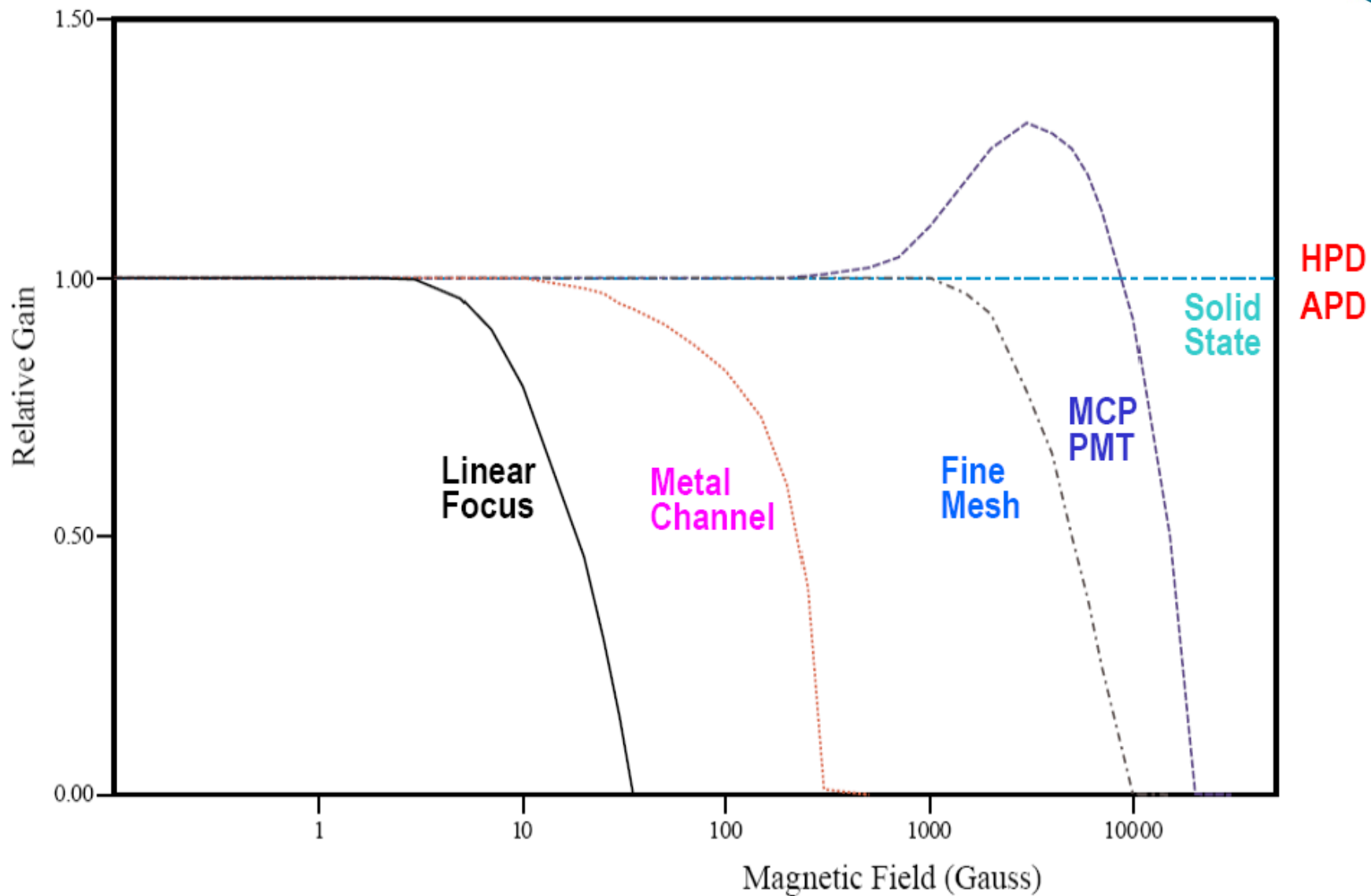


The End



Backup

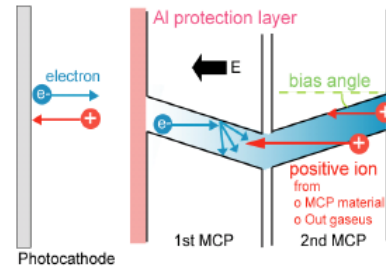




Approaches to Increase Lifetime

Protection layer

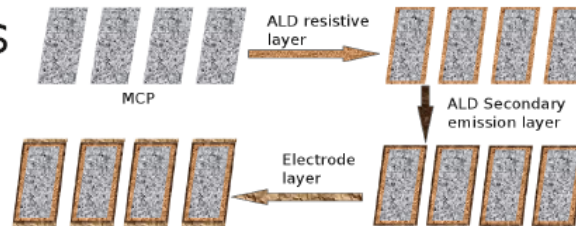
- In front of first MCP layer (older BINP and Hamamatsu)
 - disadvantage: reduction of collection efficiency
- Between MCP layers (new Hamamatsu)
 - anode region is hermetically sealed from photocathode region [NIM A629 (2011) 111]



Improved vacuum + treatment of MCP surfaces

[NIM A639 (2011) 148]

- Electron scrubbing (older PHOTONIS and new BINP)
- Atomic layer deposition (new PHOTONIS)



New photo cathode [JINST 6 C12026 (2011)]

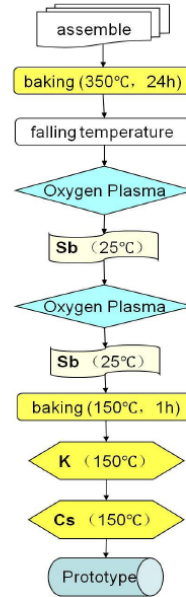
- Na₂KSb(Cs) + Cs₃Sb (new BINP)
 - disadvantage: significantly higher dark count rate

Progress on Bialkali Photocathode Production at Argonne

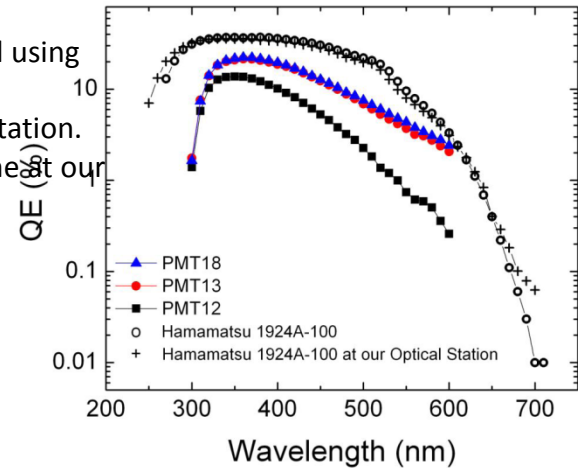
Junqi Xie, Marcel Demarteau, Ed May, Sasha Paramonov, Bob Wagner, Zikri Yusc

LAPPD Collaboration
High Energy Physics Division
Argonne National Laboratory
Tuesday, July 10th, 2012

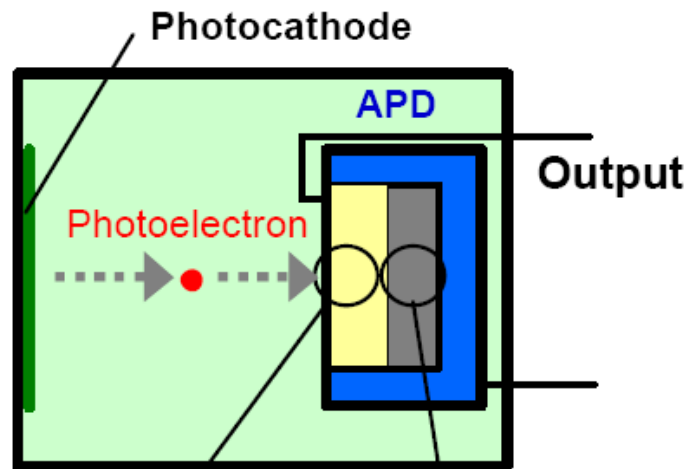
Bi-Alkali Photocathode Deposition Process



QE scans of three K-Cs-Sb bialkali photocathodes grown at Argonne using the PMT photocathode growth system acquired from Photonis. The QE values were measured using our new Optical Station system. A scan of a Hamamatsu PMT with “Super Bialkali” photocathode is also shown as part of the commissioning procedure of the Optical Station. The open circle shows the Hamamatsu’s QE scan, while the cross shows the scan done at our Optical Station.

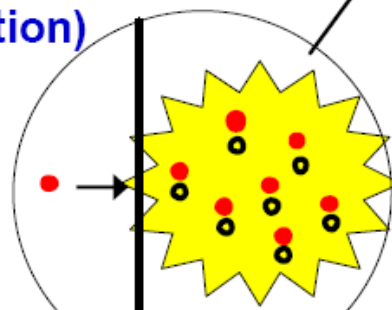


Z. Ysof, TIPP 2011

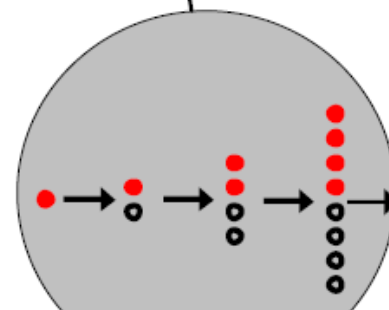


- Good PHD (Pulse Height Distribution)
- Good Uniformity
- Immunity to Magnetic Field
- Fast Time Response
- Compact (16mm in dia x 16mm)

<Photocathode>
Multi-Alkali, GaAsP, GaAs



**Electron Bombardment
X 1200**



**Avalanche Gain
X 50**

Combination of EB and avalanche gain

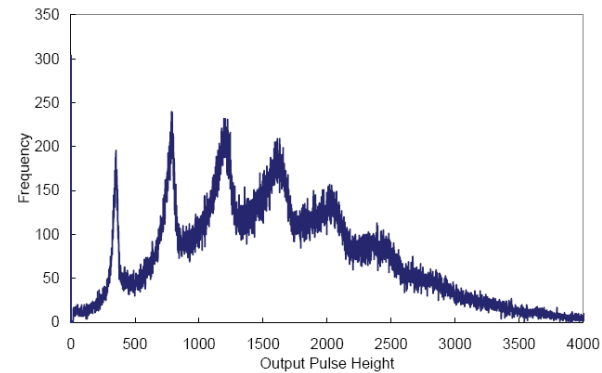
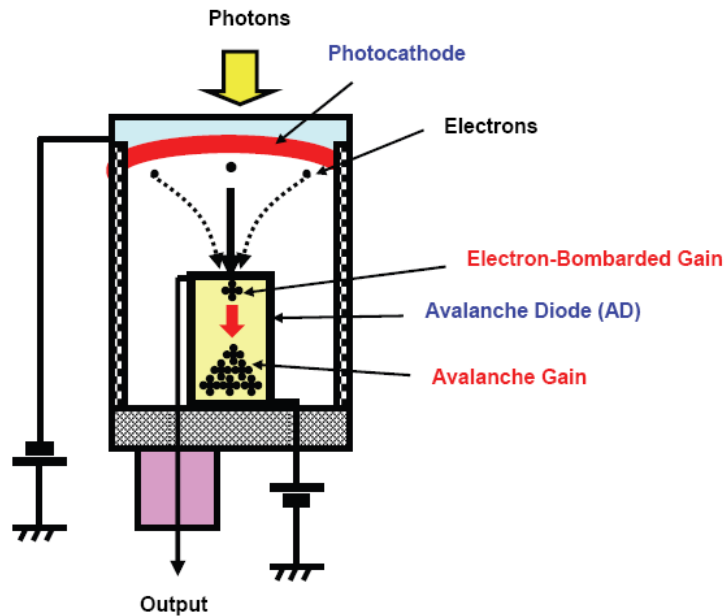
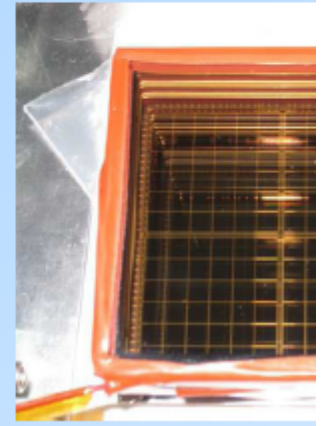
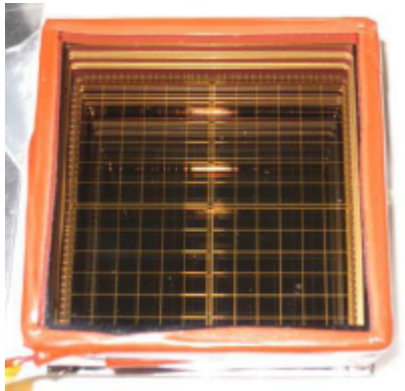


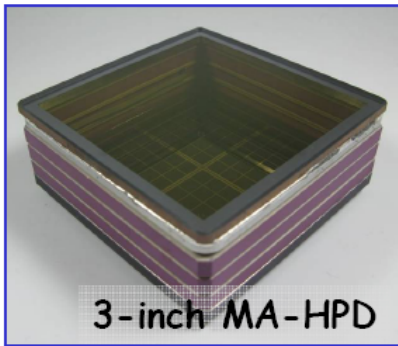
Figure 13: The pulse height spectrum for multi photons clearly shows peaks corresponding up to 6 photoelectrons.

Belle II aerogel RICH HAPD

- proximity focusing configuration → operation in magnetic field
- HV ~8kV, gain ~100k (2000x50)
- 144 channels
- ~ 65% effective area
- tested up to 1000 Gy and 10^{12} n(1MeV)/cm²
- Belle + Hamamatsu

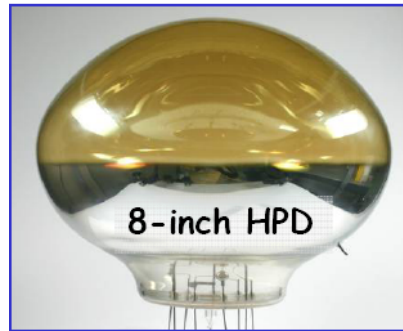


R&D on HPD



3-inch MA-HPD

RICH/Belle upgrade

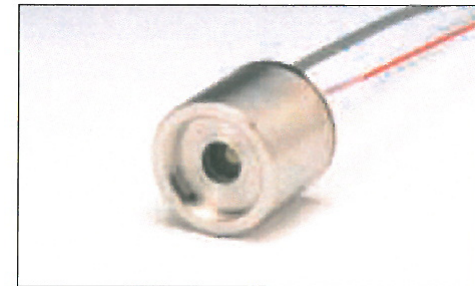


8-inch HPD

Water Tank Detector

The HPD (Hybrid Photodetector) utilizes the "electron bombardment" method in which photoelectrons are accelerated in a strong electric field to directly strike an avalanche diode (AD) in a vacuum tube. This mechanism achieves excellent quality of amplification.

Using a new AD with very low capacitance, we have developed a compact HPD with an excellent time resolution.



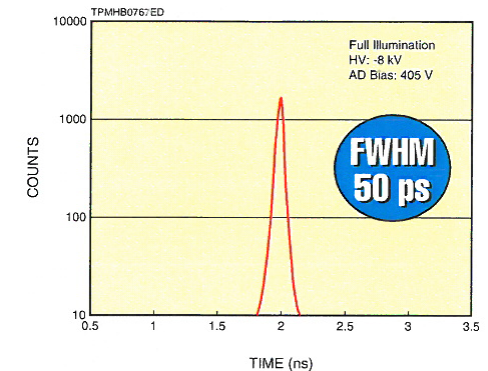
R10467U series

Parameter		R10467U-06	R10467U-40	R10467U-50	Unit
Spectral Response		220 to 650	300 to 720	380 to 890	nm
Photocathode	Material	Bialkali	GaAsP	GaAs	—
	Effective Area	$\phi 6$	$\phi 3$		mm
Quantum Efficiency		28 ^①	45 ^②	14 ^③	%
Gain ^④		1.2 × 10 ⁵			—
Rise Time		400			ps
T.T.S. (Transit Time Spread) ^⑤ (FWHM)		50	90	130	ps

① At 350 nm ② At 500 nm ③ At 800 nm

④ At the photocathode voltage of -8 kV and the AD bias voltage of $V_b -10$ V

⑤ At the single photon state and full illumination on the photocathode, specified as FWHM (Full Width at Half Maximum). These values include the jitter of the electronics of about 30 ps



SPACIROC

Analog part:

1. Photoelectron counting (20-50MHz)
2. Q-to-T converter

Digital part :

1. Digitization,
2. Memory,
3. Send data to FPGA for triggering

Crucial points

- Power consumption < 1 mW/ch
- data flow ~ 384 bits / $2.5 \mu\text{s}$
- Radiation tolerant



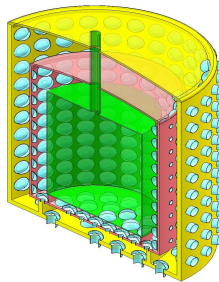
P. Barrillon, LAL, EUSO BALLON

Next generation Neutrino Experiment in China

60 km from Daya Bay and Haifeng



Daya Bay II



Huge Detector (LS + PMT

Energy resolution $\sim 3\%/\sqrt{E}$

Neutrino target: 30m(D) \times 30m(H)

LS, LAB based : ~ 20 kt

Oil buffer: ~ 6 kt

Water buffer: ~ 10 kt

• PMT (20") : $\sim 20,000$

Reactor experiments:

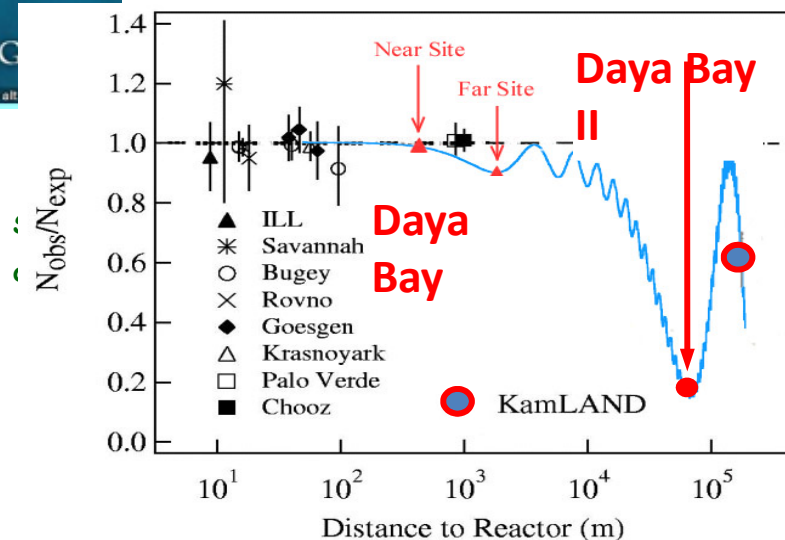
The Main Scientific goals:

\Rightarrow **Mass Hierarchy**

\Rightarrow **Mixing matrix elements**

\Rightarrow **Supernovae**

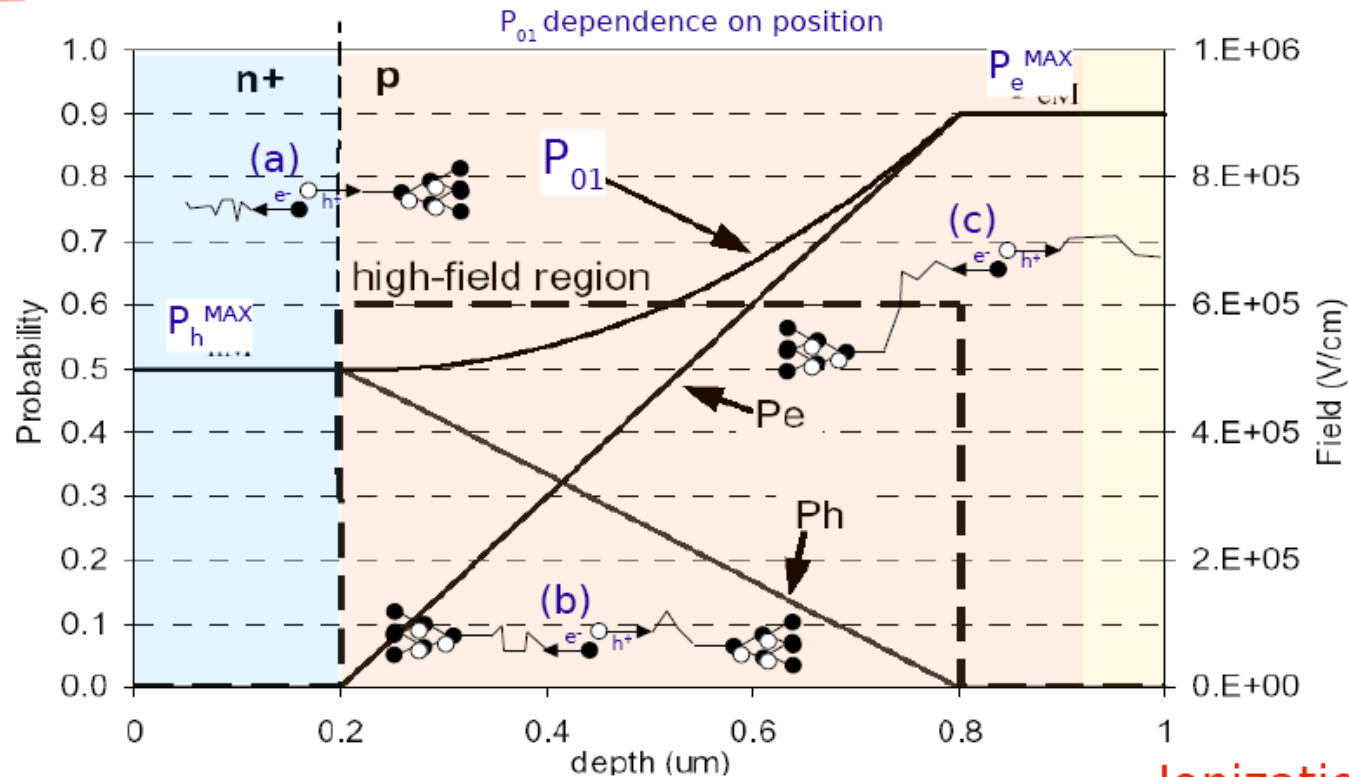
\Rightarrow **geo-neutrinos**



L. Zhan, et. al., Phys.Rev.D 78:111103,2008

L. Zhan, et. al., Phys.Rev.D 79:073007,2009

Avalanche trigger probability (P_{01})

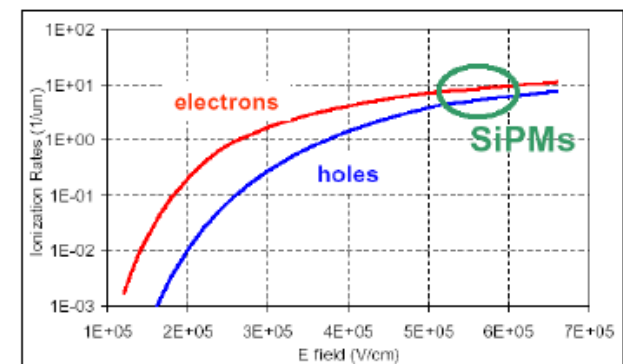


C.Piemonte
NIM A 568
(2006) 224

- Example with constant high-field:
- (a) only holes may trigger the avalanche
 - (b) both electrons and holes may trigger (but in a fraction of the high-field region)
 - (c) only electrons may trigger

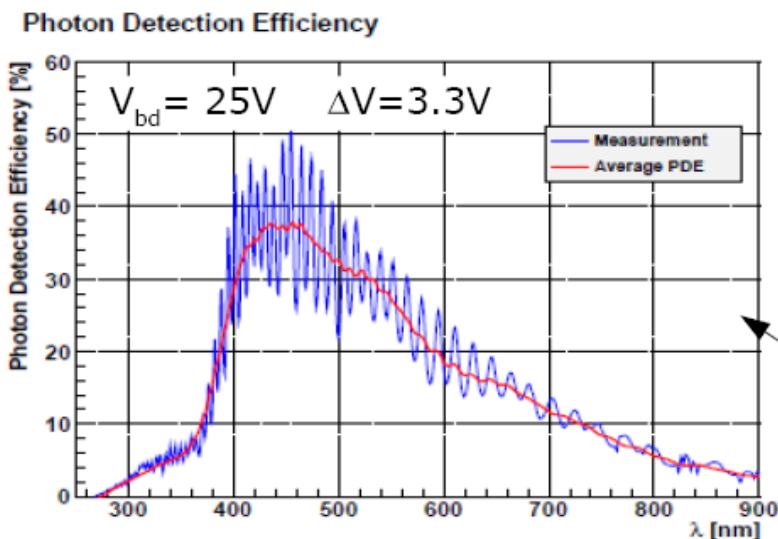
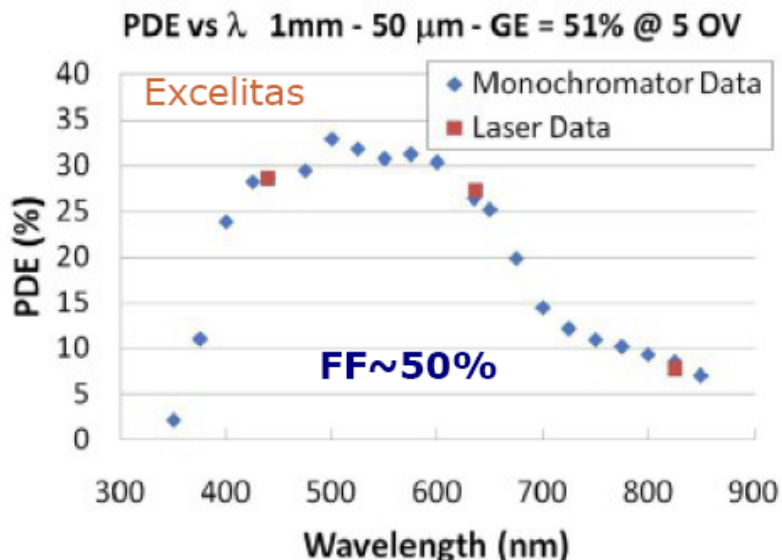
- high over-voltage
 - photo-generation in the p-side of the junction
- P_{01} optimization

Ionization rate in Silicon



Improving PDE

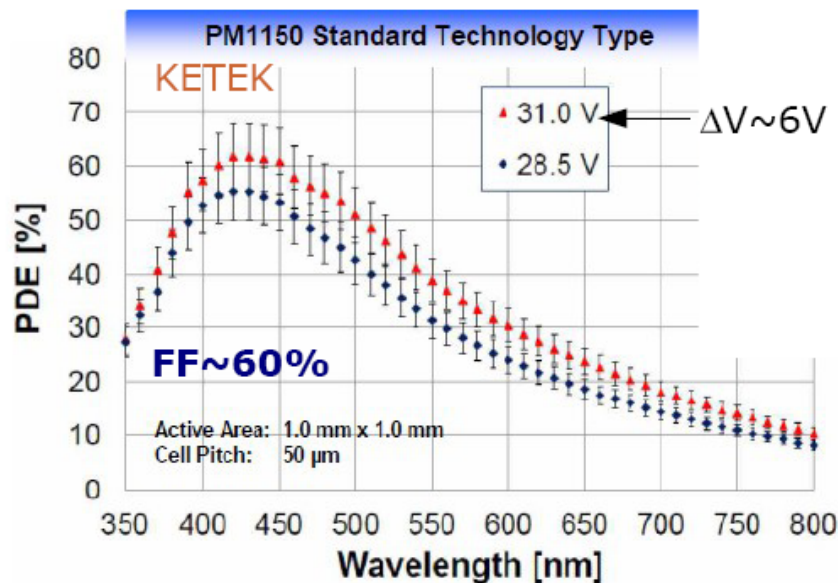
Barlow - LIGHT 2011



T.Frach 2012 JINST 7 C01112

- PDE peak constantly improving for many devices
- every manufacturer shape PDE for matching target applications
- UV SiPM eg from MePhi/Excelitas (see *E.Popova at NDIP 2011*)
- DUV SiPMs in development too

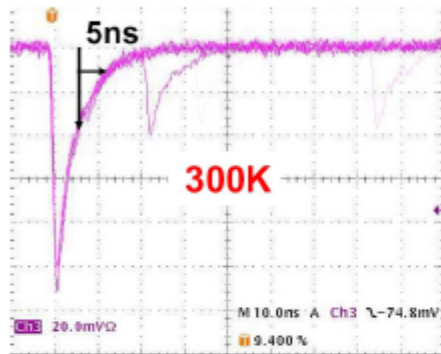
F.Wiest - AIDA 2012 at DESY



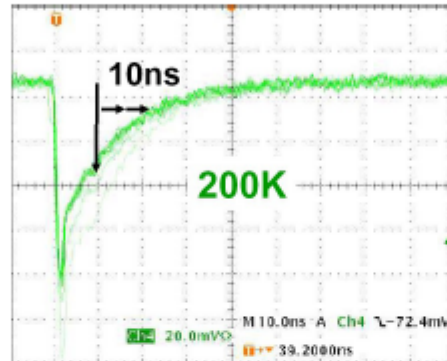
- dSiPM (latest sensor 2011)
- up to now **no optical stack optimization**
- **no anti-reflecting coating**
- potential improvement up to 60% peak PDE (*Y.Haemish at AIDA 2012*)

Pulse shape: dependence on Temperature

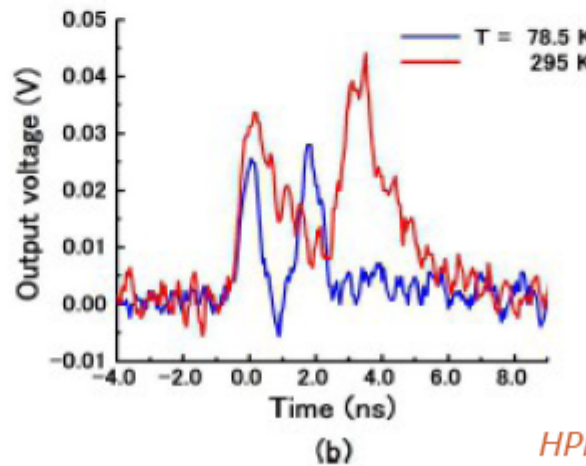
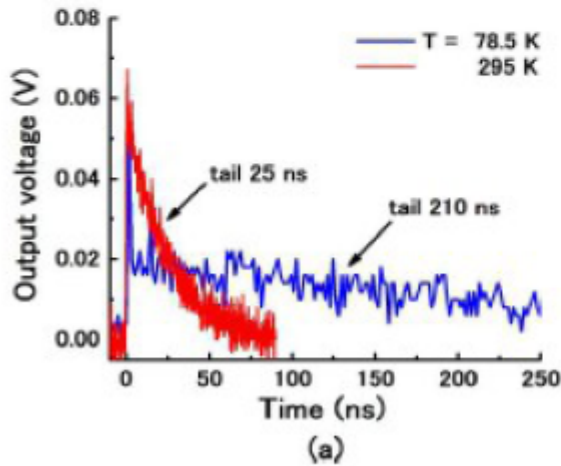
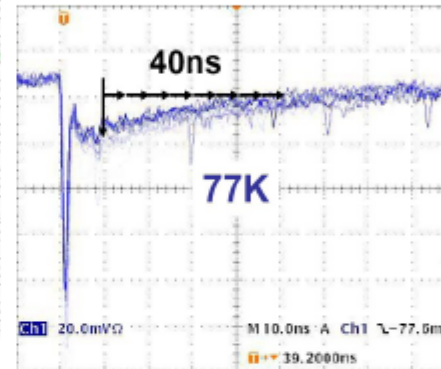
- The two current components behave differently with Temperature
- fast component is independent of T because C_{tot} couples to external R_{load}
- slow component is dependent on T because $C_{d,q}$ couple to $R_q(T)$



HPK MPPC



H.Otono, et al. PD07



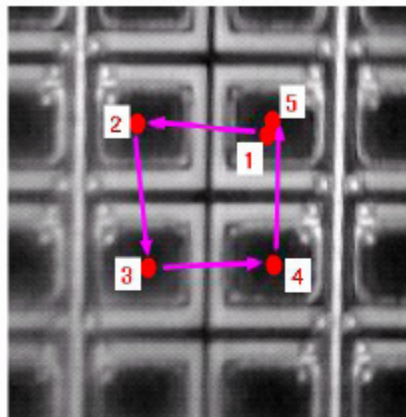
high pass filter / shaping
→ recover fast signals

HPK MPPC

Fig. 2. (a) Output signals from the MPPC when no high-pass filter is used, and (b) output signals from the high-pass filter when two pulses were generated successively.

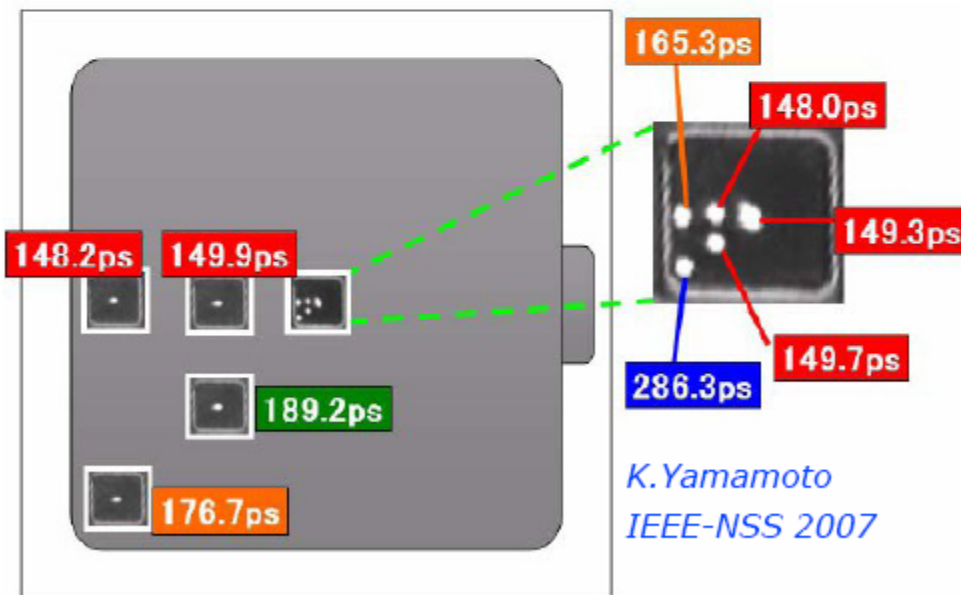
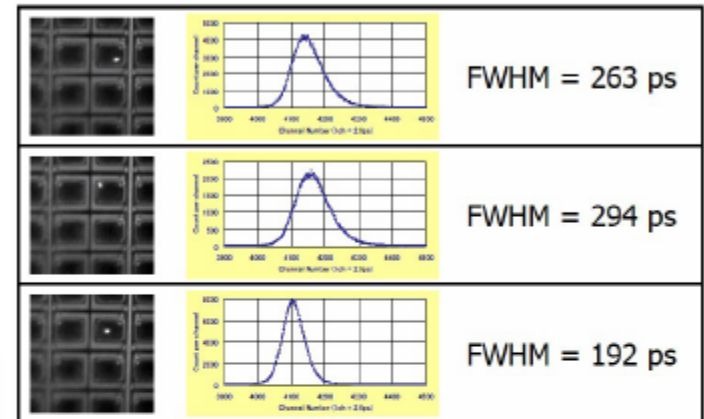
Akiba et al Optics Express 17 (2009) 16885

SPTR: position dependence → cell size



	FWHM (ps)	FWTM (ps)
1	199	393
2	197	389
3	209	409
4	201	393
5	195	383

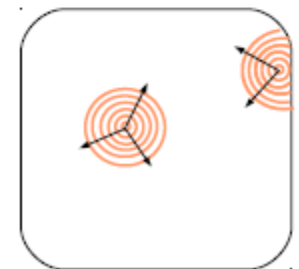
K. Yamamoto PD07



Larger jitter if photo-conversion at the border of the cell

Due to:
1) slower avalanche front propagation

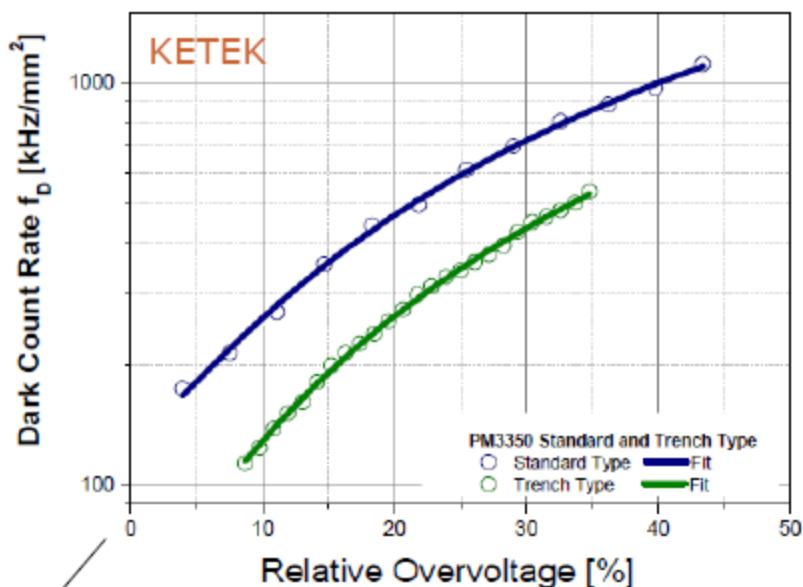
2) lower E field at edges
→ cfr PDE vs position



Data include the system jitter (common offset, not subtracted)

Dark Count Rate

KETEK PM 3350 (p⁺-on-n, shallow junction)
 3x3mm² active area pixel size 50x50 μm²



$V_{bd} \sim 25V$

F. Wiest - AIDA 2012 at DESY

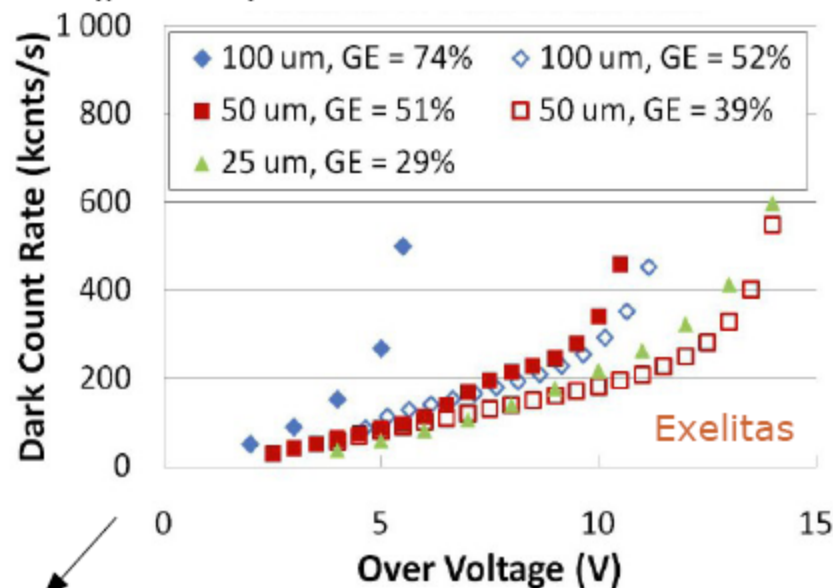
Latest **Hamamatsu** devices reached $\sim 80\text{kHz/mm}^2$

HPK claiming for additional improvements coming (*HPK at LIGHT 2011*)

Critical issues:

- quality of epitaxial layer
- gettering techniques
- Efield engineering (low T)

Exelitas 1st generation SiPM 2011 (p⁺-on-n) 1x1mm²



$V_{bd} \sim 140V$

P. Berard - NDIP 2011

Radiation damage: effects on SiPM

1) Increase of dark count rate due to introduction of generation centers

Increase (ΔR_{DC}) of the dark rate:

$$\Delta R_{DC} \sim P_{01} \propto \Phi_{eq} Vol_{eff} / q_e$$

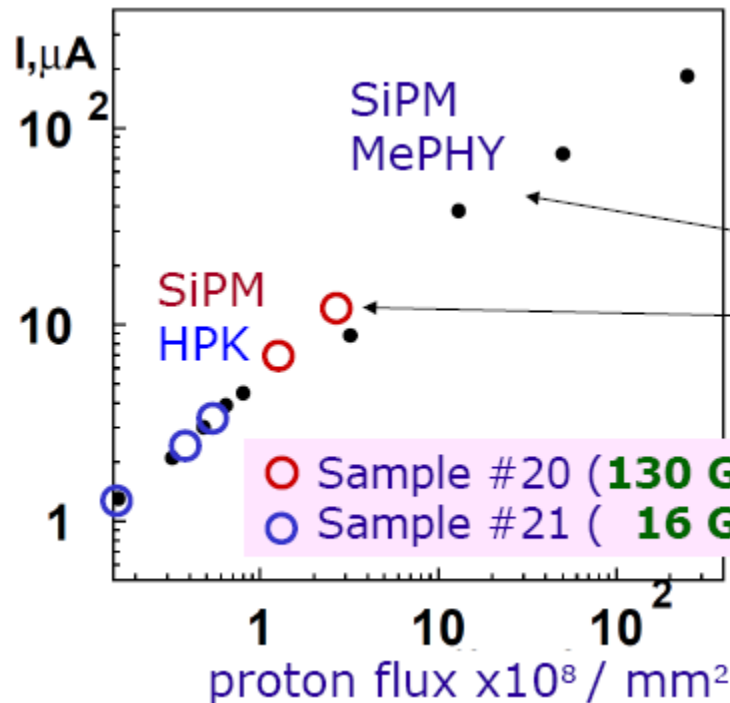
where $\alpha \sim 3 \times 10^{-17}$ A/cm is a typical value of the radiation damage parameter for low E hadrons and $Vol_{eff} \sim Area_{SiPM} \times \epsilon_{geom} \times W_{epi}$

NOTE:

- The effect is the same as in normal junctions:
- independent of the substrate type
 - dependent on particle type and energy (NIEL)
 - proportional to fluence

2) Increase of after-pulse rate due to introduction of trapping centers

→ loss of single cell resolution → no photon counting capability



Indications from measurements:

1) no dependence on the device

similar effects found for SiPM from MePHY (Danilov) and HPK (Matsumura) (normaliz. to active volume)

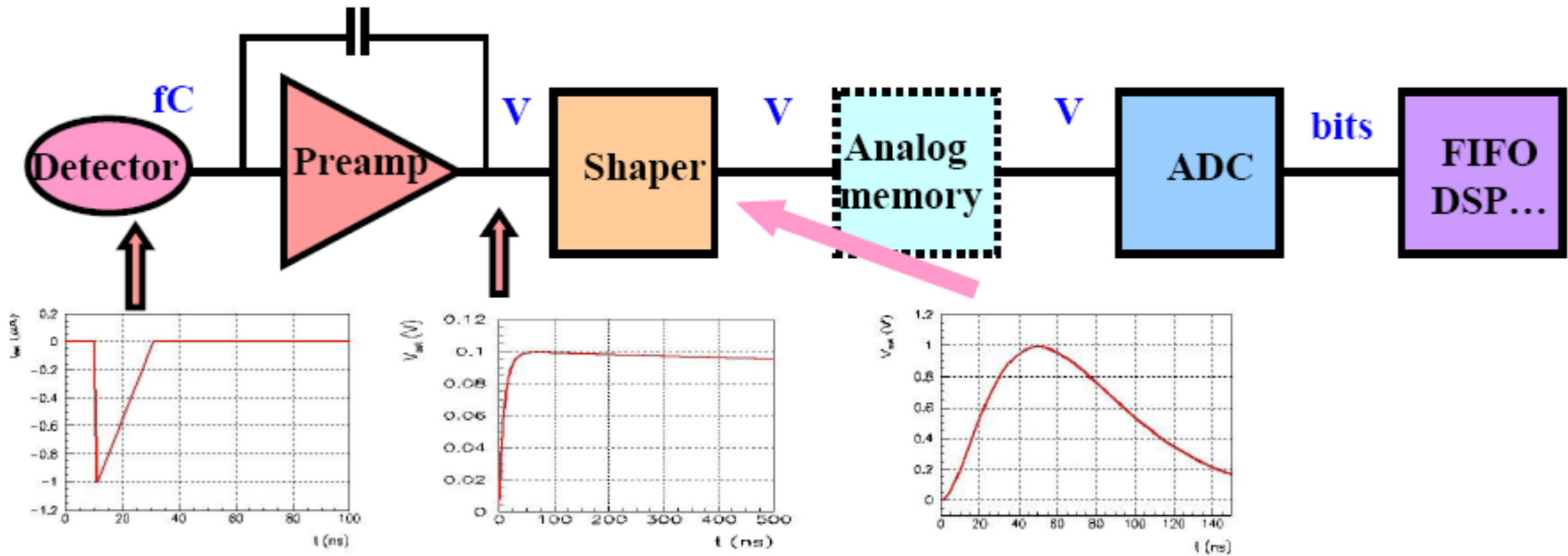
2) no dependence on dose-rate

HPK (Matsumura)

3) n similar damage than p

4) p $\times 10^1$ - 10^2 more damage than γ

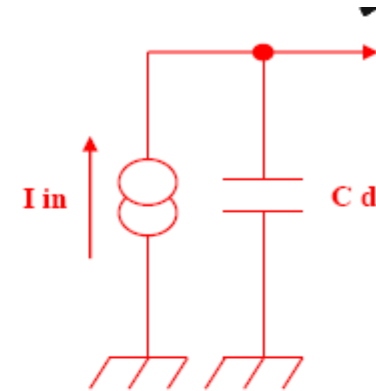
- Most front-ends follow a similar architecture



- n Very small signals (fC) -> need **amplification**
- n Measurement of **amplitude** and/or **time** (**ADCs**, **discris**, **TDCs**)
- n Several thousands to millions of channels
- n **Trends** : high speed, low power

Detector modelization

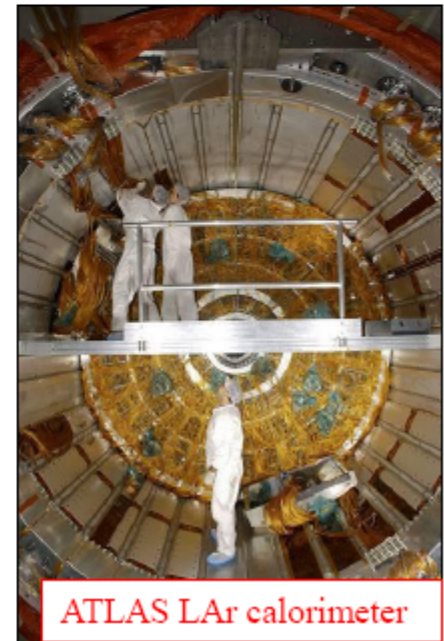
- Detector = capacitance C_d
 - Pixels : 0.1-10 pF
 - PMs : 3-30pF
 - Ionization chambers 10-1000 pF
 - Sometimes effect of transmission line
- Signal : current source
 - Pixels : $\sim 100e^-/\mu\text{m}$
 - PMs : 1 photoelectron $\rightarrow 10^5\text{-}10^7 e^-$
 - Modelized as an impulse (Dirac) :
 $i(t) = Q_0 \delta(t)$
- Missing :
 - High Voltage bias
 - Connections, grounding
 - Neighbours
 - Calibration...



Detector modelization



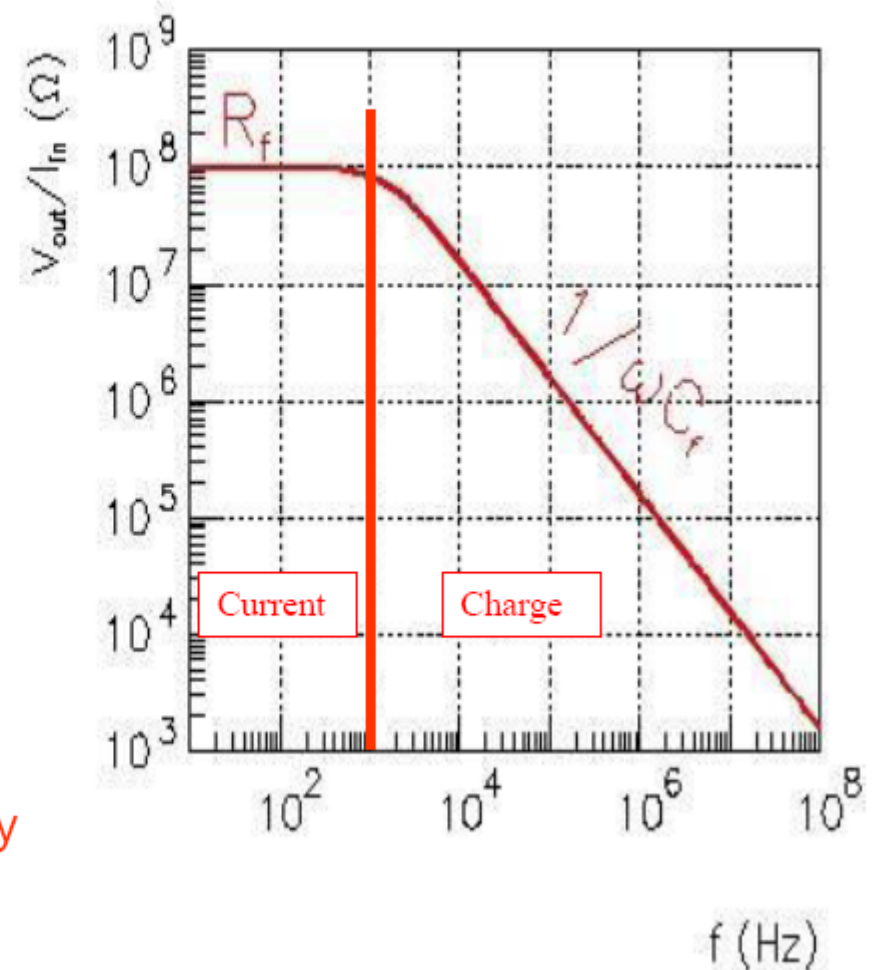
CMS pixel module



ATLAS LAr calorimeter

Charge vs Current preamps

- Charge preamps
 - Best noise performance
 - Best with short signals
 - Best with small capacitance
- Current preamps
 - Best for long signals
 - Best for high counting rate
 - Significant parallel noise
- Charge preamps are not slow, they are long
- Current preamps are not faster, they are shorter (but easily unstable)



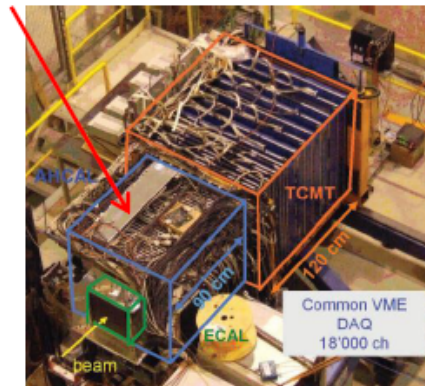
High granularity hadronic calorimeter optimised for the Particle Flow measurement of multi-jets final state at the ILC

Photodetector requirements:

- insensitive to magnetic field ($\sim 4T$)
- good sensitivity in blue-green
- cheap (10 millions channels)

studied SiPMs : MePHI/PULSAR, CPTA

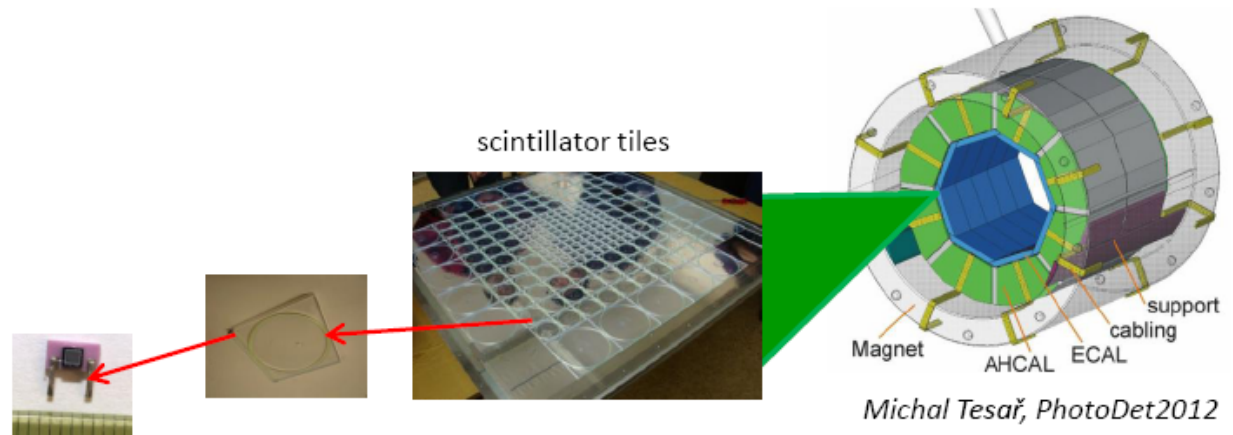
HCAL prototype (from 2007 to 2011)



38 layers - ~ 7600 SiPMs from MePHI/PULSAR

temperature dependance (variation of $PDE \times Gain : 3.7\%/^{\circ}C \%$) \rightarrow correction of response variations

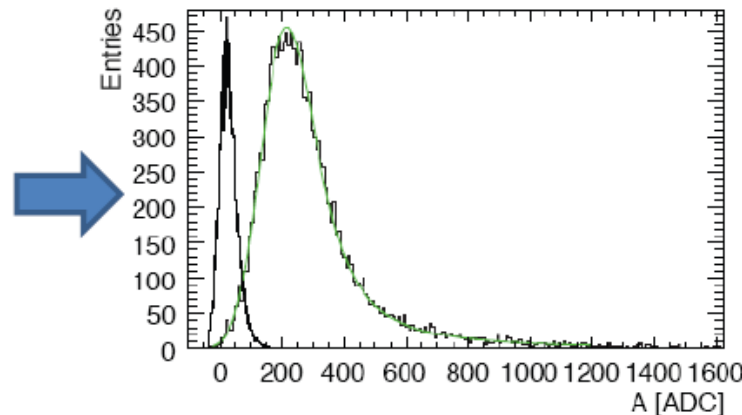
Ongoing activity : engineering prototype is now under construction with SiPM from CPTA



Michal Tesař, PhotoDet2012

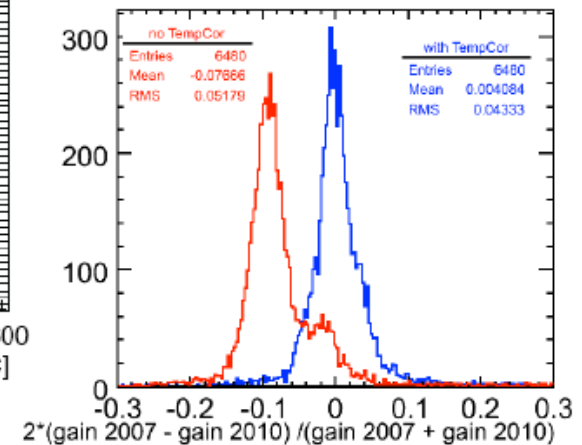
MePHI/PULSAR SiPM

HCAL test beams at SPS H8



MIP distribution of muons

CALICE Collaboration, 2010 JINST 5 P05004



S. Lu, LCWS11



Annealing

Proposal to Test Improved Radiation Tolerant Silicon Photomultipliers

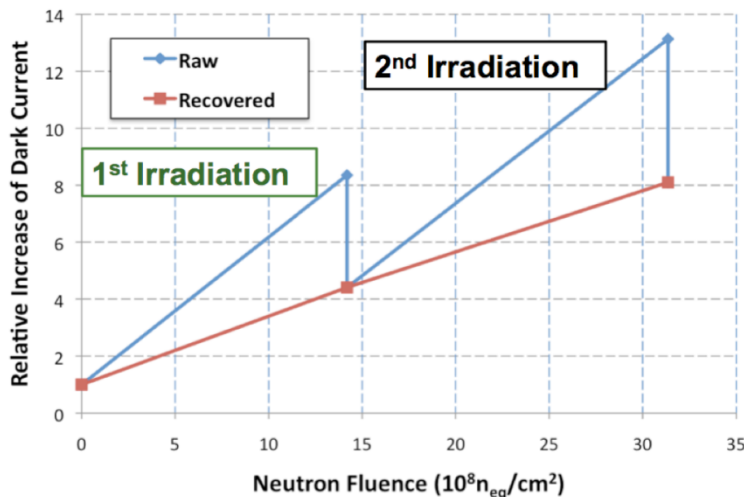
F. Barbosa, J. McKisson, J. McKisson, Y. Qiang, E. Smith, D. Weisenberger, C. Zorn
Jefferson Laboratory

How to Extend the Lifetime?

SiPMs cooled to 5°C during the beam → reduction of the dark noise by a factor 3 and minimization of the effects of neutron irradiation

Beam down period : SiPMs heated to ~40°C (post-irradiation annealing) → bring the noise down to a residual level

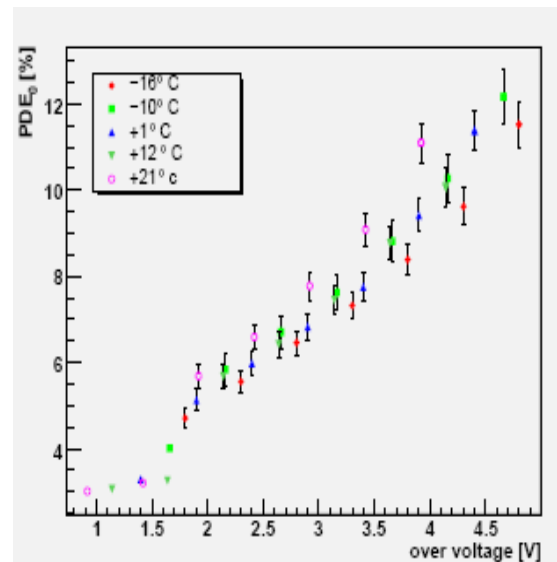
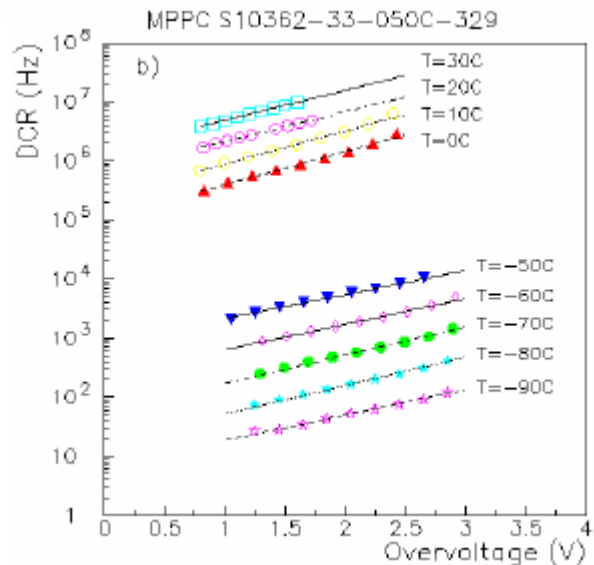
SiPM Neutron Radiation Test



At 25°C, annealing requires at least 5 days

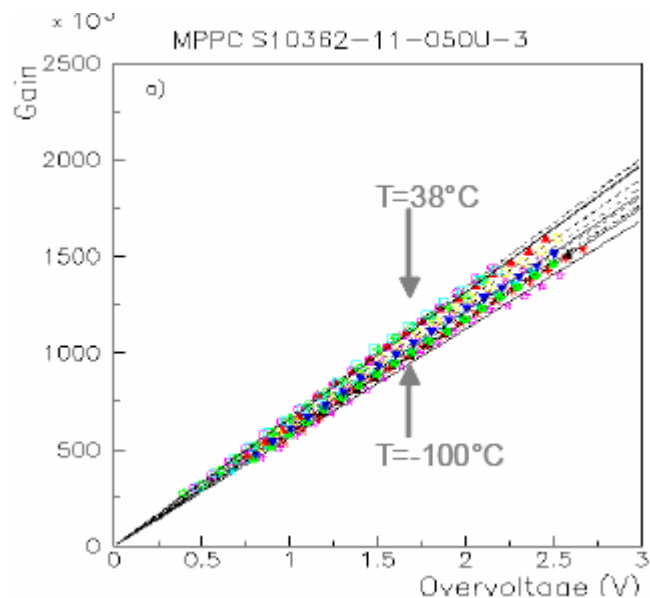
Heating to above 40°C can reduce the annealing time to less than 24 hours

Neutron Fluence with 10^8 g/s on LH_2 Target with 1/3 efficiency
→ 3×10^8 $n_{eq}/cm^2/year$



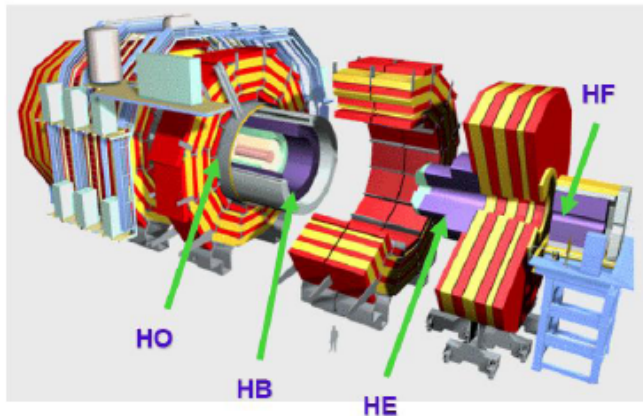
M. Ramilli

no temperature dependence of the PDE



Dinu, IEEE NSS 2010

HB & HE upgrade



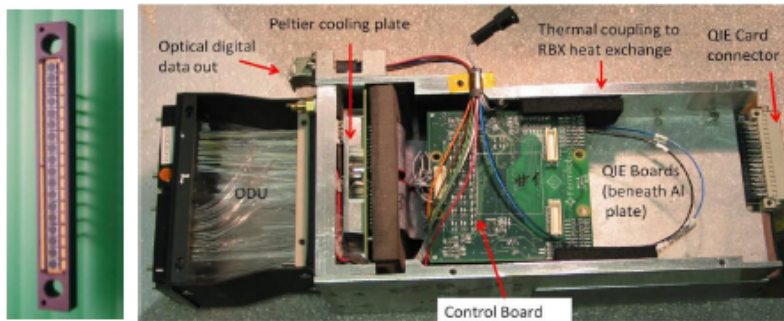
Photodetector requirements (to replace the HPD):

- very large dynamic range: a few p.e \rightarrow 2500 p.e
- high occupancy in front layers in SLHC \rightarrow fast recovery time (5 – 100 ns)
- radiation hard up to 3.10^{12} 1 MeV neutrons/cm² for 3000 fb⁻¹ (Gain*PDE change \leq 20%)

Studied SiPM :

HAMAMATSU, ZECOTEK, FBK, CPTA , ST-Micro, Sensl, NDL, KETEK

Prototype HB RM used at 2011 Testbeam

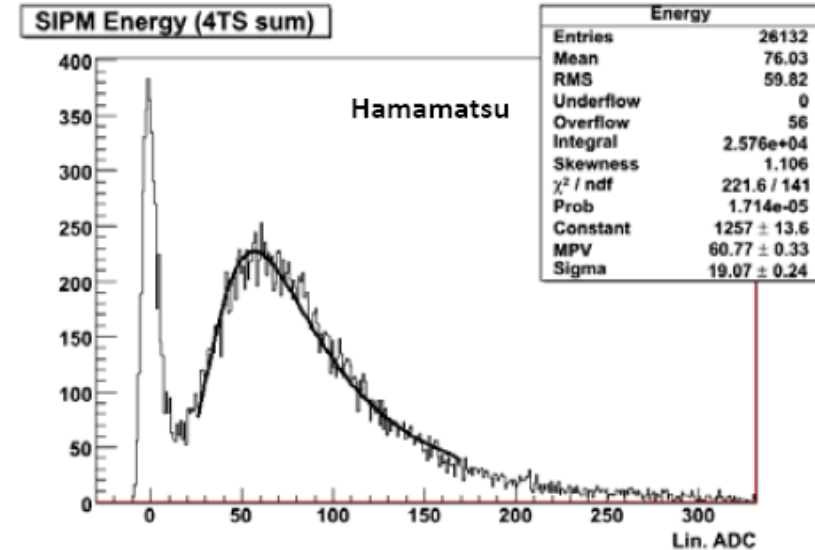


Y. Musienko, NDIP 2011

Temperature dependence \rightarrow control @ 0.2 °C

Significant progress on the SiPM development over the last 2 years (HAMAMATSU , Zecotek, NDL) \rightarrow the MPPCs from HAMAMATSU are close to satisfy most of the requirements.

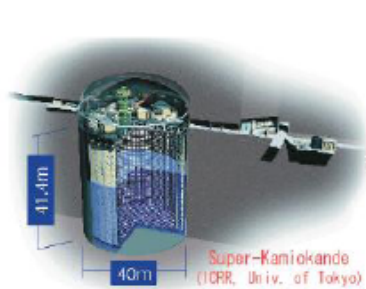
Muon response in a single tower of CMS HO



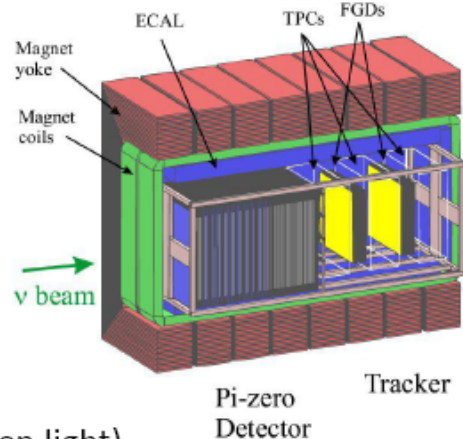
J. Freeman, FERMILAB-CONF-09-601-E



SiPMs for neutrino oscillation experiment: T2K



ND280 : near detector complex - neutrino beam flux and spectrum measurements



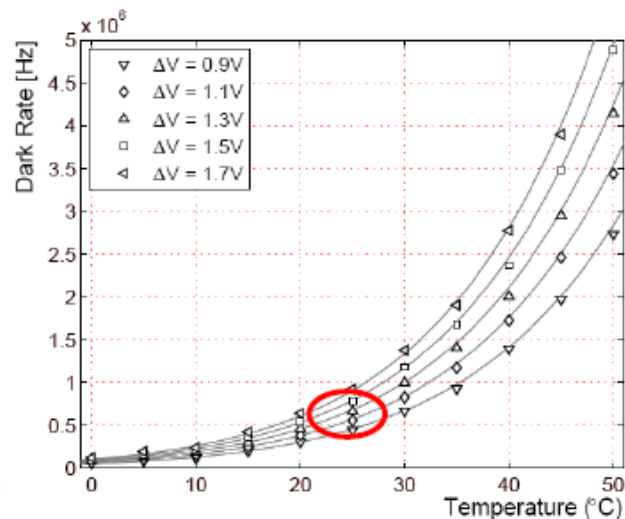
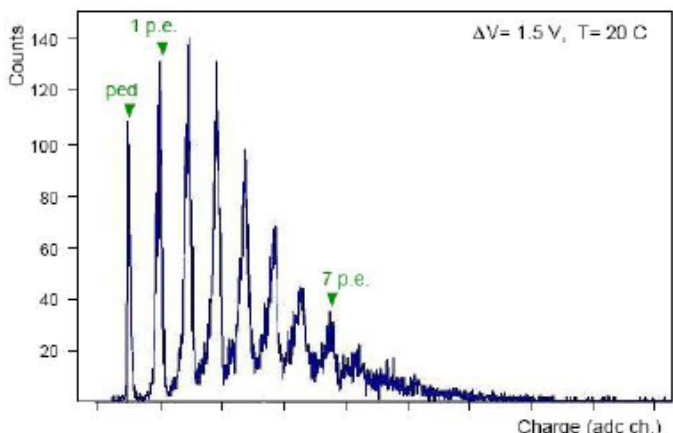
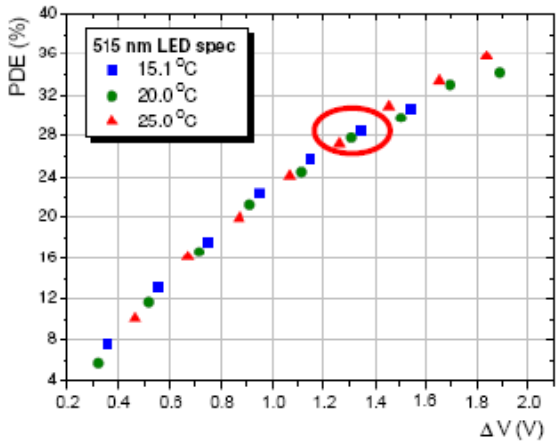
HAMAMATSU MPPC customized device



1.3 x 1.3 mm²
667 cells (50 x 50 μm²)

Photodetector requirements:

- insensitive to magnetic field
- coupling with a scintillator + WLS fiber (PDE > 20 % for green light)
- DCR < 1 MHz
- compact



55996 MPPC tested : only 0,16 % rejected

A. Vacheret, arXiv:1101.1996

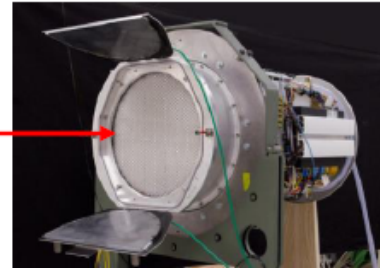
FACT: First G-APD Cherenkov Telescope



MPPC S10362-33-50C
coupled to a cone light
concentrator



1440 channels



Th. Krähenbühl, Photodet
2012

Photodetector requirements:

- PDE > 20 % for blue light
- ability to detect single photons
- stable
- robust
- compact



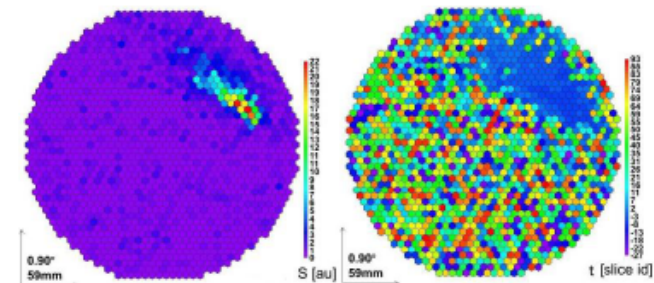
problem with the SiPM V_{BD} temperature dependence
→ regulation of the bias voltage with a feedback system

First operation on the night of October 11, 2011

After one year of routine operation:

- no indication of any problem or ageing in any SiPM
- temperature as well as ambient-light dependence of SiPM well under control
- operation under very different ambient conditions shows no problem

an Event Seen by FACT

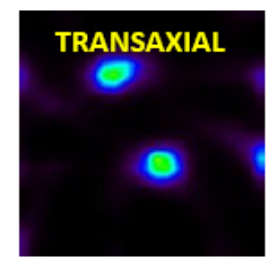
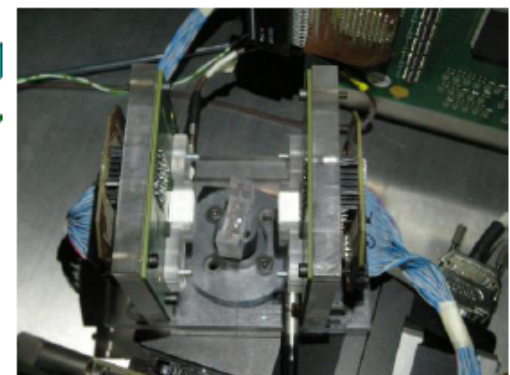
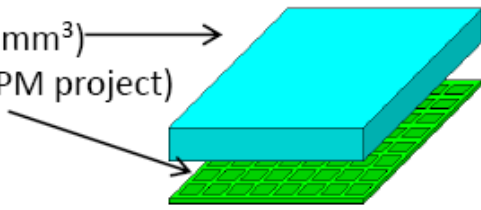


P. Voqler, TWEPP 2012

Small animal PET

miniature, high-resolution camera for a small-animal PET imaging system that is based on a combination of SiPM with a continuous scintillation crystal.

- LYSO continuous crystal ($12 \times 12 \times 5 \text{ mm}^3$)
- monolithic matrices from FBK (DASIPM project)
- $\Delta E/E \sim 15\%$ FWHM (at 511 keV)
- $\Delta x = \Delta y \sim 0.7 \text{ mm}$ FWHM

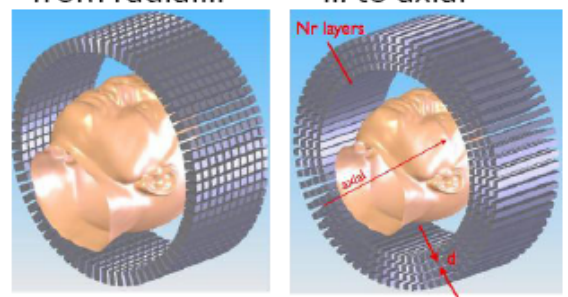


G. Llosa, PSMR 2012

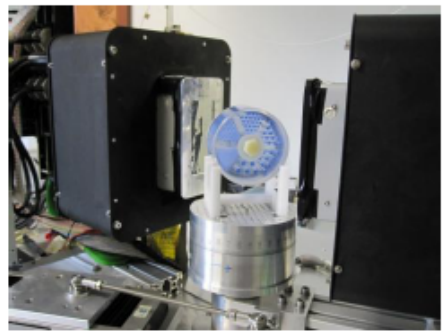
AX-PET

from radial...

... to axial



C. Joram, NIM A 654 (2011) 546-559



- long LYSO crystals ($3 \times 3 \times 100 \text{ mm}^3$)
- orthogonal WLS strips
- readout by SiPMs from Hamamatsu
- 3D reconstruction of photons

Some results

- $\Delta E/E \sim 12\%$ FWHM (at 511 keV)
- $\Delta x = \Delta y \sim 2 \text{ mm}$ FWHM
- Δz (axial) = 1.8 mm FWHM

Latest development:

Use of Digital SiPM (Philips) for AX-PET with TOF \rightarrow CRT < 200 ps FWHM.